Sedimentology, Diagenesis and Trapping Style, Mississippian Tar Springs Sandstone, Inman East Consolidated Field, Gallatin County, Illinois

David G. Morse

Illinois Petroleum 157 2001

George H. Ryan, Governor

Department of Natural Resources
ILLINOIS STATE GEOLOGICAL SURVEY
William W. Shilts, Chief

Sedimentology, Diagenesis and Trapping Style, Mississippian Tar Springs Sandstone, Inman East Consolidated Field, Gallatin County, Illinois

David G. Morse

Illinois Petroleum 157 2001

George H. Ryan, Governor

Department of Natural Resources
ILLINOIS STATE GEOLOGICAL SURVEY
William W. Shilts, Chief
Natural Resources Building
615 East Peabody Drive
Champaign, IL 61820-6964
(217) 333-4747

DISCLAIMER

This report was prepared by the Illinois State Geological Survey (ISGS) as part of a project sponsored by the State of Illinois. It presents reasonable interpretations of available scientific data. Any opinions, findings, conclusions, or recommendations expressed herein are those of the author. Neither the ISGS, any individual members of the ISGS staff, the Illinois Department of Natural Resources, nor the U.S. Department of Energy assumes any liability with respect to the use of any information contained in this report. Trade names cited in this report are provided solely for the purpose of informing the public. Use of a particular product does not constitute an endorsement by the ISGS.

ACKNOWLEDGMENTS

Donald F. Oltz initially suggested that I study the Tar Springs Sandstone. Preliminary work by Richard Howard at Sailor Springs Field provided some insight about how to attempt this study. Beverly Seyler was particularly helpful in the scanning electron microscopy/energy dispersive x-ray analyses and interpretation of the Tar Springs samples, along with advice on thin-section preparation. Duane M. Moore made the x-ray diffraction analyses and their interpretation and took particular interest in the ankerite cements, in addition to the whole rock and clay mineral analyses. Janet K. Pitman at the U.S. Geological Survey helped arrange for and interpret the carbon and oxygen isotope data from the ankerite cements. Bruce W. Fouke of the University of Illinois Geology Department made a cathodoluminescence examination of the ankerite and helped with the ankerite isotope data interpretation. Thomas Davis extracted the Tar Springs data from the Illinois core analysis database. Members of the Oil and Gas Section at ISGS, particularly Hannes Leetaru, John P. Grube and Beverly Seyler, provided a good sounding board for reservoir, geological and sedimentological ideas and interpretations that are presented here and also made a careful review of and suggestions for this paper. Jonathan H. Goodwin helped provide technical clarity with his editorial review and suggestions. The responsibility for the accuracy of the interpretations and ideas, however, rests with me. I acknowledge the support of this research by Landmark Graphics via the Landmark University Grant Program.

Cover Photo *Cross-bedded Tar Springs Sandstone at an outcrop near Alto Pass in Union County in southwestern Illinois. Foresets on the cross-beds consist of pairs of thin and thick beds, interpreted as "tidal couplets." Cross-bedding is diverse in orientation but generally unimodal, dipping predominantly to the southeast. The field of view is approximately four feet high. (photo by D. G. Morse)*

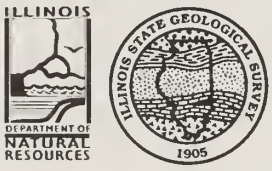

printed by authority of the State of Illinois/2001/700

⊛ Printed with soybean ink on recycled paper

CONTENTS

FIGURES

TABLE

ABSTRACT

The Mississippian Tar Springs Sandstone in southern Illinois is often overlooked as a potential oil-producing horizon, yet it can be a prolific reservoir. The East Inman Consolidated Field, discovered in 1940, produces from the Tar Springs as well as from several other Chesterian cyclic sandstones. The reservoirs are structural-stratigraphic traps formed by the Wabash Valley Fault System of southeastern Illinois. The source of the oil was the Devonian New Albany Shale. The oil is believed to have migrated vertically along faults to its present location, thus charging many of the Chesterian and lower Pennsylvanian sandstones in the field. The Tar Springs Sandstone produces from stacked distributary channel sandstone reservoirs. The sandstones, which are up to 125 feet thick, fill valleys up to 40 feet deep that were incised in laterally equivalent, non-reservoir, delta-fringe facies and the underlying Glen Dean Limestone. The reservoir sandstones are well-sorted, fine- to medium-grained quartz arenites with less than 5% feldspar and chert. Quartz grains have quartz overgrowths. Feldspar grains appear clouded in thin section and show pronounced etching, dissolution and alteration to clay in scanning electron microscopy (SEM) photomicrographs. Diagenetic kaolinite and lesser amounts of mixed-layer illite-smectite, illite and chlorite occur in intergranular pores. Sparry, iron-rich dolomite or ankerite that fills pores in irregular millimeter-size patches locally occupies up to 10% of the volume of reservoir rock. Typical reservoir porosity ranges from 16% to 19% and permeability ranges from 60 to 700 millidarcies (md). By contrast, non-reservoir delta-fringe sandstones typically have porosities of 6% to 12% and permeabilities of 1 to 20 md. Shales deposited in the delta-fringe environment act as impermeable lateral and vertical seals that aid in stratigraphic trapping.

EXECUTIVE SUMMARY

This paper provides the first comprehensive study of the regional geology and hydrocarbon reservoir character of the Upper Mississippian Tar Springs Sandstone in the Illinois Basin. For this study, the regional depositional patterns and sedimentary environments of this formation in Illinois were examined, and the reservoir geology at a typical location, Inman East Consolidated Field, located in Gallatin County in southeastern Illinois, was characterized in detail. The results of this study can serve as an analogue for the exploration and development of other oil fields in the Tar Springs Sandstone in southern Illinois.

The Tar Springs Sandstone was deposited across Illinois, western Indiana and western Kentucky during the Mississippian Period about 320 million years ago as a tidally influenced, river-dominated delta. The Tar Springs Sandstone is 40 to 150 feet thick and consists of well-sorted sandstone bodies formed in delta distributary channels that were part of a basin-wide, generally north to southward prograding delta complex. The rivers that formed the channel sandstones in the lower part of the Tar Springs scoured downward as much as 40 feet into the underlying Glen Dean Limestone. The channel sandstones that form the bulk of the formation may total, in places, more than 100 feet of clean sandstone. Between the channels are interdistributary sandstones and shales that formed in bays, tidal flats and crevasse splays and as channel overbank deposits. The formation is vertically and laterally heterogeneous and variable in thickness. The top of the Tar Springs is commonly shaley. Thin coal stringers or carbonaceous shales have been found in the uppermost shales. The contact with the overlying, fossiliferous, Vienna Limestone is sharp and without apparent relief.

The sandstones of the Tar Springs at Inman East Consolidated field are composed primarily of fine-to very fine-grained, well-sorted, quartzose sand originally with 2% to 5% feldspar grains; feldspar grains appear clouded in thin section and typically are partially altered to clay minerals. The primary cement is quartz, occurring as

overgrowths on the quartz grains. Later cements include ankerite (an iron-rich dolomite) and a variety of clay minerals consisting mostly of kaolinite and lesser amounts of chlorite, mixed layered illite/smectite and illite.

The hydrocarbon trap for the Tar Springs Sandstone at Inman East Consolidated Field is a combination of anticlinal closure and up-dip stratigraphic pinchout. Inman East Consolidated Field occurs on an arching horst block formed as part of the Wabash Valley Fault System. The eastern compartment has up-dip closure against the Inman East Fault. Each of the three Tar Springs compartments at Inman East Consolidated Field is delimited by the distribution of the channel sandstones and their up-dip closure against laterally equivalent shaley channel plugs and overlying shales. Porosity in the channel sandstones averages about 17%, and the geometric mean permeability is 107 md. Thinner crevasse splay sandstones, sandstones interbedded with shales or flaser-bedded sandstones have significantly lower porosity and permeability. Primary pores constitute about 80% of the pore volume. The remaining secondary pores were formed largely by partial dissolution of feldspar grains. Quartz overgrowths along with some diagenetic clay and carbonate minerals also are present in the pores.

INTRODUCTION

The Tar Springs Sandstone is a well-sorted, mature sandstone deposited during the late Mississippian (Chesterian) in the Illinois Basin. In addition to sandstone, the formation contains siltstone, shale and local thin beds of coal. It conformably overlies the Glen Dean Limestone, although local scouring has removed at least 40 feet of the Glen Dean (Swann 1963). Overlying the Tar Springs is the Vienna Limestone, a thin, but persistent, Chesterian marker in the southern Illinois Basin. The Tar Springs forms part of one cycle in a series of alternating siliciclastic/carbonate units that typify the upper Mississippian Chesterian Series in the Illinois Basin.

The Tar Springs Sandstone produces oil in 52 oil fields in Illinois (fig. 1) and extends widely throughout the Illinois Basin, including western Indiana and northwestern Kentucky (fig. 2). It is a major producing horizon in the Inman East Consolidated Field (162 completions) and Benton Field (249 completions) and is significant at Sailor Springs Field (67 completions). Nevertheless, the Tar Springs Sandstone is an overlooked pay horizon that operators routinely drill through to reach the more productive reservoirs of the Cypress, Aux Vases or Ste. Genevieve Formations.

Previous studies of the Tar Springs are limited, largely focusing on the areas where it outcrops in southern Illinois. Weller (1920) described the Tar Springs in Hardin, Pope and Johnson Counties as having an upper and lower sandstone body, separated by a persistent shale that at widely varying locations may contain a layer of impure coal 1 inch to 1 foot thick. Butts (1925) described a persistent coaly/carbonaceous shale bed in the middle part of the Tar Springs in a 40-foot-thick, dark gray to black, shaley interval that contains well-preserved, land-plant fossils. Weller et al. (1952, p. 102) noted a locally persistent thin coal bed up to 6 inches thick near the top of the Tar Springs Sandstone. Devera (1991) mapped this coal in the Glendale Quadrangle of Johnson and Pope Counties.

Grote (1949), in examining the subsurface characteristics of the Tar Springs Formation in Hamilton, White and parts of Gallatin and Saline Counties, noted that the formation was generally sandy at the base and became more shaley upward. By examining more than 5800 well logs and mapping the Tar Springs, he found that lithologies varied over short lateral distances, thus limiting well-to-well correlations. From compiled core analysis data, he determined that the average porosity was about 17% and the average permeability was about 50 md. The sandstone is composed primarily

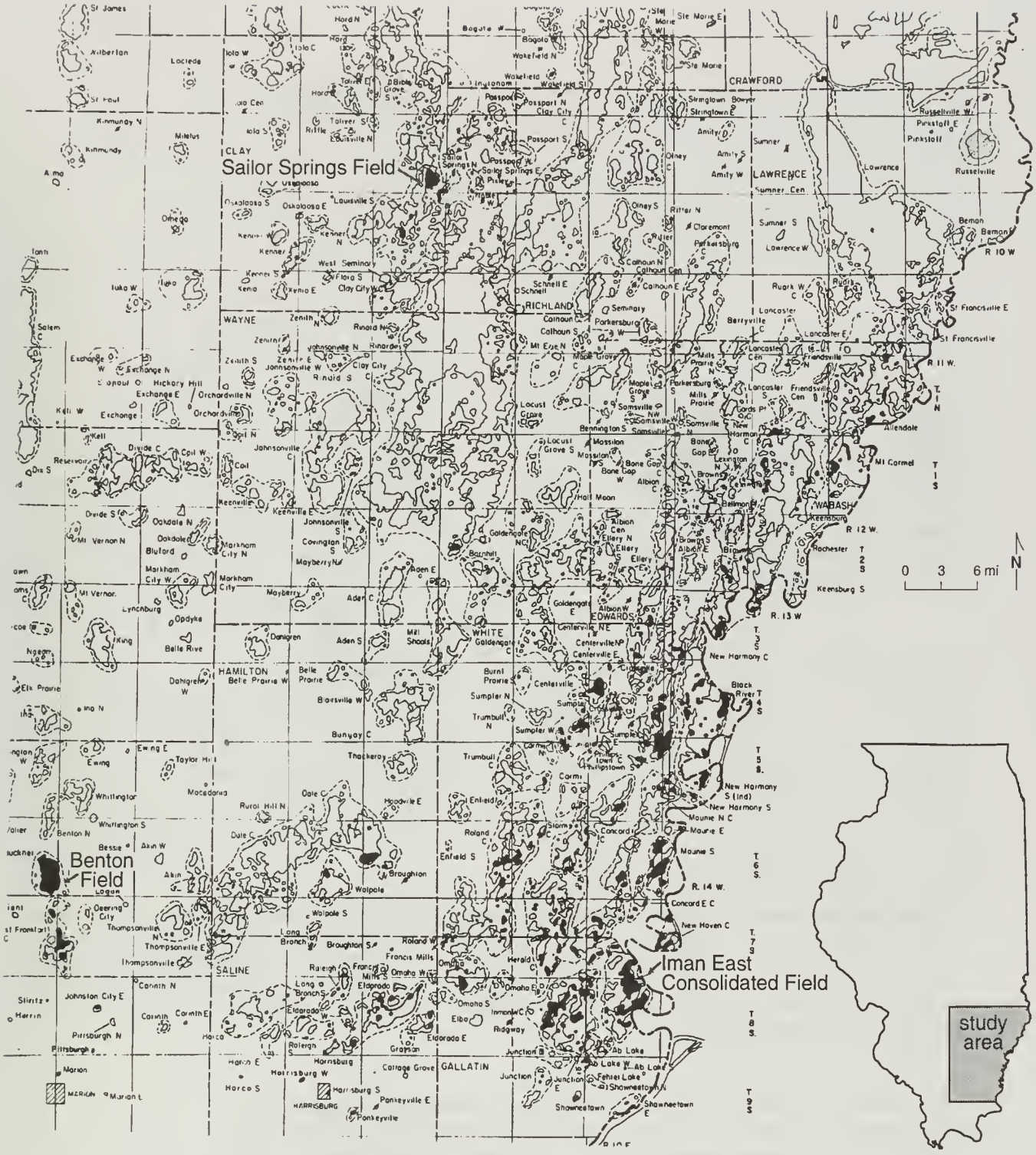

Figure 1 Tar Springs production map in the southeastern Illinois Basin. Fields that produce from the Tar Springs are blackened. The major fields include Inman East Consolidated, Benton and Sailor Springs. Production typically occurs on anticline closures, but the extent of the reservoir rock is determined by the sedimentological variation in sandstone distribution (from Howard 1987).

of very fine-grained quartz sand that is cemented by quartz, carbonate and clay. Howell (1948) described Benton Field, the major Tar Springs reservoir in Franklin County, Illinois, in detail. Other workers who have studied the Tar Springs include Worthen (1860), Lamar (1925), Workman (1940), Weller and Ekblaw (1940), Dana and Scobey (1941), Folk and Swann (1946), Swann (1963, 1964) and Simon and Hopkins (1966).

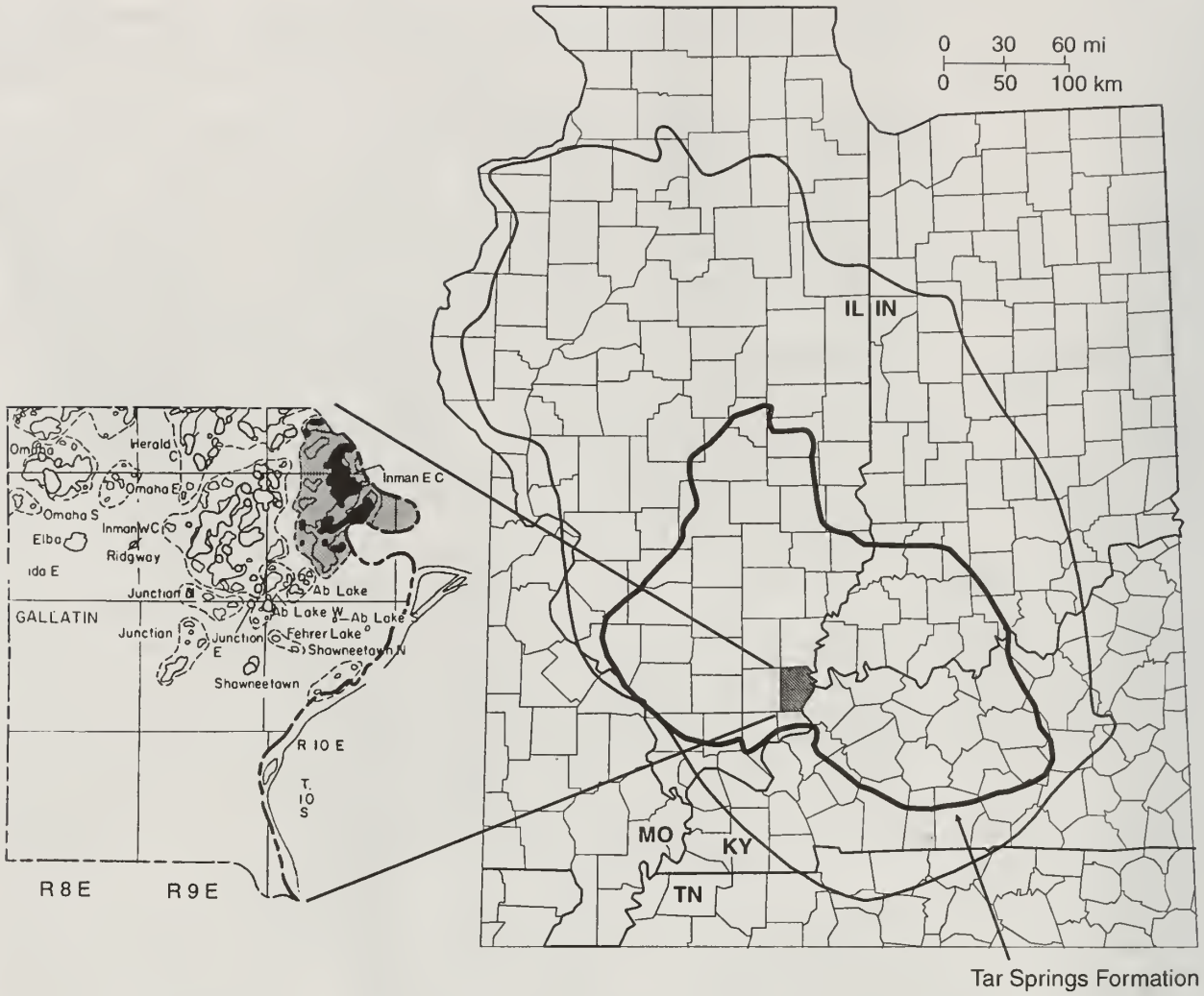

Figure 2 Regional extent of Tar Springs Sandstone. Outlined area of the Illinois Basin (light line) and occurrence of the Tar Springs and equivalents (dark line) in Illinois, Indiana and Kentucky. Outcrops occur in the southern Illinois Basin, but in the central and northern Illinois Basin, the edge of the Tar Springs is truncated along an unconformity below the overlying Pennsylvanian rocks (in part from Willman et al. 1975, p. 159). Gray area of the inset map of Gallatin County outlines the Inman East Consolidated Field. All fields that produce from the Tar Springs Sandstone are colored black (from Howard 1987).

More recently, Wescott (1976, 1982) measured and described nine stratigraphic sections across southern Illinois. Unfortunately, his two sections near New Columbia (nos. 7 and 8) occur in rocks that have now been mapped as Cypress Sandstone (Devera, personal communication). Wescott recognized four lithofacies in the Tar Springs, which he interpreted as having been deposited in fluvial-deltaic distributary channels, shoreface, foreshore, tidal flats and interdistributary bay environments. He suggested that wave-dominated deltaic sedimentation in southeastern Illinois became more tidally dominated to the northwest. This interpretation refines Swann's (1963, 1964) commonly accepted model for the cyclic late Valmeyeran through Chesterian deltaic deposition in the Illinois Basin, in which repeated advances and abandonments of deltaic lobes of the ancient Michigan Delta successively deposited the sediments of the Aux Vases, Cypress, Hardinsburg, Tar Springs, Waltersburg, Palestine, Clore and Degonia Formations (fig. 3). Swann's fluvial-deltaic system migrated laterally

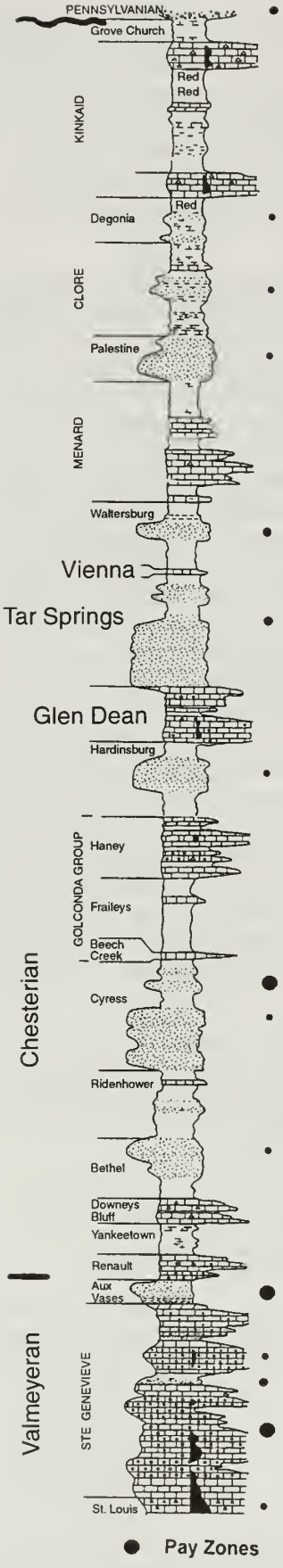

several hundred miles, and advancing deltaic lobes pushed seaward up to 600 miles in a generally southerly direction across the shallow, subsiding craton. Between these clastic units, widespread carbonate marker formations were deposited. These included the Renault, Downeys Bluff, Beech Creek, Haney, Glen Dean, Vienna and Menard Limestones and the Negli Creek and Goreville Limestone Members of the Kinkaid Formation.

Modern sequence stratigraphy suggests that eustatic changes in sea level could have played a major role in the late Valmeyeran and Chesterian cyclic siliciclastic/carbonate deposition in the Illinois Basin (Smith 1996, Leetaru 1997, Treworgy et al. 1997). In general, the transgressive system deposits include either the basal limestone or a transgressive lag or a mixed siliciclastic/carbonate sequence. The highstand deposits include the progradational siliciclastic units. When the sea level lowered, soils, karst and incised valleys formed and marked the boundary with the next sequence.

This report studied the reservoir character of the Tar Springs Sandstone, the regional depositional patterns of the sandstone, and details of the reservoir geology at a typical location, Inman East Consolidated Field, located in Gallatin County in southeastern Illinois. The reservoir sedimentology, petrography, trapping mechanism and reservoir rock parameters were examined in detail. Rock analyses used for the study included thin-section optical microscopy, SEM, x-ray diffraction, and isotope geochemistry. The results of this study may serve as an analogue for other Tar Springs Sandstone reservoirs in southern Illinois.

BACKGROUND

The Tar Springs Sandstone was named for an oil-bearing sandstone at an oil seep and its associated tar build-up in Breckenridge County, Kentucky (Owen 1857, Butts 1917). It crops out along the southern and eastern margins of the Illinois Basin in Illinois, Indiana and Kentucky and continues throughout the Illinois Basin to its truncated limits beneath the sub-Pennsylvanian unconformity (fig. 2).

Figure 3 Geologic column of upper Valmeyeran and Chesterian sediments in southern Illinois. Oil-bearing reservoirs are indicated by black dots whose size varies according to the relative magnitude of their contribution to oil production in the basin (from Bell et al. 1961). The Vienna Limestone, Tar Springs Sandstone, and Glen Dean Limestone are discussed in detail in this report. They are middle Chesterian.

The Tar Springs Sandstone is bounded by the underlying Chesterian Glen Dean Limestone and the overlying Chesterian Vienna Limestone (fig. 3). Minor disconformities may be present at each of these contacts. For example, as discussed later, the Tar Springs locally cuts down into the Glen Dean, removing up to 40 feet of dark shale and limestone. The uppermost Tar Springs includes localized thin coal stringers and terrigenous deposits that are sharply overlain by the bioclastic, marine limestone beds of the Vienna. Such an abrupt change in lithology and depositional conditions suggests that some transitional upper Tar Springs sediments may have been removed by erosion.

Inman East Consolidated Field was discovered in 1940 at a depth of about 2,000 feet with 30 barrels per day of production from the Tar Springs Sandstone in the Leach and Fuhrer, No. 2 Egyptian Tie and Timber well located in Section 16, T8S, R10E. It was one of many discoveries in that area as drillers explored the many anticlinal structures along the Wabash Valley Fault System in Gallatin and White Counties, Illinois. The Tar Springs Sandstone was but one of 15 pays discovered in the field. Records show that 491 producing wells were drilled on 10-acre spacing in this area and delineated three producing pools or compartments (informally called in this report, "Inman," "Inman East" and "Inman South") that are collectively known as the Inman East Consolidated Field (fig. 4). A total of 165 of the wells were Tar Springs producers. Initial Tar Springs potential production from these wells ranged from a few barrels per day to1,200 barrels per day (fig. 5). At its peak in 1948, Inman East Consolidated Field was producing more than 6,000 barrels per day from all reservoir pays in 41 leases (fig. 6). Cumulative production from all pay horizons in Inman East Consolidated Field had reached 24,378,896 barrels of oil by December 1997 (*Petroleum Information Pipeline Production Report* December 1997) (see fig. 6a), for an average total production per well of just fewer than 50,000 barrels. Average cumulative production per well from all reservoirs in Inman East Consolidated Field varies by location from about 7,600 barrels to about 83,500 barrels per well, as is shown in Table 1. Today, the field produces only 70 barrels per day from just 27 active leases. Most of the wells drilled in the field's heyday have been shut in or plugged and abandoned. Two waterflood units, the East Inman and the Big Barn, were established to increase recovery when the field was being developed. Today, wells in the East Inman Unit are in the Illinois Plugging and Restoration Program, and all producing wells in the Big Barn Unit have been plugged (Larry Bengal, Oil and Gas Division, Illinois Department of Natural Resources, personal communication).

The Tar Springs pay at Inman East Consolidated Field averages 13 feet thick. Many of the wells are cased down to the top of the Tar Springs and then drilled into the top of the pay sandstone and completed as open holes without casing and perforating. The Tar Springs reservoir interval has 16% to 19% porosity and 60 to 700 md permeability.

Table 1 Cumulative oil production and field totals from all reservoirs in selected parts of Inman East Consolidated Field and for the field as a whole.

location	cumulative production[1] of all wells in section (no. barrels)	producing wells per section (no.)	average cumulative oil per well (no. barrels)
34 7S 10E	751,121	25	30,044
3 8S 10E	511,292	51	10,025
10 8S 10E	3,680,909	48	76,685
14 & 11 8S 10E	2,673,501	32	83,546
15 8S 10E	885,296	40	22,132
16 8S 10E	253,018	33	7,667
Inman East	24,378,896	491	49,651

[1] Cumulative production data from *Petroleum Information Pipeline Production Report*, December 1997.

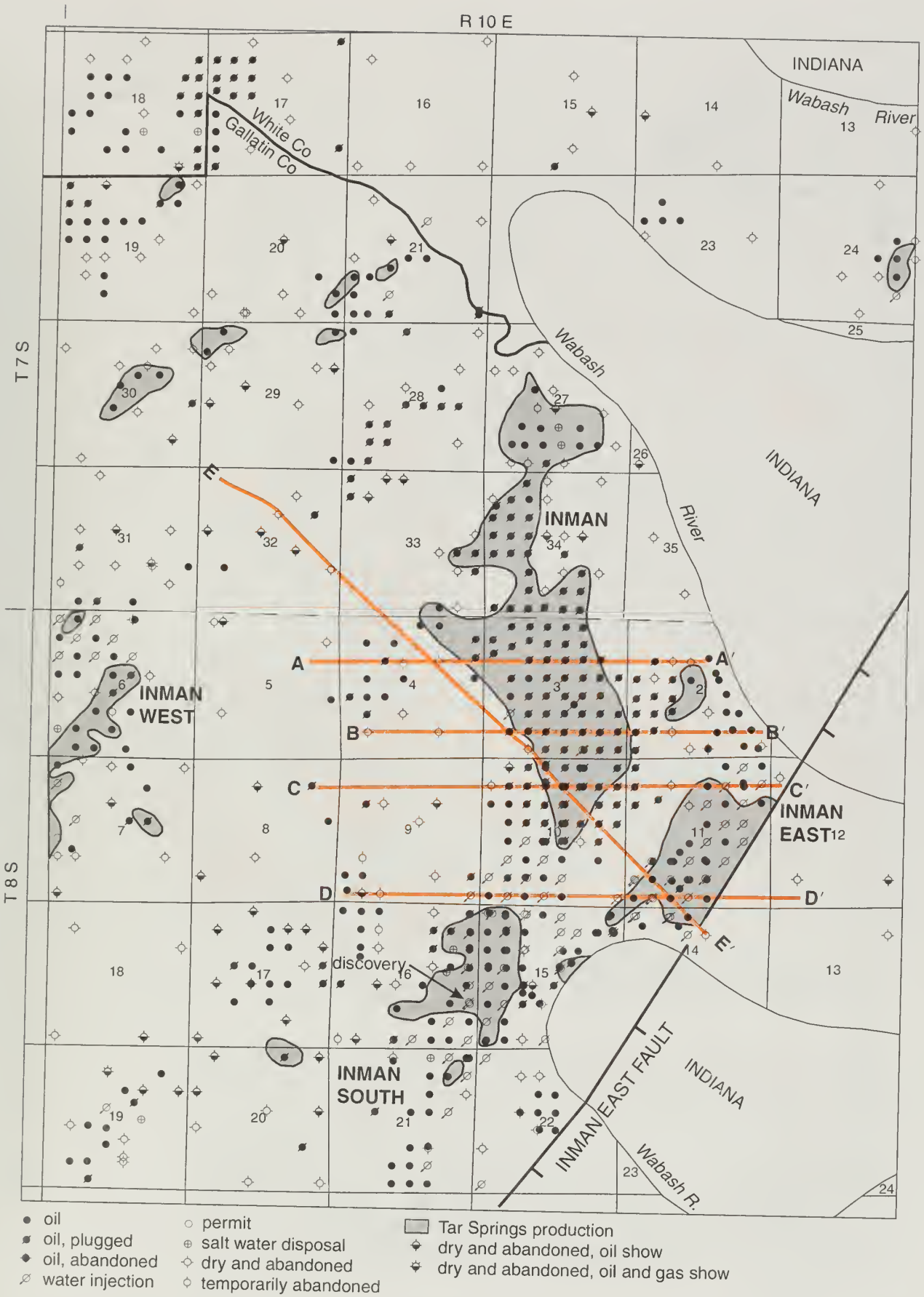

Figure 4 Inman East Consolidated Field index map. Locations of cross sections, faults and the main producing pools, named "Inman," "Inman East" and "Inman South." The Inman West Consolidated Field lies two to three miles to the west. Areas of Tar Springs production are outlined. The Tar Spring Sandstone Field discovery well is located in Sec. 16, T8S, R10E.

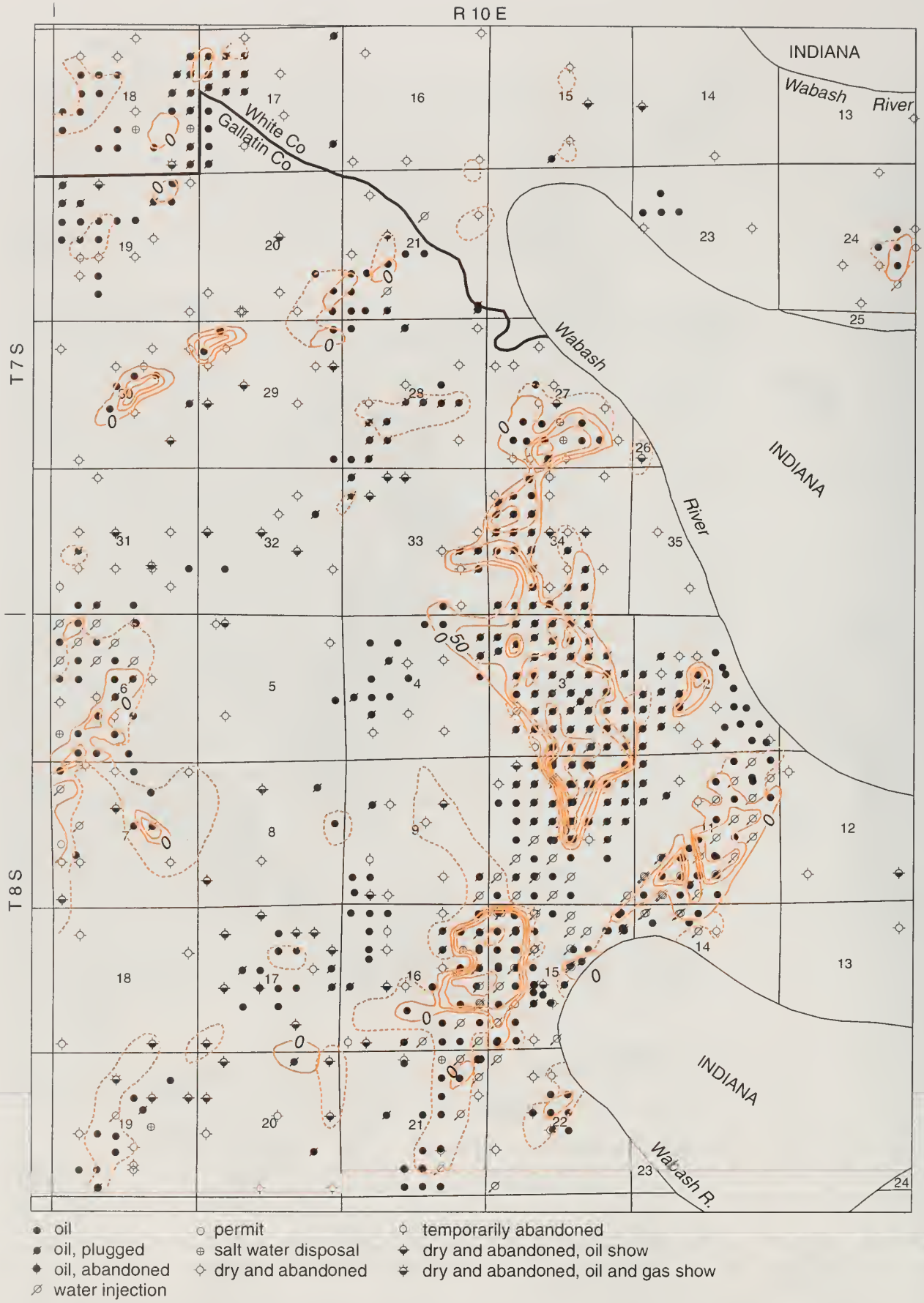

Figure 5 Inman East Consolidated Field initial potential. Rate for wells completed in the Tar Springs Sandstone at Inman East Consolidated Field. Contours indicate "shows" (dotted) and 0, 50, 100, 250 and 500 barrels of oil per day.

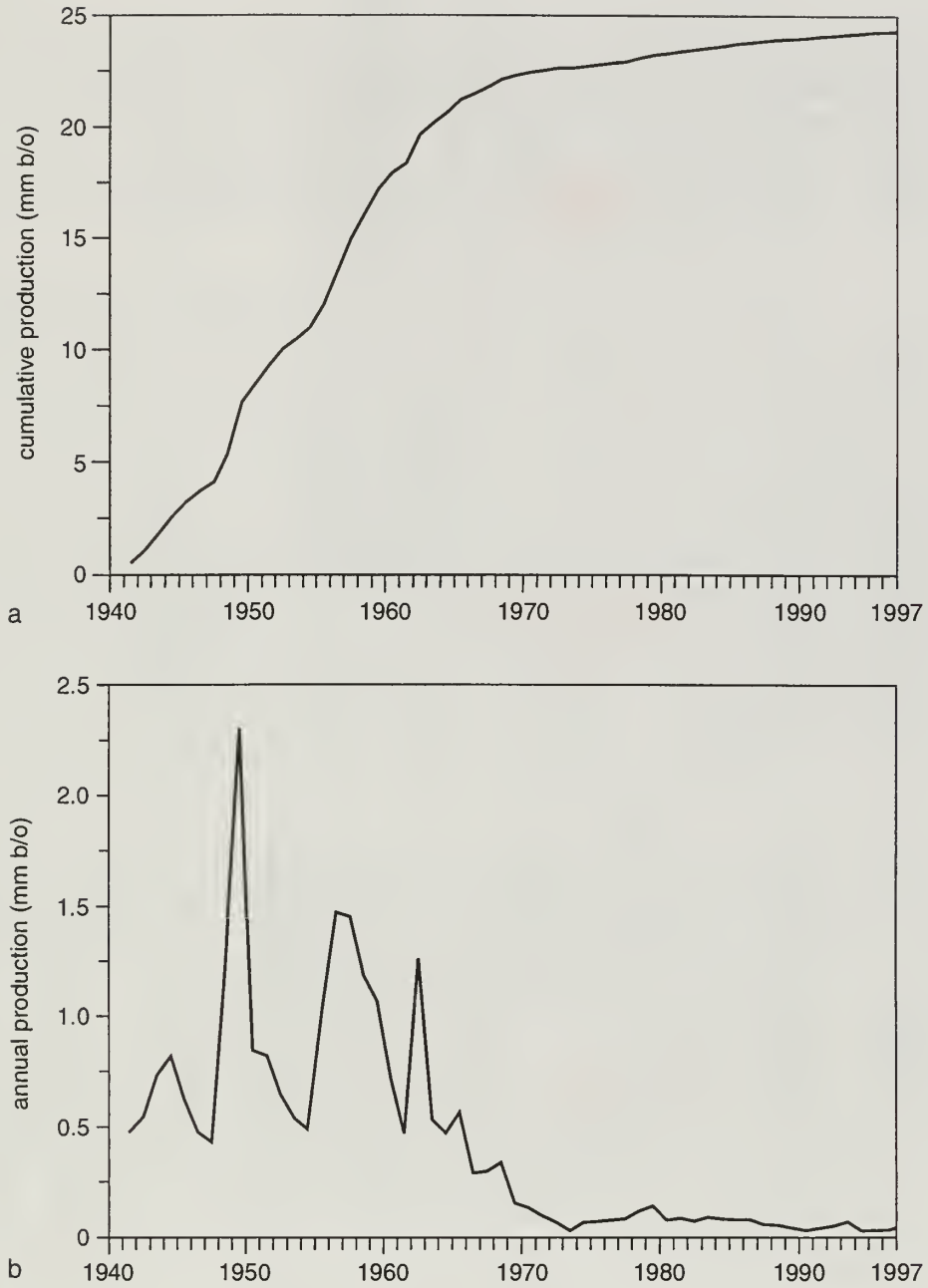

Figure 6 Inman East Consolidated Field production history. This includes (a) cumulative production and (b) annual production, for all producing horizons in the field (data from *Petroleum Information Pipeline Production Reports*—1940 through 1997). mm b/o, million barrels of oil.

Analyses indicate that the oils in the Mississippian reservoirs in White and Gallatin Counties were derived from the Devonian New Albany Shale. The oil apparently migrated vertically along faults of the Wabash Valley Fault System, thus charging many of the Chesterian and lower Pennsylvanian sandstones and limestones in the area with similar oil of about 37 degree API Gravity (Hatch et al. 1991, p. 408). The Tar Springs accumulations were formed by a combination structural-stratigraphic trap.

Typical electric wireline well logs (e-logs)(fig.7) from Inman Field illustrate the variable log and lithologic character of the Tar Springs. The logs also illustrate the character of

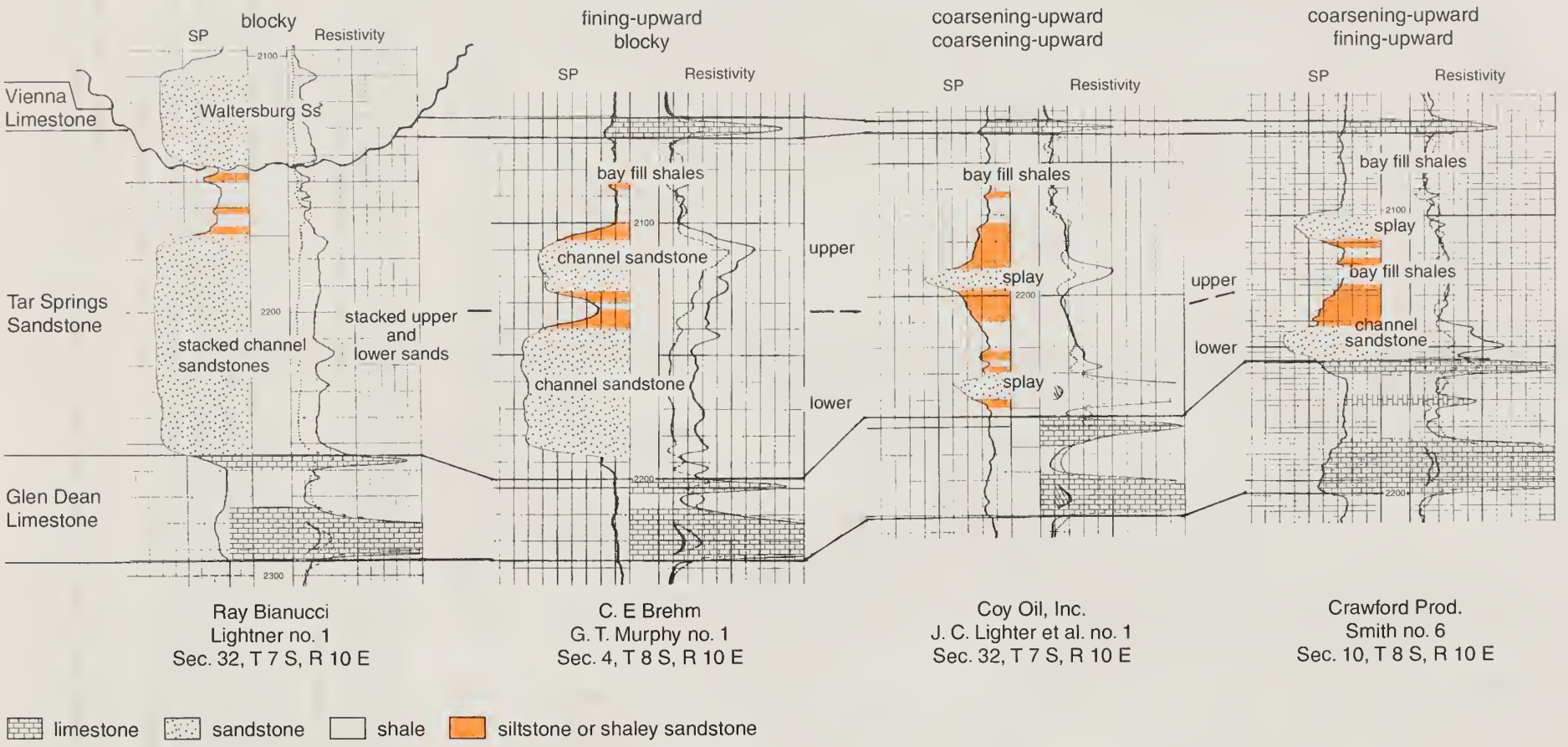

Figure 7 Tar Springs type logs. Typical electric wireline well logs (SP and Resistivity) from Inman East Consolidated Field showing the variable log and lithologic characteristics of the Tar Springs as well as the typical expression of the limestone formations that delimit the top and base of the Tar Springs. Log motifs (fining-upward, coarsening-upward and blocky) are indicated for both the upper and lower parts of the Tar Springs Sandstone.

Typical electric wireline well logs (e-logs)(fig.7) from Inman Field illustrate the variable log and lithologic character of the Tar Springs. The logs also illustrate the character of the limestones of the Vienna and Glen Dean Formations that, respectively, overlie and underlie the Tar Springs and the variations in spontaneous potential (SP) log response in the Tar Springs that were used to help determine depositional environments. Net sandstone and basic lithologies of the Tar Springs were determined from the SP and resistivity log traces.

REGIONAL GEOLOGY

Although the Tar Springs Sandstone is found throughout the southern and central part of the Illinois Basin, its total thickness, net sandstone thickness and continuity indicate it is not a blanket sandstone deposit. The regional maps of the Tar Springs Sandstone formational isopach (base of Vienna Limestone to top of Glen Dean Limestone, fig. 8) and the net sandstone isolith (fig. 9) indicate that the formation ranges in thickness from about 40 feet to more than 150 feet. Areas where the formation is thickest occur in narrow, long, linear, sinuous to branching, very generally north-south-oriented bands (fig. 8) that are generally coincident with the thickest areas on the net sand isolith (fig. 9). These thick intervals of the Tar Springs form bands 1 to 6 miles wide that can be traced up to 150 miles across the Illinois Basin from their subcrop truncations beneath the sub-Pennsylvanian unconformity in the north and northeast to their limits at the outcrop in southern Illinois. Paleocurrents, inferred from cross-bed dip directions along the outcrop belt (cover photo), indicate variable transport directions, but generally are from the north-northeast toward the south-southwest (Potter et al. 1958, p. 1029; Wescott 1982, p. 361).

In Indiana, Shaver et al. (1986) noted that the Tar Springs is primarily shale with thin beds of limestone and scattered lenses of sandstone. However, one local sandstone lens, called the "Tick Ridge Sandstone Member," located south of Taswell in Crawford County, Indiana, is up to 85 feet thick and forms local bluffs. East of Taswell, the thickness of the entire Tar Springs formation increases to 190 feet.

The stratigraphic definition of the Tar Springs in Indiana differs from that used in Illinois. Gray (1978) revised the base of the Tar Springs in Indiana to be the top of the massive Glen Dean Limestone. He notes that in Indiana, unlike in Illinois, there are many intervals with shale and limestone stringers throughout the Tar Springs. The Vienna Limestone is found in Indiana and, as in Illinois, its base marks the top of the Tar Springs. In Illinois, the top of the Glen Dean is put at the limits of "well-defined" limestone strata (Willman et al. 1975). In the present study, limestone and shale beds found just above the massive, lower Glen Dean limestone interval but below the first Tar Springs sandstone bed are considered to be in the upper part of the Glen Dean Limestone.

Grote's (1949) subsurface study of more than 5,800 Tar Springs well records, logs and some cores in Hamilton, White and parts of Gallatin and Saline Counties in southeastern Illinois found that lithologic correlations could only be made for short distances and, in general, that the Tar Springs was more sandy at its base with increasing amounts of shaley sand and shale upwards. His cross sections document a basal erosional contact with the Glen Dean Limestone. He found that the thickness of the Tar Springs Sandstone ranged from 48 to 158 feet and was thickest where the basal sandstone was in direct contact with the Glen Dean Limestone. He further interpreted the upper contact with the Vienna Limestone to be conformable. The percentage of sandstone in the Tar Springs ranged from 0 to nearly 100%. Grote did not find any marine fossils in the Tar Springs shales or sandstone. Wescott (1976, 1982), however, identified numerous marine trace fossils and molds of brachiopods, crinoids and bryozoans in outcrops at the Coles Mill section near Chester in Randolph County, Illinois, 50 to 60 miles west of Grote's study area.

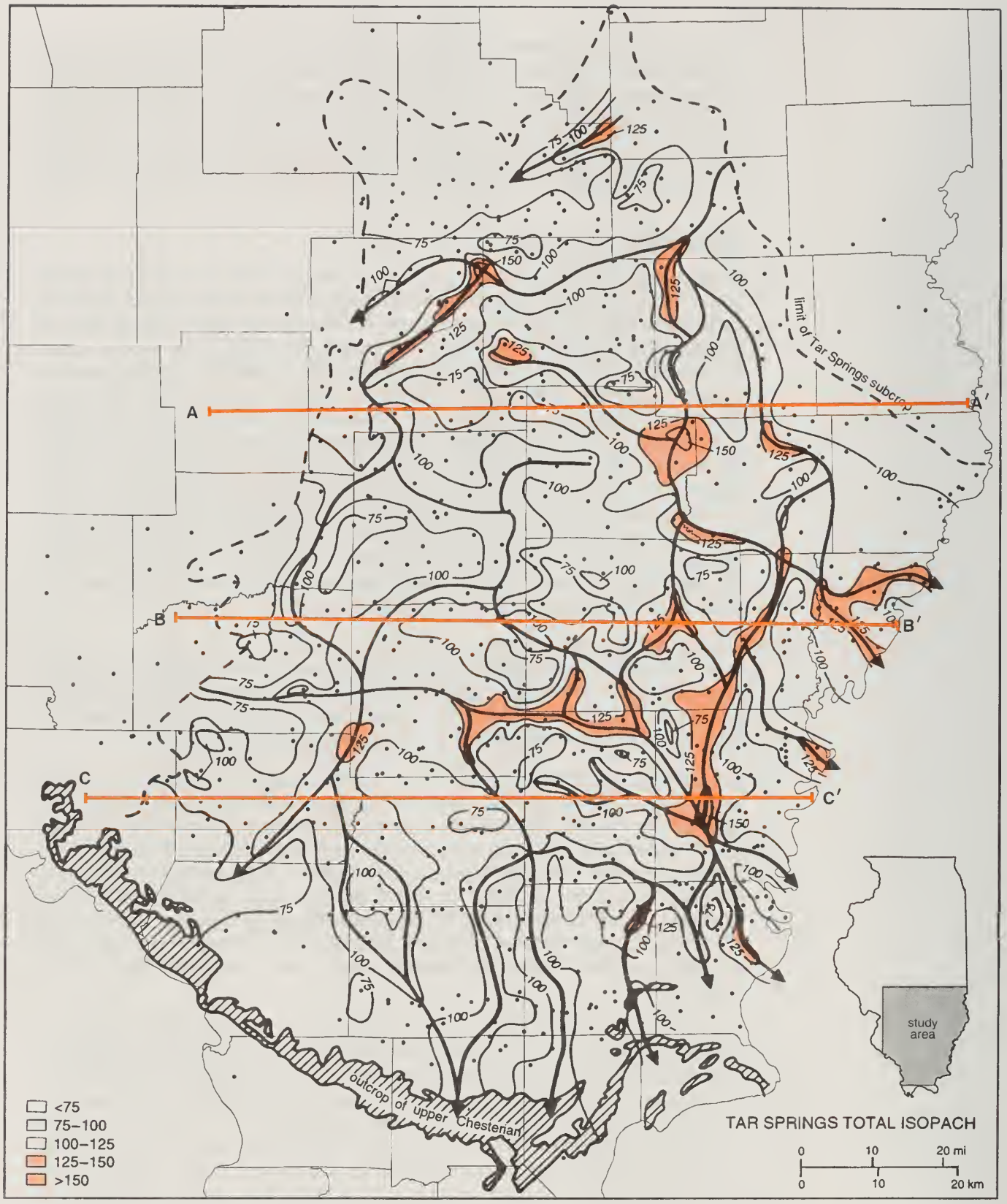

Figure 8 Regional isopach map of the Tar Springs Sandstone. Outcrop zone in southern Illinois has diagonal hachures. The subcrop limit of the Tar Springs beneath the basal sub-Pennsylvanian unconformity is delineated with a dashed line. Axes of areas of thick Tar Springs Formation are shown with bold lines, and the inferred paleotransport direction is indicated by the arrowheads. The locations of the cross sections shown in figure 10 are indicated. The approximately 800 wells used to construct this map are indicated by dots. Contour interval is 25 feet.

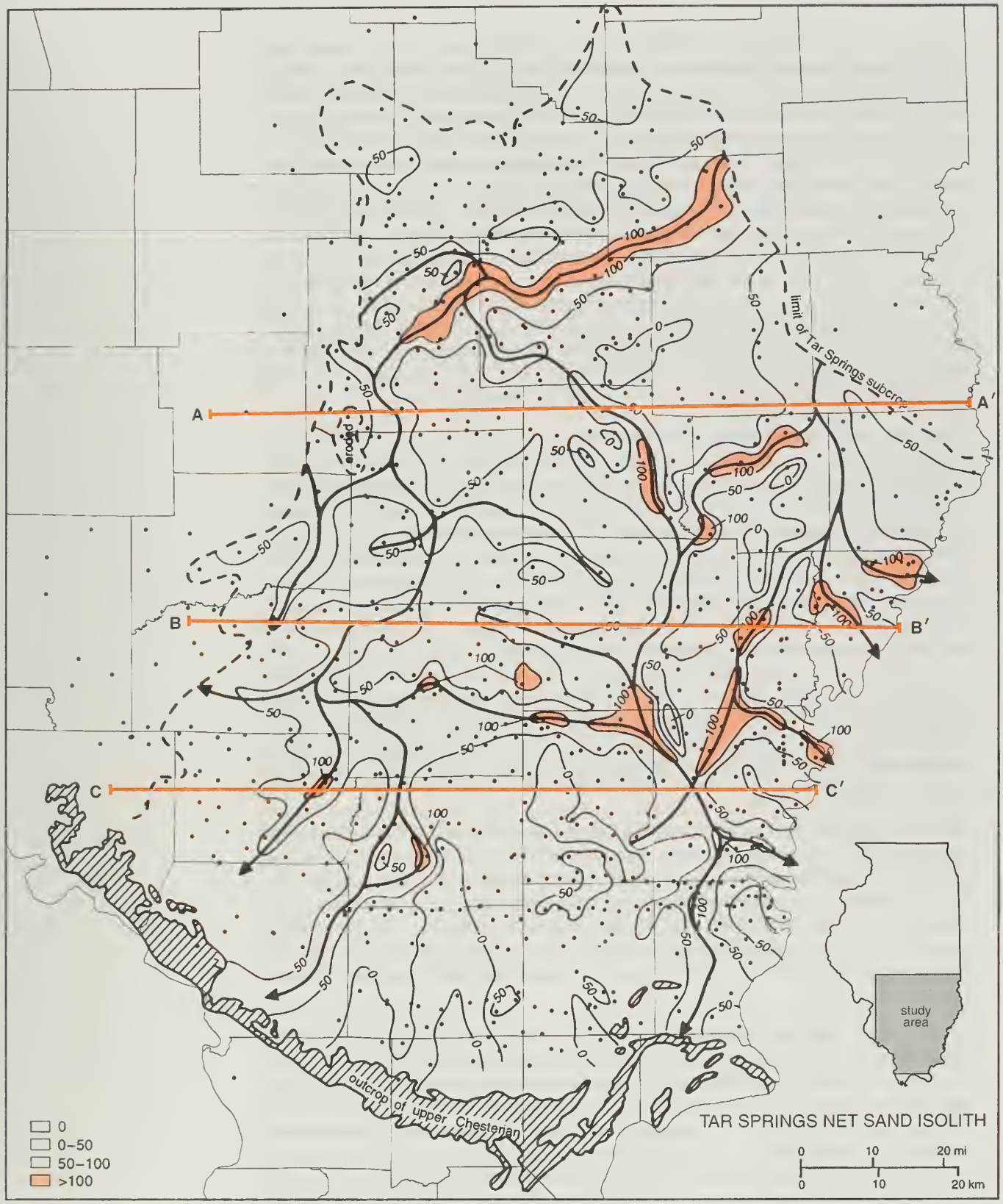

Figure 9 Regional Tar Springs net sandstone isolith. Outcrop in southern Illinois has diagonal hachures. The subcrop limit of the Tar Springs beneath the basal sub-Pennsylvanian unconformity is delineated with a dashed line. Axes of areas of thick Tar Springs sandstone are shown with bold lines and the inferred paleotransport direction is indicated by the arrowheads. The locations of the cross sections shown in figure 10 are indicated. The approximately 800 wells used to construct this map are indicated by dots. Contour interval is 50 feet.

A series of east-west regional stratigraphic cross sections across the Illinois Basin (fig. 10) illustrate the continuity and variation in the Tar Springs lithologies. These sections are oriented roughly perpendicular to the paleoflow directions of the Tar Springs and extend from the subcrop pinchout below the sub-Pennsylvanian unconformity in the west to the eastern Illinois state border along the Wabash River. The cross sections are hung on the base of the Vienna Limestone and extend to the base of the Glen Dean Limestone. Basic lithologies (clean sandstone, siltstone or shaley sandstone, shale and limestone) were identified by SP and Resistivity log character. Clean sandstone includes the intervals with 75% to 100% of the SP deflection of a typical clean, water-bearing sandstone; siltstone or shaley sandstone includes intervals with 25% to 75% of the SP deflection of a clean sand; and shale includes intervals that range from the shale baseline to 25% deflection. The shale baseline is the typical low SP response value generated by thick clean shales located within a few hundred vertical feet of the Tar Springs. Limestone was identified from the low SP deflection coupled with a high Resistivity value. Sandstone bodies were subdivided within the sandstone interval where thin, minor SP deviations occur.

The cross sections show that individual sandstone units range in thickness from a few feet to more than 70 feet. Up to five or six sandstone bodies, each 5 to 15 feet thick and separated by a thin interval of shale, may be stacked in some wells. Thick sandstone bodies also may be composites of multiple beds that lack shale breaks or where shale breaks were not discernible in SP logs. Where sandstone bodies occur right at the base of the Tar Springs, they commonly replace limestone and shale intervals of the upper part of the Glen Dean Limestone, which suggests that they filled channels scoured into the Glen Dean. Locally, over a distance of just a few miles, up to 40 feet of the Glen Dean have been removed. Although the lower half of the Tar Springs appears to contain more sandstone than the upper half, no clearly identifiable shale marker could be identified to regionally divide the Tar Springs into an upper and a lower member. Areas on the regional net sand isopach with high values are commonly composed of clusters of composite or stacked sandstone bodies, which in aggregate may be up to 6 or 8 miles wide. Siltstone or shaley sandstone bodies, commonly 5 to 12 feet thick, may be laterally correlative to clean sandstone bodies.

The log motif of the sandstone bodies near Inman East Consolidated Field is examined in more detail in the next section, but, in general, includes primarily sandstone bodies with bases defined by sharp upward transitions from shale into the clean sandstone. Less common are sandstone bodies that have progressively cleaner sandstone upward. The top contacts of the sandstone bodies most commonly have gradational upward transitions into more silty or shaley strata. Thus, the sandstone bodies typically have sharp bases and fine upward; less common are those thinner sandstone bodies that coarsen upward.

Wescott (1976, 1982) interpreted the Tar Springs Sandstone along its southern outcrop belt to have been deposited as a progradational sequence in a variety of lateral environments, including fluvial-deltaic, shoreface-foreshore and tidal flat settings. Marine processes varied from wave dominated in the southeast to tide dominated in the southwestern parts of the outcrop belt. Fluvial deltaic facies include fluvial channels, prodelta-distal bar, interdistributary bay, upper delta plain overbank deposits and delta destructional bars. Shore face-foreshore facies include widely abundant gray, parallel laminated mudstones formed in the prodelta; thick, bluff-forming, parallel laminated and hummocky cross-bedded sands of the mouthbar and shoreface; and parallel laminated and low-angle cross-bedded sandstone of the foreshore. Tidal flat and tidally influenced sands include herrringbone crossbedded sands, flaser and lenticular beds, mudcracks and reactivation surfaces. In the western part of the

outcrop belt at the Coles Mill section, a trace fossil assemblage in the uppermost six inches of the Tar Springs, diagnostic of the *Skolithos* ichnofacies (Seilacher 1967, 1978), indicates deposition in a sandy litoral environment where the substrate is frequently reworked by waves or tidal currents. At the same locality, Wescott (1976) also reported fine-grained sandstone units near the top of the Tar Springs with flaser and wavy bedding, load casts, clay intraclasts, macerated plant fragments, parting lineation, thin shale parting laminae, bi-directional cross-bedding and mud cracks, all of which are indicative of tidal flat, tidal channel and tidal levee deposition. Thin coal seams found in the central and eastern part of the outcrop belt (Workman 1940, Swann 1963, Devera 1991) indicate both sub-aerial exposure and the existence of local swamps on an alluvial or delta plain at the top of the Tar Springs.

The regional pattern of sand deposition shown in figures 9 and 10 suggests that the major sandstone bodies of the Tar Springs were deposits that filled channels scoured into pre-existing prodelta or underlying Glen Dean Limestone deposits. The channels may become filled with shale if abandoned, a situation illustrated on figure 10 A–A′ at township 6E, where the upper Glen Dean limestones are missing and a thick shale overlies the lower Glen Dean limestone bed. The presence of a series of channel sandstone bodies in 6-mile-wide bands and the lack of channel sandstone between the bands suggests the Tar Springs channel deposits may have become amalgamated. The entire depositional system is highly variable laterally, suggesting periodic lobe switching or channel avulsing to produce new sets of stacked channels (see fig. 10). The paths of these channel systems form an interweaving network of thick channel sandstones with siltstone, interbedded sandstone and shale, and pure shale deposited in areas between these channels (see figs. 8 and 9). This type of depositional system is typical of a river-dominated deltaic system (Coleman and Gagliano 1965, Coleman 1976, Coleman and Prior 1982) with tidal influence (Allen et al. 1979, Kvale and Archer 1990).

When applied to the Tar Springs, the typical modern analogue model for river-dominated deltaic deposition, the modern Mississippi River "bird-foot" delta, has to be modified to reflect deposition in a shallow cratonic sea where little accommodation space is created for clastic deposition. Furthermore, the model has to allow periodic cessation of clastics deposition and the formation of shallow marine limestones such as the Glen Dean and the Vienna. The model should be able to explain the presence of the tidally influenced deposition interpreted from outcrop exposures at Alto Pass and reported from the Tar Springs in Indiana (Kvale, personal communication). Lastly, the model should support deposition of long sinuous sandstone bodies that traverse roughly north to south across the length of the Illinois Basin. Thus, a mixed fluvial-tidal delta may be a better regional model for the Tar Springs depositional system than the modern Mississippi River delta system.

An analogue for such a system that includes more tidal influence is the modern Mahakam River delta on the east coast of the Indonesian island of Kalamantan, a mixed, fluvial-tidal delta (Allen et al. 1979, Kvale and Archer 1990). The Mahakam delta is located in the tropics, as was Illinois when the Illinois Basin was located at 6 to 8° south paleolatitude in Chesterian time (Lavin, p. 344, 1991). The Mahakam has low wave energy. Tidal amplitudes range annually from less than 3 feet in neap tides to 9 feet in extreme spring tides. Interdistributaries are about 6 to 9 miles wide between channels and are dominated by subtidal to intertidal mud-rich deposits. Small-scale tidal channels are rare. Planar bedding with flaser to lenticularly bedded sands and abundant muds are the primary bedding type on the interdistributary intertidal to subtidal flats. Faunas are restricted and bioturbation is minimal, probably because the tidal creeks are hyposaline, or fresh, due to abundant tropical rainfall. Major distributary channels contain cross-bedded and ripple-bedded sand deposits up to 30 feet thick and are generally fluvially dominated.

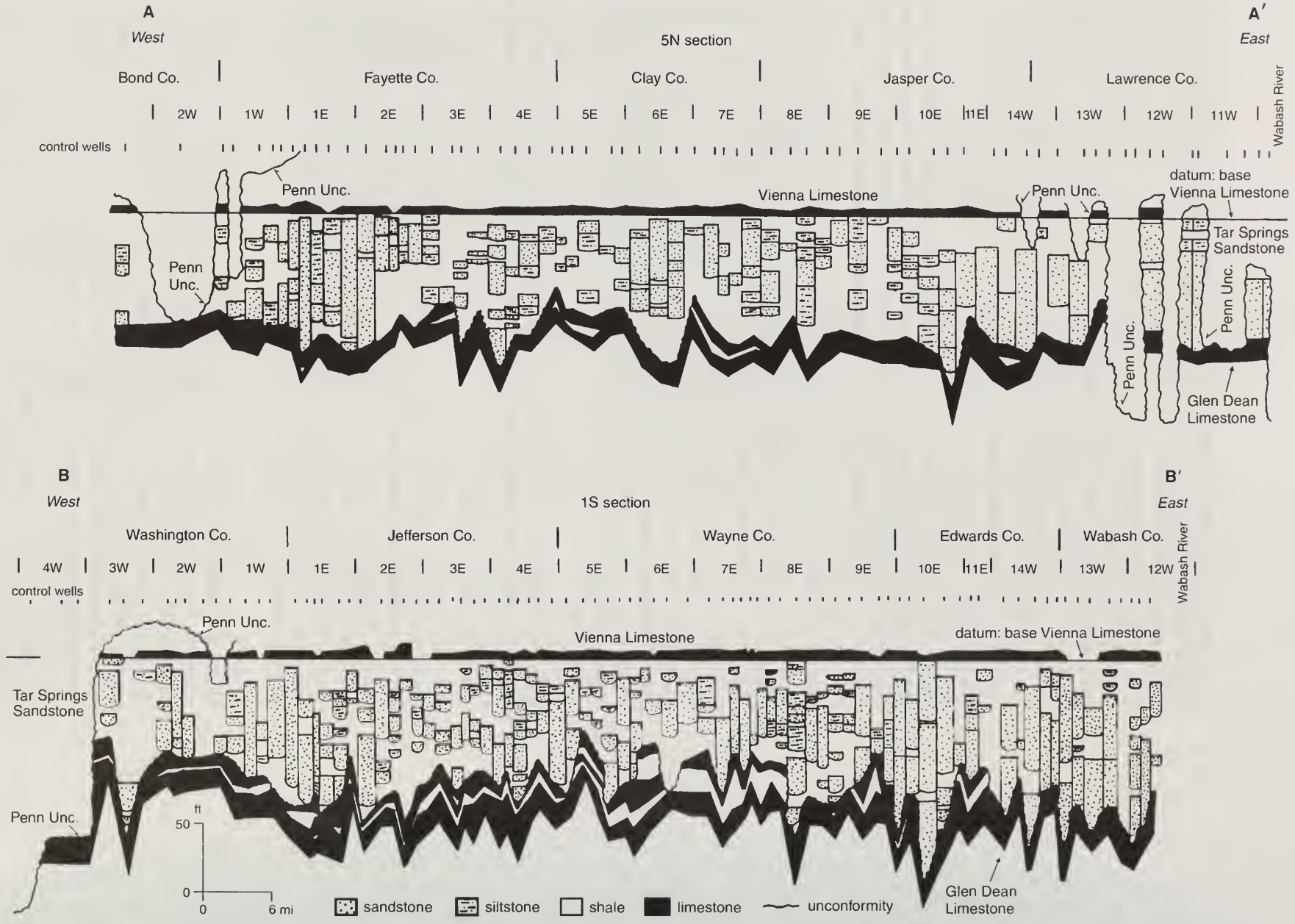
A
West
5N section
A′
East
Bond Co.
Fayette Co.
Clay Co.
Jasper Co.
Lawrence Co.
Wabash River
2W
1W
1E
2E
3E
4E
5E
6E
7E
8E
9E
10E
11E
14W
13W
12W
11W
control wells
Penn Unc.
Vienna Limestone
Penn Unc.
datum: base Vienna Limestone
Penn Unc.
Tar Springs Sandstone
Penn Unc.
Penn Unc.
Penn Unc.
Glen Dean Limestone
B
West
1S section
B′
East
Washington Co.
Jefferson Co.
Wayne Co.
Edwards Co.
Wabash Co.
Wabash River
4W
3W
2W
1W
1E
2E
3E
4E
5E
6E
7E
8E
9E
10E
11E
14W
13W
12W
control wells
Penn Unc.
Vienna Limestone
datum: base Vienna Limestone
Tar Springs Sandstone
Penn Unc.
ft
50
0
0
6 mi
sandstone
siltstone
shale
limestone
unconformity
Glen Dean Limestone

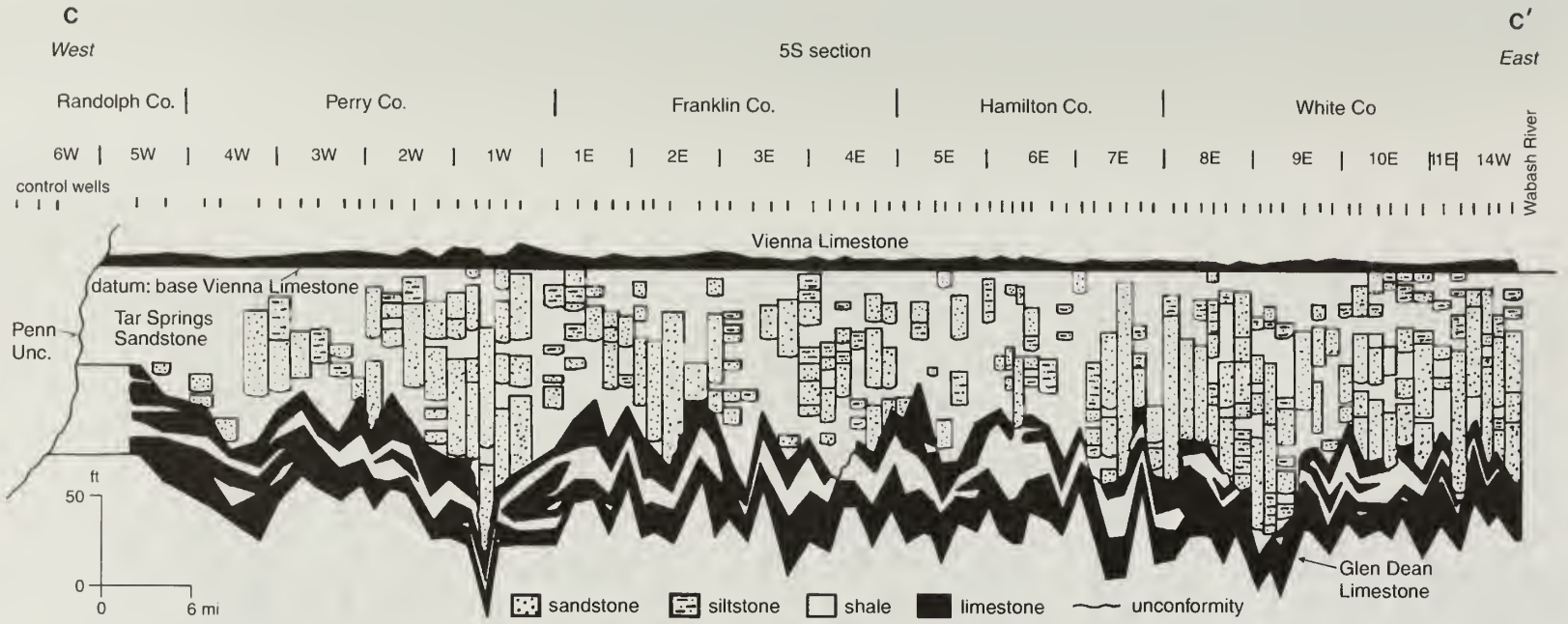

Figure 10 East-west regional stratigraphic cross-sections of the Tar Springs Sandstone (see figure 9 for location). The base of the Vienna Limestone is the datum. The Glen Dean Limestone thickens to the south. Its wavy appearance is probably due to both differential compaction of the Tar Springs and the extreme vertical exaggeration of the sections. A-A′, Section along the Five North Township line shows thick sandstone accumulations centered around T1E, T6E and T14W. B-B′, Section along the One South Township line shows thick sandstones are centered around T1W, T10E and T13W. C-C′, Section along the Five South Township line shows thick sands centered around T1W, T2E, T8-9E and T 14W. Note that marker beds in the Upper Glen Dean Limestone are absent in local areas where the sandstone is thick. These areas reflect scouring by the Tar Springs channels.

To form the clean, bioclastic-rich limestones of the Glen Dean and the Vienna requires clear, oxygenated, unrestricted sea water and the absence of active clastic sedimentation that would typify a delta. A rise in sea level or an avulsion of the channel system to a location several hundred miles away, as suggested by Swann (1964), could clarify the water and permit limestone to form. The rise in sea level moves the erosional base level landward (northward) on the craton, and thus the Illinois Basin becomes less proximal to siliciclastic sediments formed by erosion on the exposed craton. Swann (1964) suggests a rise in sea level would shift the shoreline more than 600 miles and shift the deltaic depo-center a similar distance. There is, however, no comparable sedimentary record in Canada to confirm this hypothesis. These processes temporarily would reduce the ability of the river system to transport clastics far out onto the shelf, thus creating conditions favorable for carbonate deposition. With time, the accommodation space created by this rise would be filled with prograding clastics of the next parasequence (i.e., the Tar Springs Sandstone after the Glen Dean or the Waltersburg Formation after the Vienna).

INMAN EAST CONSOLIDATED FIELD

A detailed examination of the Tar Springs Sandstone at the Inman East Consolidated Field, where it is one of the important oil-producing horizons, will provide additional characteristics about the log character, sedimentology, petrography, trapping mechanism, petrophysical properties and production history of this reservoir sandstone.

The map of initial potential for wells completed in the Tar Springs (fig. 5) outlines the three productive areas of the field and the defined local study area for this paper. The three productive pools or compartments are referred to as the "Inman," "Inman East" and "Inman South" compartments (fig. 4). To the west of the study area is another Tar Springs producing area called "Inman West Consolidated Field." Inman East Consolidated Field was intensely drilled on a 10-acre spacing after its 1940 discovery in the Tar Springs. Development of other reservoir formations followed. The Tar Springs initial potential ranged from a few to 1,200 barrels per day, with a typical producer having 100 to 250 barrels per day initial potential. Boundaries of the producing areas are sharp and well-defined by the stratigraphy and structure.

Log Character and Sandstone Distribution

The SP-Resistivity log character of the Tar Springs Sandstone is highly variable from well to well and reflects the variation in lithology that plays an important role in the formation of the Inman reservoirs. The four example logs shown in figure 7 have distinctive shapes or patterns, particularly in the SP log; these signatures include blocky-shaped logs, coarsening-upward logs and fining-upward logs.

Sandstones with blocky logs (fig. 7, Lightner no. 1 and G.T. Murphy no. 1) have abrupt shifts to negative SP values at their base and then sharply return to more positive SP values at the top of the sandstone. Logs with this signature correspond lithologically with clean sandstone beds that have sharp basal lithologic contacts with the underlying shale, siltstone or limestone. The upper sandstone contact is relatively sharp, but typically is gradational over a few feet to overlying silt or shale. Within the blocky sandstones are thin zones with slight increases or breaks in the SP value that reflect the presence of thin siltstone or shale beds. Intervals with the blocky motif are generally interpreted as channel sandstone deposits. The shale breaks delineate separate channel sandstones in a stacked channel sequence.

Fining-upward log patterns (fig. 7, G.T. Murphy no. 1 and Smith no. 6) are similar to blocky patterns except that the transition to more positive SP values at the top of the sandstone occurs over a thicker interval. This upward transition reflects the presence of thinly interbedded sandstone and siltstone or shale that becomes predominantly siltstone and shale upward. This motif is also interpreted as a channel sandstone, where overbank or tidal flat fines are preserved at the top.

Coarsening-upward log patterns (fig. 7, J. C. Lightner et al. no. 1 and Smith no. 6) show a gradational upward progression from shales and siltstones to the more negative SP sandstones. The sandstones are typically thinner and less clean than the blocky or fining-upward motif sandstones. The sandstones with this log motif are interpreted as open shelf or distributary mouth bars or crevasse splay deposits.

Siltstones and shales have SP responses that deflect to the right (positive) relative to clean sandstones. Shales typically have SP values along a baseline to the right (more positive) on the log, as at the top of the Tar Springs Sandstone in the Murphy no. 1 well on figure 7. Siltstones or interbedded sandstone and shale intervals (colored orange on figure 7) have values a few SP units to the left (negative) from this baseline.

Net thickness of sandstone was measured from the SP logs. An interval was considered sandstone when its negative SP value exceeded the 75% SP value between the shale baseline and clean sandstone. Good examples of sandstone occur in the Lightner no. 1 and Murphy no. 1 wells on figure 7. When sandstone overlies limestone, as was commonly the case at the basal Tar Springs contact with the Glen Dean Limestone, the inflection point in the resistivity curve was used to separate the sandstone from the limestone (fig. 7). In some wells, the sandstone intervals had both a negative or "sand" SP value and a moderate Resistivity. This occurred where the sandstones were oil saturated or where the sandstone was cemented with carbonate, as at the base of the Tar Springs. The SP values in an oil-bearing interval may be depressed slightly more positive than those normally seen in clean sandstone, but were included in the net sand calculations because they exceeded the 75% SP cutoff.

In Inman East Consolidated Field, the Tar Springs Sandstone was commonly divisible into an upper and lower sandstone member about midway through the formation as shown in figure 7. Maps of these two divisions were prepared because the individual members had distinct and overlapping geometries and trapping configuration and were deposited at different times. These members merged in the thick, stacked sandstones of some wells. For mapping purposes, the division into upper and lower in these stacked sandstone channels was chosen where a subtle break in the SP log was detected near the middle of the formation. Where massive sandstones were present, the division between upper and lower was arbitrarily chosen near the mid-point in the formation.

The Upper Tar Springs is the prime reservoir interval at Inman East Consolidated Field. Two maps were made from the log data for this interval: a net sandstone thickness (fig. 11) and a sandstone log character map (fig. 12). Both of these maps illustrate the heterogeneity of this unit. The net sandstone thickness of the Upper Tar Springs varies from 0 to more than 40 feet in the study area. Each of the three main producing compartments (Inman, Inman East and Inman South) contain thick, clean sandstones, but they are constrained laterally by areas with very thin sandstones or no sandstone. The limits of clean sandstone correspond to the edges of the productive compartments. Thick unproductive sandstone intervals in the study area also occur to the southwest (e.g. Sec. 17, T8S, R10W), but are not surrounded by potential sealing, non-sand strata. Thus, the presence of seals and clean, oil-bearing sand in close lateral proximity indicate that stratigraphic trapping played a role in this field.

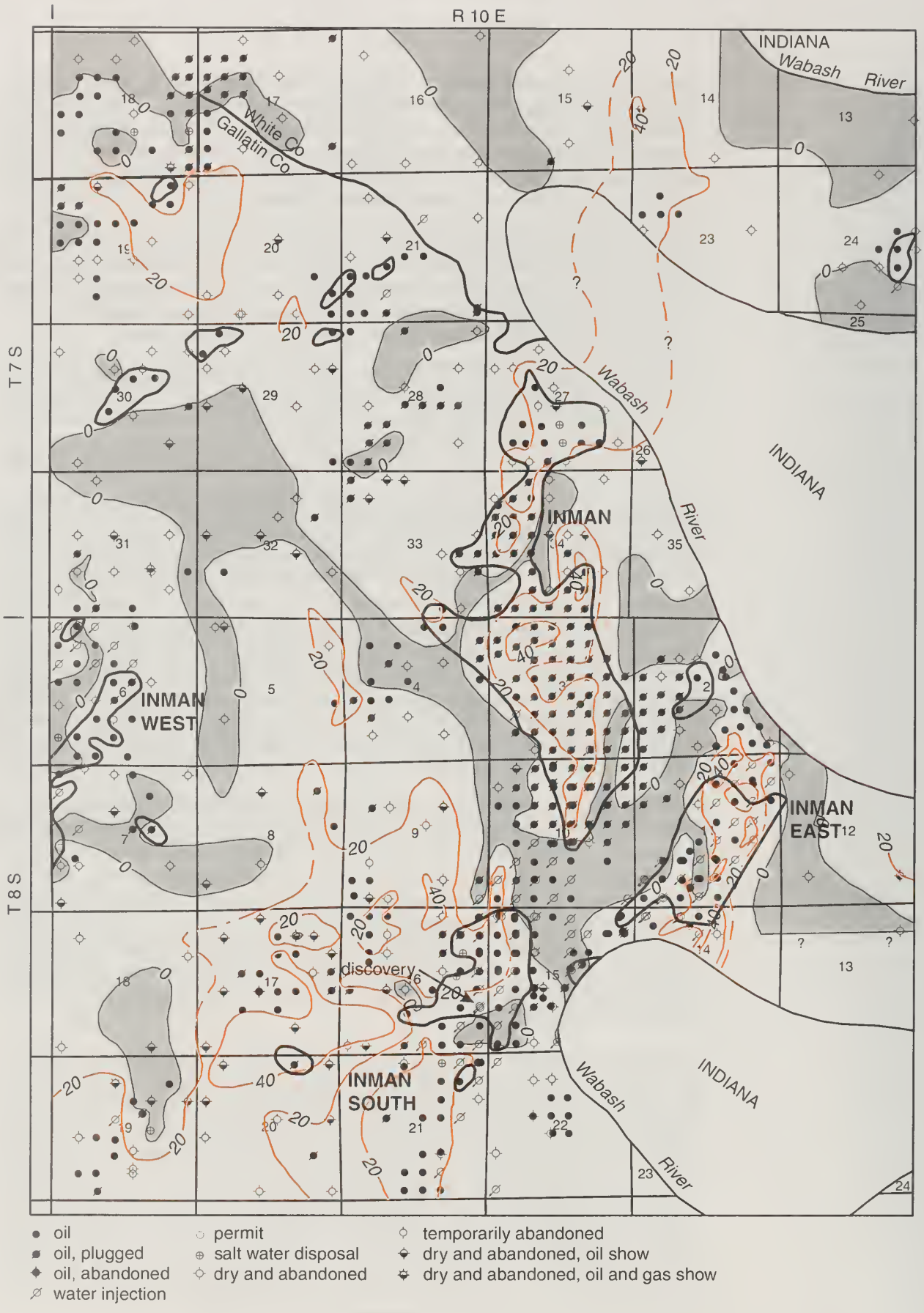

Figure 11 Upper Tar Springs net sandstone isolith at Inman East Consolidated Field. Areas with no sandstone (shaded) are particularly important in the stratigraphic trapping component of the Inman pool, which is centered in Sec. 3, T8S, R10E. Contour interval is 20 feet. Areas of Tar Springs production are enclosed by heavy black lines.

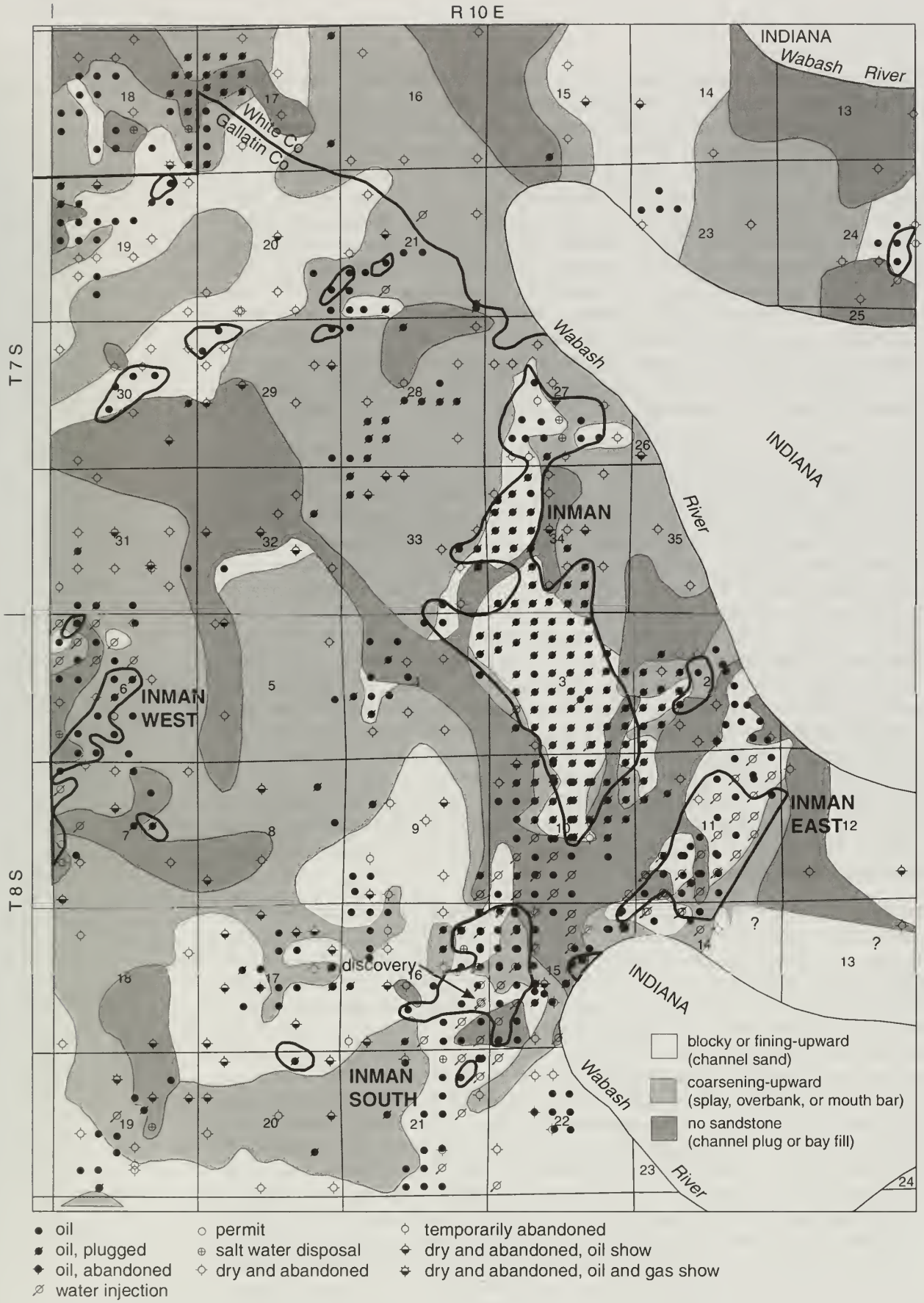

Figure 12 Upper Tar Springs log character map at Inman East Consolidated Field. Areas with blocky and fining-upward SP log character are separated from areas with coarsening-upward logs or areas with no sandstone. The reservoir sandstones at each of the three pools in Inman East Consolidated Field show blocky or fining-upward e-log motifs. Areas of Tar Springs production are enclosed by heavy black lines.

The map of the log character of the Upper Tar Springs Sandstone also helps to define or characterize the producing areas. The distribution of three log characteristics is plotted in figure 12. The first includes areas with either blocky or fining-upward log motifs. These two motifs were combined on the map because both could be formed by channels and have sharply defined bases, but only vary in the thickness of their overlapping fine-grained deposits. Areas with this motif included all the thick sandstones, all the areas of significant production and some areas without production. The second motif includes all sandstones with coarsening-upward e-log profiles. These occur in areas where the net clean sandstone is 25 feet or less, commonly only 10 to 15 feet. These sandstones typically have not developed as low (clean) an SP value as the blocky or fining-upward sandstones, which indicate that they contain more interbedded or intermixed siltstone and shale, and they do *not* form hydrocarbon reservoirs, even where they occur adjacent to productive blocky sandstone in an area of closure. The last motif plotted in figure 12 is the interval that consists of siltstone or shale with no net sandstone. These areas provide potential sealing strata.

The net sandstone isolith (fig. 11) and the log character (fig. 12) maps indicate that the three producing compartments at Inman East Consolidated Field are elongate, sharp-based, clean sandstone bodies, one-half to one mile wide and up to two miles long, which are largely surrounded by areas with no sandstone. Based on their blocky and fining-upward log motif and the purity of the sandstone, as indicated by their low SP values, the producing sandstones are interpreted to be fluvial, delta distributary or tidal channel sands. The fact that the blocky sandstones may be stacked one on top of another does not eliminate either of the two channel types. The areas with shale and/or siltstone adjacent to the producing fields provide seals, and some have the same width and curving outline as the channel sandstones, which suggests they may have formed as silt and clay-filled channel plugs. Thus, they could form by fluvial channel avulsing, delta lobe switching or tidal channel abandonment. The coarsening-upward sandstones were formed in an environment where energy increased up-section as the depositional package thickened. Shallow marine shoal bars, tidal bars, distributary mouth bars or crevasse splays would all form this e-log motif. The proximity to channel deposits precludes offshore, shallow marine bars, but ebb or flood tidal bars, distributary mouth bars or crevasse splays remain a likely depositional setting. Examination of the lower Tar Springs member provided some additional evidence for the depositional setting.

The lower part of the Tar Springs is considerably more sandy than the upper, but has a similar log character motif and sand body distribution. The net sandstone isolith map (fig. 13) shows that the sandstone in the lower part is more widespread, but highly variable in thickness—from a trace to more than 80 feet. Thick sandstones form curving bands that are typically about a mile in width and extend across the map. The regional map of net sandstone thickness (fig. 9) indicates that thick sandstone trends extend for tens of miles to the north and south of Inman East Consolidated Field. The major, non-producing, thick sandstone on the Inman East Consolidated Field map (fig. 13), which trends approximately north-south to the west of the producing Tar Springs compartments, is cut by an east-west–oriented thin sand body with a coarsening-upward log character (fig. 14). At the three Inman Field pools, the Lower Tar Springs sand is 60 feet thick or less, more typically about 10 to 30 feet thick, with a log motif that may be either blocky/fining-upward or coarsening-upward. Because the Tar Springs is not fully charged with hydrocarbons here, these sandstones, which have good porosity and permeability, are not productive. The SP logs in thicker sandstones may have deflections indicating shale breaks that separate 10- to 20-foot thick individual sandstone beds. Immediately to the east of Inman Field is an area with only siltstone and shale. The siltstone beds in this zone have a coarsening-upward log motif and are interpreted as a clay plug formed in an abandoned

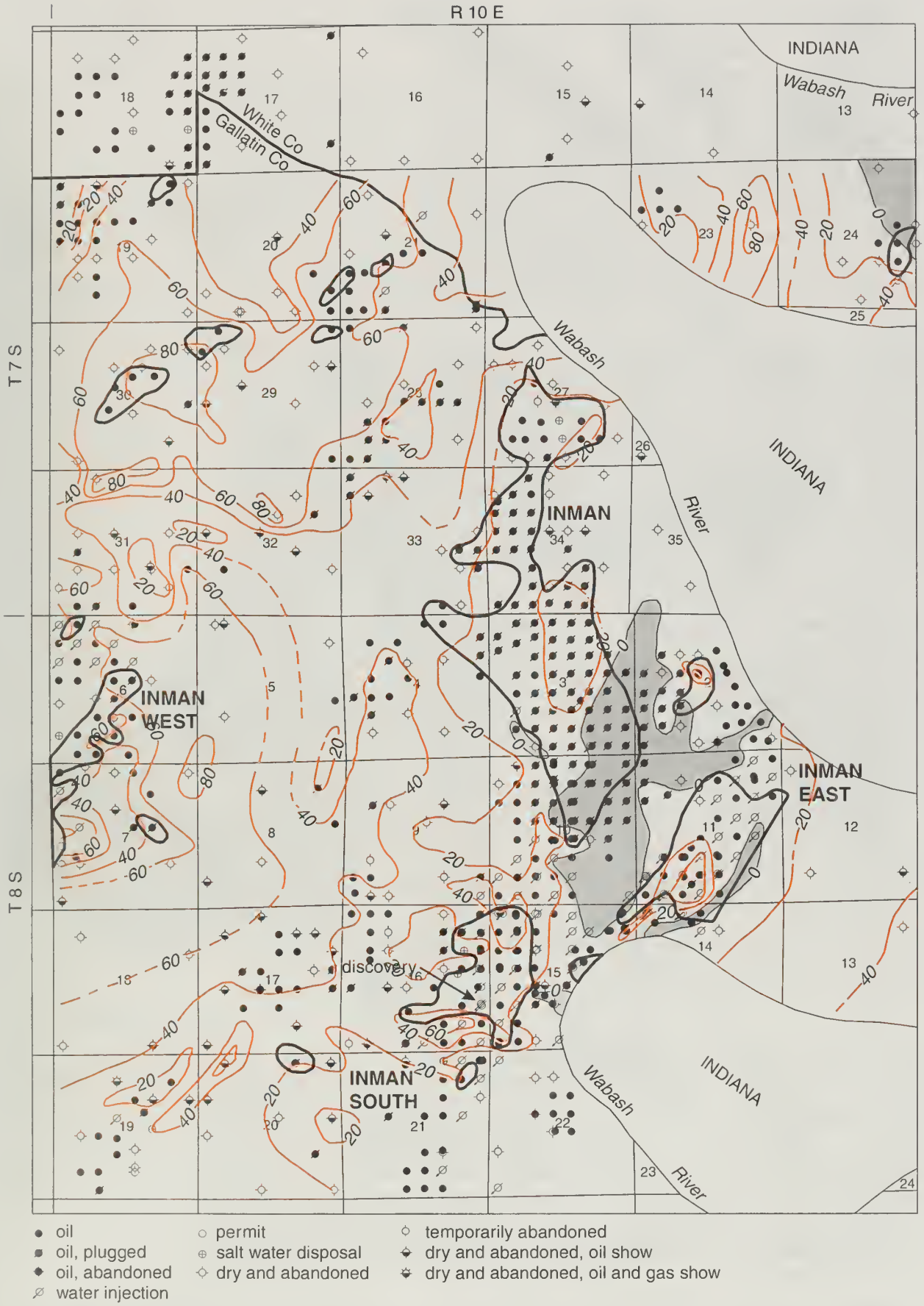

Figure 13 Lower Tar Springs net sandstone isolith at Inman East Consolidated Field. Areas with no sandstone (shaded) are important in the stratigraphic trapping component of the Lower Tar Springs. This lower sandstone is thicker and more widespread than the Upper Tar Springs at Inman East Consolidated Field. Areas of Tar Springs production are enclosed by heavy black lines.

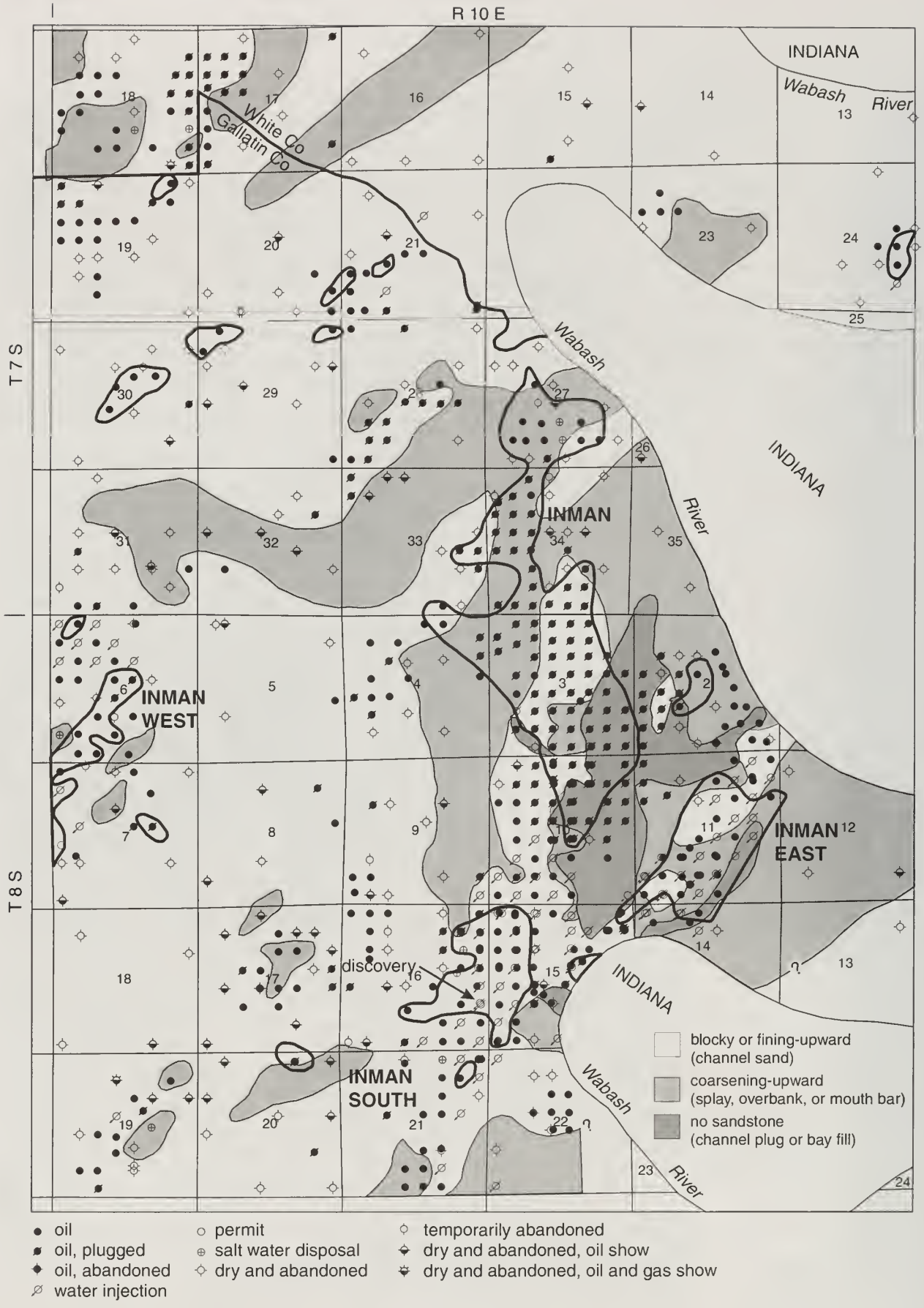

Figure 14 Lower Tar Springs log character map at Inman East Consolidated Field. Areas with blocky and fining-upward log character are distinguished from areas with coarsening-upward logs and areas with no sandstone. The reservoir at each of the three pools in Inman East Consolidated field consists of blocky or fining-upward sandstone. Lateral to the Inman pool are coarsening-upward sandstones and shales that are interpreted to be channel splay or overbank deposits. Areas of Tar Springs production are enclosed by heavy black lines.

channel that was about three-fourths of a mile wide, the same dimension as the Inman pool channel sandstone.

The regional cross sections of the Tar Springs (fig. 10) indicate that the Lower Tar Springs is thick where it has a blocky log motif. Up to 40 feet of shale and thin limestone beds considered to be part of the upper member of the underlying Glen Dean Limestone are removed locally and replaced with clean blocky sandstone that has a sharp basal contact. This indicates that either subaerial incisement or subaqueous scouring formed channels that were subsequently filled with clean sandstone. The lower Tar Springs channels are similar in width and orientation to those in the upper Tar Springs, but are offset in location.

Detailed stratigraphic cross sections across Inman East Consolidated Field (fig. 15) illustrate the lithologic complexity of the Tar Springs Sandstone. The sections are oriented east-west, approximately perpendicular to the elongation trend of the sandbodies. The sections are spaced about one-half mile apart (see index map, fig. 4). Lithologies were interpreted from the SP-Resistivity logs. Note that many of the wells in Inman East Consolidated Field itself were only drilled to the top 10 feet or so of the Tar Springs, where the well was "open hole" completed. Division of the Tar Springs into upper and lower members is indicated, but was difficult to determine where massive thick sandstones occur so a mid-formation point was used. The sections use the base of the Vienna Limestone as a datum because the base was presumably close to a horizontal surface when the Vienna was being deposited.

The detailed stratigraphic cross sections (figs. 10 and 15) illustrate many features of the Tar Springs. First, the thickness of the Tar Springs Sandstone is quite variable. It is thickest where the upper beds of the Glen Dean have been removed. However, the thickness of the removed strata is not matched everywhere by an equivalent amount of Tar Springs. Differential compaction also played a role. Where no sandstone beds occur and siltstone and shale predominate, the Tar Springs compacted more than in areas where there were thick, stacked sandstone beds. Thus, formational thick areas occur where sands are abundant. The apparent waviness of the top of the Glen Dean in figure 10 is probably due in part to this differential compaction, which is accentuated by the very large vertical exaggeration used to show details in these sections.

Second, Tar Springs sandstones form in sand bodies about 1 mile in width. Many of these are complex sand bodies composed of stacked sandstone units. Correlation of individual sand body units is limited. Blocky sandstones appear to have filled scours or incisements cut into older Glen Dean limestones as well as silts, shales and other sandstone beds of the Tar Springs. Some sandstones correlate laterally with crevasse splay siltstone or silty sandstone beds, but only for short distances of less than a mile or two.

Third, the upper one-third of the Tar Springs (about 20 feet) consists primarily of shale with local silt and silty sand stringers. This unit forms the upper seal for the Inman Tar Springs oil reservoirs. In the outcrop belt, the top of this unit is known to contain some very thin carbonaceous shale or coally stringers (Devera 1991). The 2- to 5-feet-thick silt and silty sandstone stringers that occur in this unit may be correlated for up to one mile. Commonly, a thin silty sandstone bed occurring in one well may correlate to a siltstone bed in an adjacent well. However, typically these sandstone beds do not extend beyond one well location spacing (660 feet) and do not appear to have been charged with hydrocarbons. This upper siltstone and shale unit is interpreted as bay fill and/or as overbank marsh deposits.

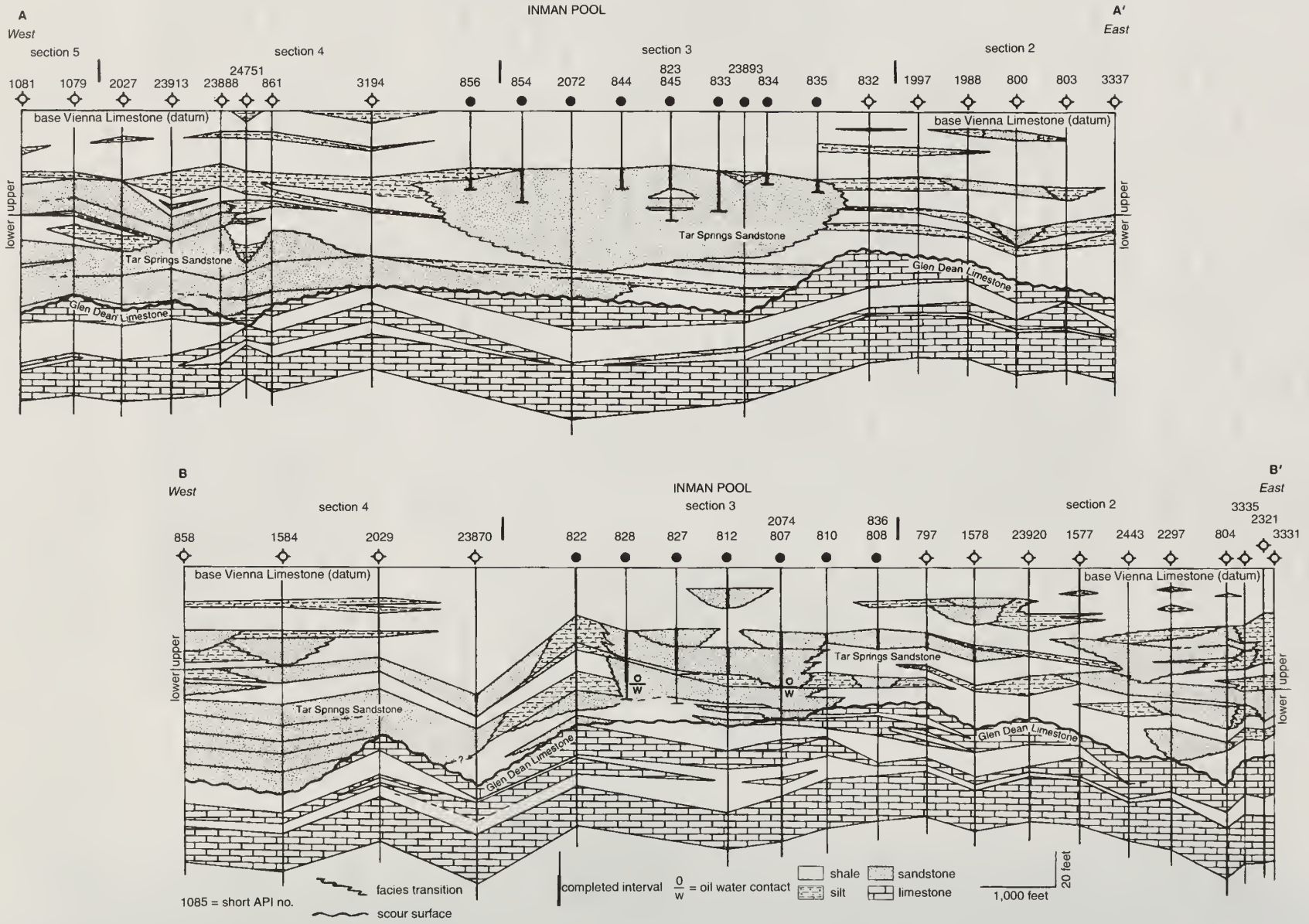
A
West
INMAN POOL
A′
East
section 5
section 4
section 3
section 2
1081 1079 2027 23913 23888 24751 861 3194 856 854 2072 844 823 845 833 23893 834 835 832 1997 1988 800 803 3337
base Vienna Limestone (datum)
base Vienna Limestone (datum)
lower upper
lower upper
Tar Springs Sandstone
Tar Springs Sandstone
Glen Dean Limestone
Glen Dean Limestone
B
West
INMAN POOL
B′
East
section 4
section 3
section 2
858 1584 2029 23870 822 828 827 812 2074 807 810 836 808 797 1578 23920 1577 2443 2297 3335 804 2321 3331
base Vienna Limestone (datum)
base Vienna Limestone (datum)
lower upper
lower upper
Tar Springs Sandstone
Tar Springs Sandstone
O/W
O/W
Glen Dean Limestone
Glen Dean Limestone
?
1085 = short API no.
facies transition
scour surface
completed interval
0/w = oil water contact
shale
silt
sandstone
limestone
20 feet
1,000 feet

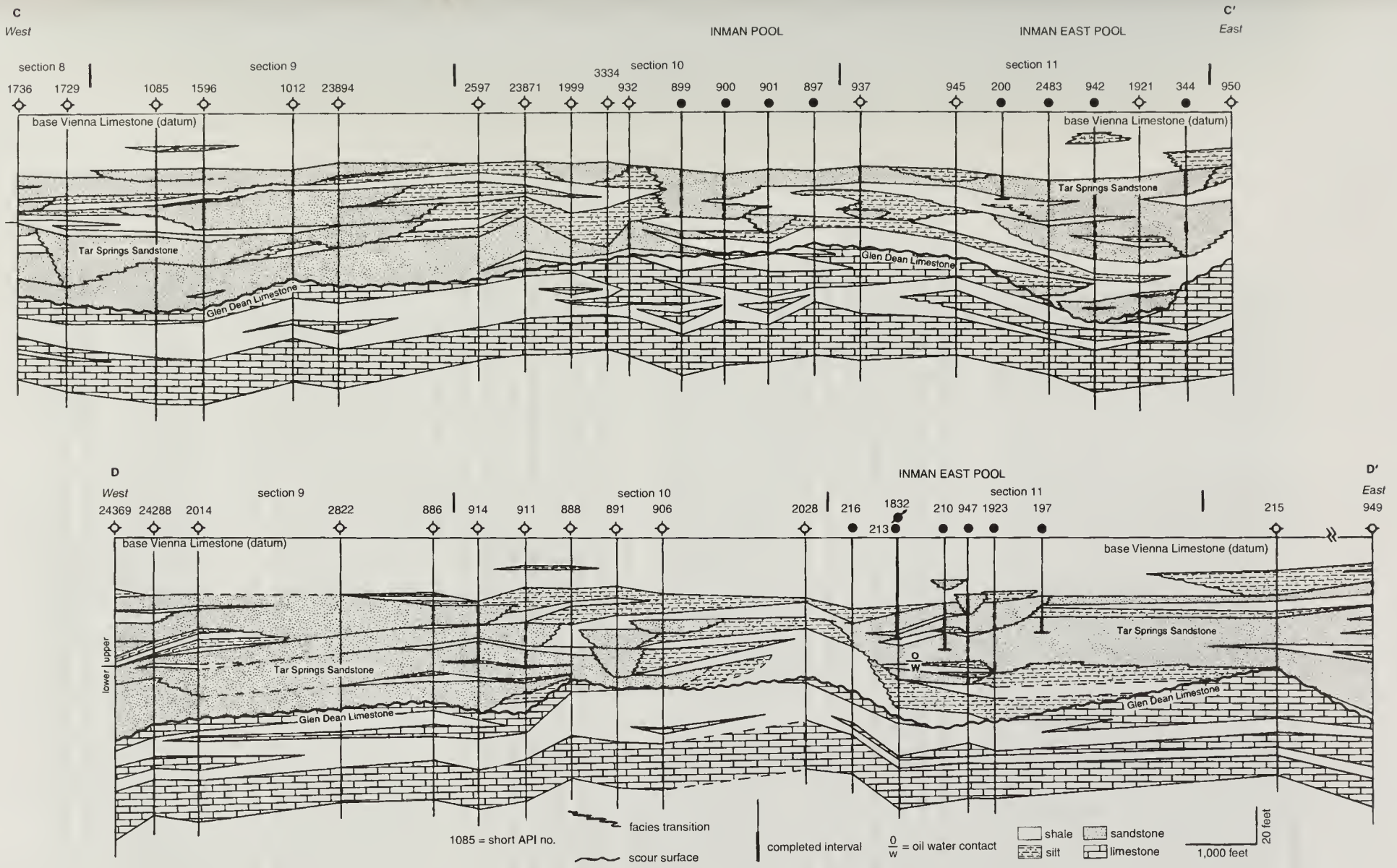

Figure 15 Stratigraphic cross sections at Inman East Consolidated Field. Sections A–A′, B–B′, C–C′, D–D′ are about one-half mile apart and oriented east-west (see figure 4 for location). The sections are spatially aligned east-west and from north (A–A′) to south (D–D′) to help visualize the three-dimensional geometry of lithofacies. These cross sections show the stratigraphic variations in the sandstone that create reservoirs and lateral seals. Solid symbols indicate wells that produced oil from the Tar Springs Sandstones. Many of the producing wells, particularly on section A–A′, were drilled just into the top of the sandstone and completed as an "open hole." The oil-water contacts, particularly on section B–B′, suggest that the reservoir is not fully charged with oil. Datum is the base of the Vienna Limestone.

Sedimentology

The Tar Springs Sandstone consists of fine to very fine sandstone, interbedded fine sand and silt, and gray and black shale. Only 1-inch-thick wafers or biscuits collected from one-foot intervals of several Tar Springs cores taken in Inman East Consolidated Field have been preserved in the ISGS Samples Library (see Appendix A). These biscuits show some of the sedimentary structures of the Tar Springs and were sampled for SEM and thin-section petrographic analysis. The thick sandstones of the Tar Springs contain abundant cross-bedding, ripple cross-lamination and planar bedding. Scattered flakes of muscovite, fine black sand grains (magnetite?) and zircon lie along bedding planes. The sandstone is white to gray, clean, sugary and locally oil-stained. Flaser bedding is observed in intervals that correspond to "siltstone" on SP logs. Several silty shale beds were also found to be carbonaceous. No distinct bioturbation traces were seen, although some clean sandstone beds lacked internal stratification and appeared to be massive.

The Tar Springs sediments at Inman East Consolidated Field are interpreted as the deposit of a river-dominated, tidally influenced, deltaic system that prograded across a shallow cratonic shelf. Prodelta and distributary mouth bar facies are thin to non-existent because of limited accommodation space or later reworking by the channel facies. The basal contact of the Tar Springs with the Glen Dean may be conformable in areas where interbedded shales and limestone beds of the Glen Dean are overlain by shales of the Tar Springs. However, the more common removal of limestone markers and the presence of a channel sandstone directly above a hard Glen Dean Limestone bed indicates a widespread, minor disconformity. The top of the Glen Dean is considered to be the top of the uppermost limestone bed (Willman et al. 1975, p. 158). The basal Tar Springs shales are all that remain of the prodelta. Overlying or interbedded with this shale are rare, scattered thin (6 to 12 feet) sandstone beds with coarsening-upward log motifs that may have been deposited as distributary mouth bars, bay fills or crevasse splays.

Most commonly, lying directly on the limestones of the Glen Dean are blocky, clean, stacked or massive sandstones that were deposited in channels scoured up to 40 feet deep into the Glen Dean. These sandstones are interpreted to be channel deposits based on their sharp base, good sorting, long and narrow areal geometry, abundant cross-bedding and cross-lamination. Tidal features such as tidal couplets and rhythmic tidal bundles, which are seen in outcrop at Alto Pass (Wescott 1982), were not observed at Inman East Consolidated Field, although flaser bedding was seen in some intervals of the limited sets of core chips and biscuits. The isopach map and regional net sandstone isolith maps (figs. 8 and 9) of the Tar Springs show that the vertically stacked channel sandstones at Inman East Consolidated Field can be traced as a 6- to 10-mile-wide unit that extends tens of miles to the north and south. The individual channel sands are approximately one mile wide and are locally cut off by later channels that were subsequently filled with sand or silt and shale. The channels are at least 10 to 20 feet deep, a typical thickness of individual sands in the stacked sand sequence. The variation in thickness of the whole stacked sandstone package reflects deposition in a fluvial-deltaic valley 6 to 10 miles wide and a composite valley fill in excess of 100 feet of sandstone locally.

Interbedded with the channel sandstones and laterally in areas that lack the stacked sandstone channel deposits are siltstones, shales and thin-bedded sandstones that were deposited as channel overbank deposits, interdistributary bay and tidal flat deposits and some small isolated crevasse-splay deposits.

Overlying the coarser clastics of the Tar Springs is a widespread shale and then the Vienna Limestone. Locally, this shale may be carbonaceous or contain thin coal

beds. To the south of Inman East Consolidated Field, along the Tar Springs outcrop belt, these shales have been interpreted to be marginal marine, fluvial overbank or estuarine deposits (Wescott 1982). Although Inman East Consolidated Field lies paleogeographically up-dip (shoreward) from the outcrop belt, the same depositional facies likely persist northward beyond the oil field. Because the overlying Vienna limestone, with its abundant, diverse marine fossil content, directly overlies this uppermost Tar Springs shale without any thickness irregularities, it is presumed that the paleotopography on top of this shale is nearly flat. The lack of fossils in the Tar Springs shale suggests a restricted environment without direct access to open marine conditions and probably with fresh or brackish water. Thus, the shale could have formed in a restricted interdistributary bay or tidal mud flat. The thin coals seen in outcrop near the top of this shale (Devera 1991) suggest freshwater marsh deposition and occasional subaerial exposure. The contact with the base of the overlying transgressive limestone (Vienna) could be an eroded surface, or it might represent a primary depositional surface formed at the top of a bay-fill succession that was capped by thin organic-rich marshes. Deltaic marsh and bay fill deposits would have very low relief and could have been preserved by a rise in sea level. The abrupt changes in facies, fossil types and lithology suggest that the base of the widespread Vienna is a parasequence boundary, perhaps a sequence boundary, that marks the base of a transgressive systems tract.

Trapping Mechanism

The Inman fields are among many located along the Wabash Valley Fault System. The fault system is composed of a series of high-angle, normal faults that trend north-northeast in the lower Wabash River valley area of southeastern Illinois and southwestern Indiana (Nelson 1995, p. 65, 123). Between the nearly planar faults are arched horsts and grabens that have formed many oil fields in southeastern Illinois. The greatest vertical displacement on a single fault in the Wabash Valley Fault System is 480 feet, recorded on the Inman East Fault (Nelson 1995, p. 68). This fault forms the eastern edge of the Inman East Consolidated Field and has a local displacement here of about 300 feet. The fault appears to have at least two splays as indicated by the position of the Glen Dean Limestone in an intermediate block in the well in Section 14, T8S, R10E (Short API no. 363) and shown on figures 16 and 17. The Inman Fault lies to the west of Inman East Consolidated Field. The horst block between these two faults has formed traps for the McClosky, O'Hara, Aux Vases, Cypress, Hardinsburg, Tar Springs, Waltersburg, Palestine and a lower Pennsylvanian sandstone. The Tar Springs and Cypress are the major reservoirs.

The structural contour map on the base of the Vienna Limestone (fig. 16) indicates that the Tar Springs reservoirs of the Inman East Consolidated Field compartments occur on a west dipping, arched horst block between the Inman East and the Inman Faults. The Inman East compartment or pool occurs on the arched structural culmination of the fault block that is located on the east edge of the horst and adjacent to the East Inman Fault. The Inman and Inman South pools lie on the west dipping portion of the horst block.

Structural cross-section E-E′ (fig. 17) indicates the partial anticlinal closure of the Inman and Inman East compartments. The Inman compartment is formed by a combination structural-stratigraphic trap where the channel sandstone has up-dip closure against siltstone and shale to the west, south and east. The Inman East compartment is also a structural-stratigraphic trap where the producing area is defined by the limits of a channel sandstone that lies at the anticlinal crest of the horst block adjacent to the steeply southeast dipping Inman Fault that provides the up-dip seal. The Inman South compartment is similar to the Inman compartment in that it is formed by an up-dip stratigraphic pinchout of the Tar Springs channel sandstone.

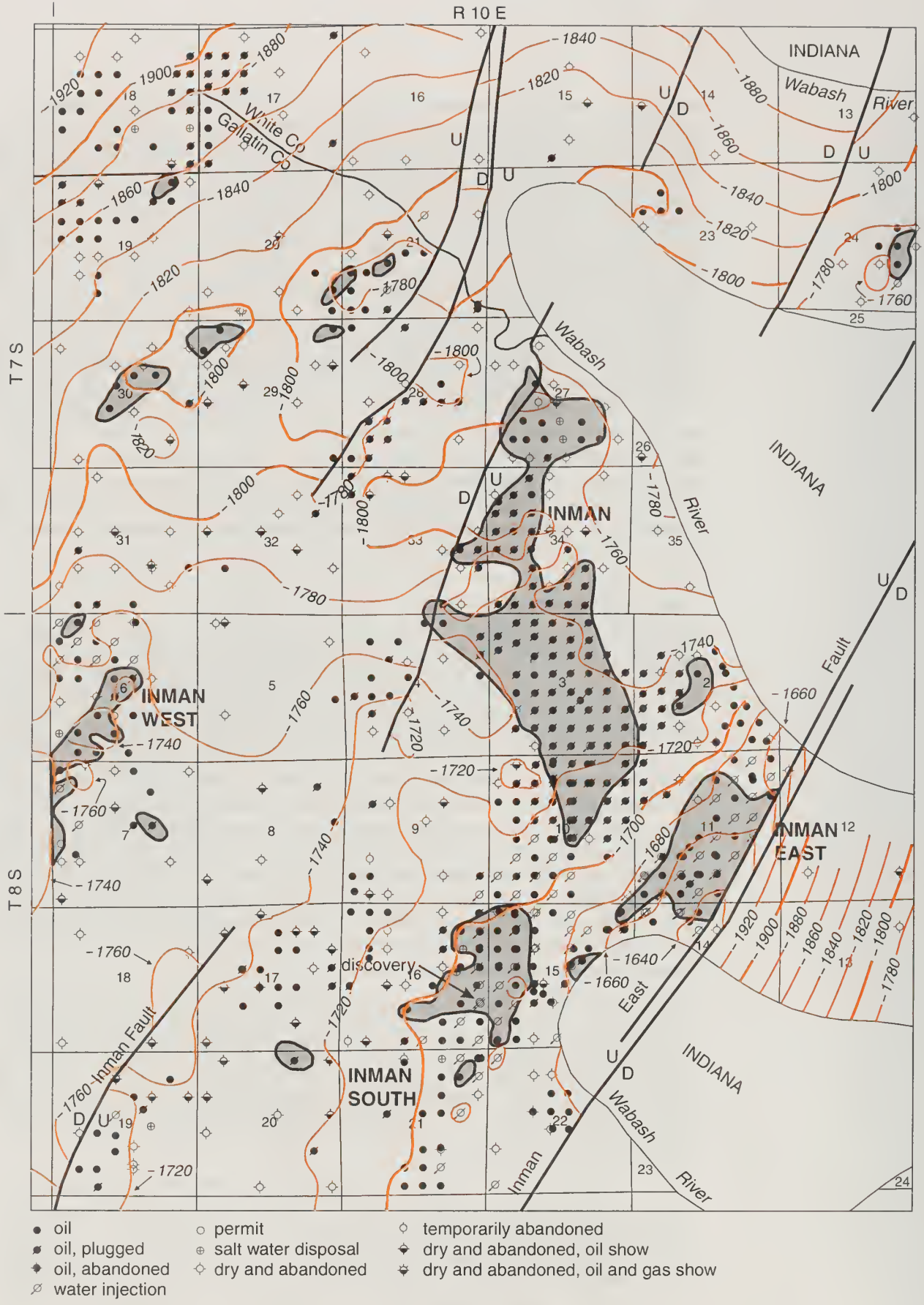

Figure 16 Structure map on base of Vienna Limestone at Inman East Consolidated Field. The field occurs in a horst block between the Inman Fault and the Inman East Fault. The Inman and Inman South compartments have up-dip stratigraphic traps on the east to southeast sides. The Inman East compartment is delineated by both the sandstone distribution and the anticlinal roll-over bordering the Inman East Fault. The contour interval is 20 feet. Areas of Tar Springs production are shaded.

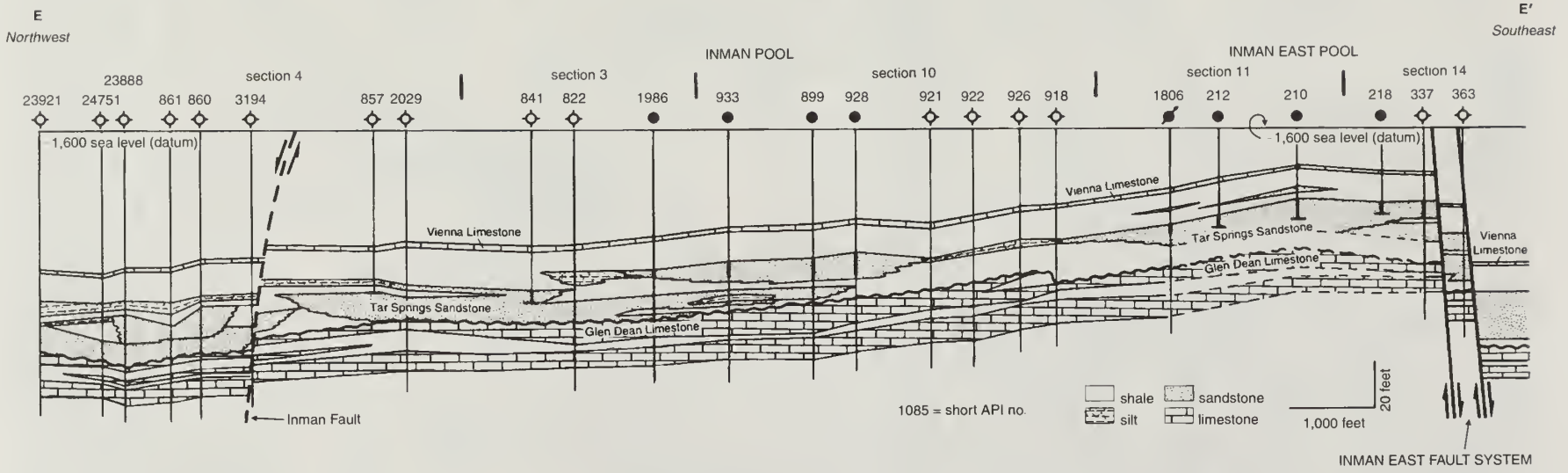

Figure 17 Structural cross section at Inman East Consolidated Field. Section E–E′, oriented northwest-southeast, shows stratigraphic trapping of the Inman pool and structural closure of the Inman East pool against the Inman East Fault (see figure 4 for location).

Petrography

The mineralogy and texture of sandstones from the Tar Springs Sandstone at Inman East Consolidated Field were analyzed using thin section (66 samples), SEM/energy dispersive x-ray analysis (EDX)(8 samples), x-ray diffraction (12 samples whole rock, 5 samples clays), and isotope geochemistry (8 samples) in order to characterize the composition of the framework grains, their alteration products, the cements and the porosity. Sandstones from 6 cores were sampled in detail. Samples included cross-bedded, rippled and homogeneous sandstones from cores of the blocky and fining-upward facies. Visual estimates of thin-section composition are summarized in Appendix B; point counting was not performed because feldspar identification stains were not made, and thus, feldspar variety could not be reliably identified.

Composition of Primary Detrital Components of Sandstones

Quartz is the predominant framework grain, constituting 70% to 80% of the rock volume (fig. 18). The grains are generally monocrystalline with rare polycrystalline grains and microcrystalline (chert) grains. They are well-sorted and very fine to fine in grain size. Roundness generally could not be observed because of abundant quartz overgrowths, although rounded grain dust rims are seen beneath the euhedral overgrowths of some quartz grains (figure 19b).

Altered feldspar, now mostly replaced by clay minerals, is next in abundance and typically ranges from a few percent to as much as 10% of the rock volume in rare instances. Originally deposited as feldspar grains, most grains are now clouded (fig. 18a), highly altered (fig. 20, a and b; fig. 22b), or partially dissolved (fig. 21a, c) and replaced by clay minerals or in some cases by diagenetic albite. A few isolated, unaltered grains of fresh feldspar with albite twinning are seen locally. Untwinned, commonly cloudy grains are likely to be orthoclase, but the cloudy appearance could mask twinning, typical of plagioclase and microcline. Thus, feldspar is generally identified only in the most generic sense.

Trace minerals, which include opaques, heavy minerals and carbonaceous matter, occur in most samples but occupy less than 1% of the rock volume. Up to one-third of the samples have laminae with streaks or concentrations of opaque or "heavy mineral" grains consisting of pyrite, magnetite and unidentified minerals along with subrounded to subhedral zircons and lesser amounts of rounded tourmaline and possibly hornblende grains (fig. 23b). Silty laminae contain fine fragments of carbonaceous plant material and wispy, wavy laminae of detrital clay material (fig. 23a).

Diagenetic Cements The framework grains are cemented by a variety of minerals.

Quartz is the predominant cement, typically forming euhedral, syntaxial overgrowths on detrital quartz grains (figs. 19 and 24a). It typically forms a partial pore-filling cement and leaves pores lined with euhedral quartz surfaces, which may or may not be coated with diagenetic clays. Pore throat sizes of 10 to 30 μm are still preserved in the sandstones.

Diagenetic clay minerals consist of abundant kaolinite, with lesser amounts of illite, mixed-layered illite/smectite and chlorite. Typically, except for some chlorite, all these clays formed after the quartz cement formed (figs. 19b and 25b). The source of the aluminum and silica for the authigenic clays is most likely the original feldspar grains, which now appear clouded in thin section and range from pitted, pockmarked and partially dissolved to completely replaced by clay in SEM images (fig. 20, a and c; fig. 22b). Where partially altered feldspar grains are observed, small amounts of diagenetic clay and fresh albite (fig. 21c) are also observed. Diagenetic kaolinite is the most abundant clay mineral (figs. 19d; 20, a and b; 22, a and d). It fills pores with vermiform books or lines pores where it may be intermixed with illite and/or chlorite

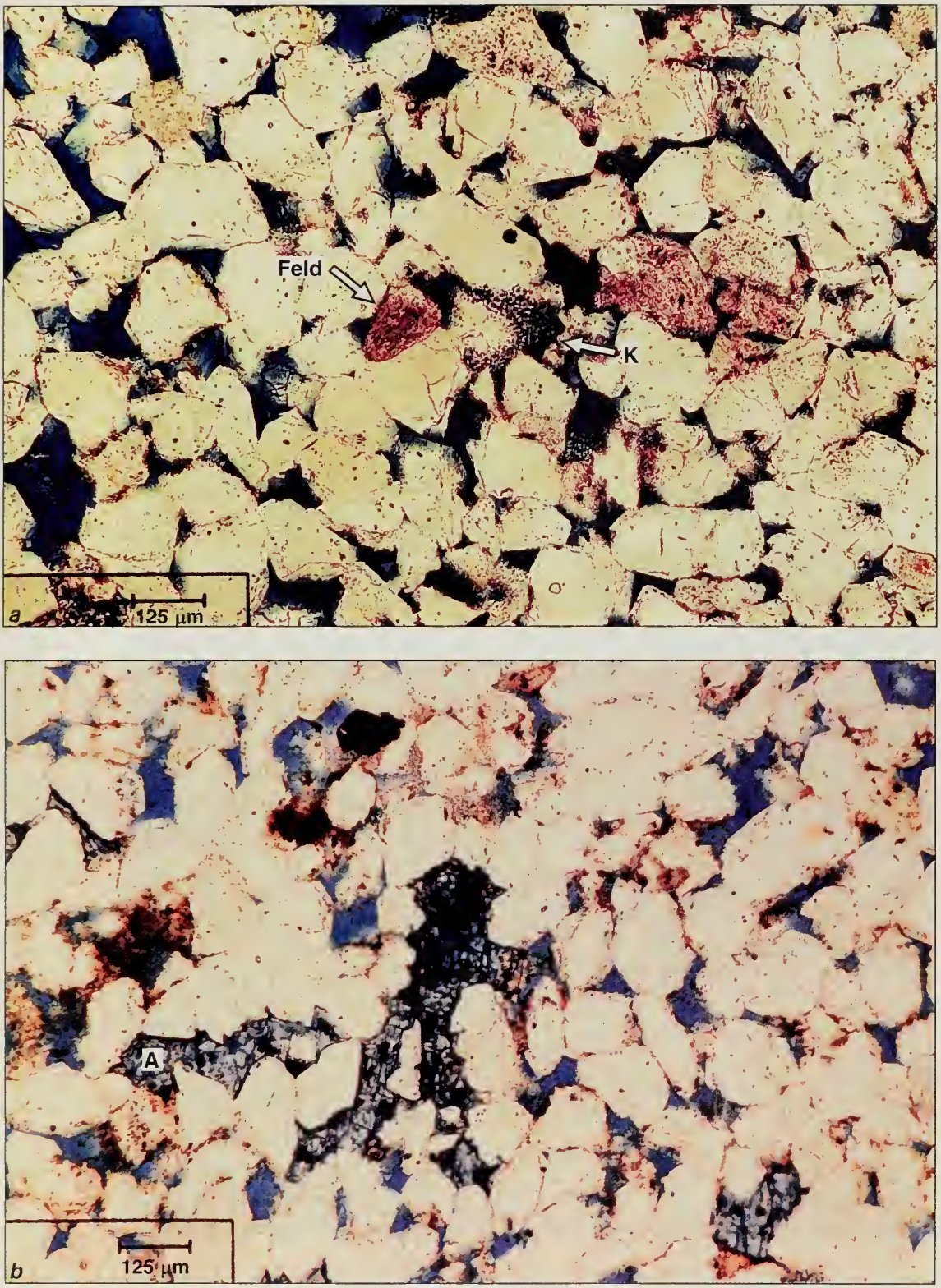

Figure 18 Thin-section photomicrographs of reservoir sandstone. Images from the Shakespeare, no. 3 Moye, Sec. 20, T8S, R10E at the Inman West Consolidated Field. (*a*) Clean sandstone with dusty, altered, feldspar grains (Feld) and kaolinite clusters (K). Quartz grains have quartz overgrowths. Sample is from 2,252.7 feet. Bar scale = 125 μm. Plane light. (*b*) Clean sandstone with patchy ankerite (A) cement (stained blue) that locally completely fills pores. Sample is from 2,251 feet. Bar scale = 125 μm. Plane light.

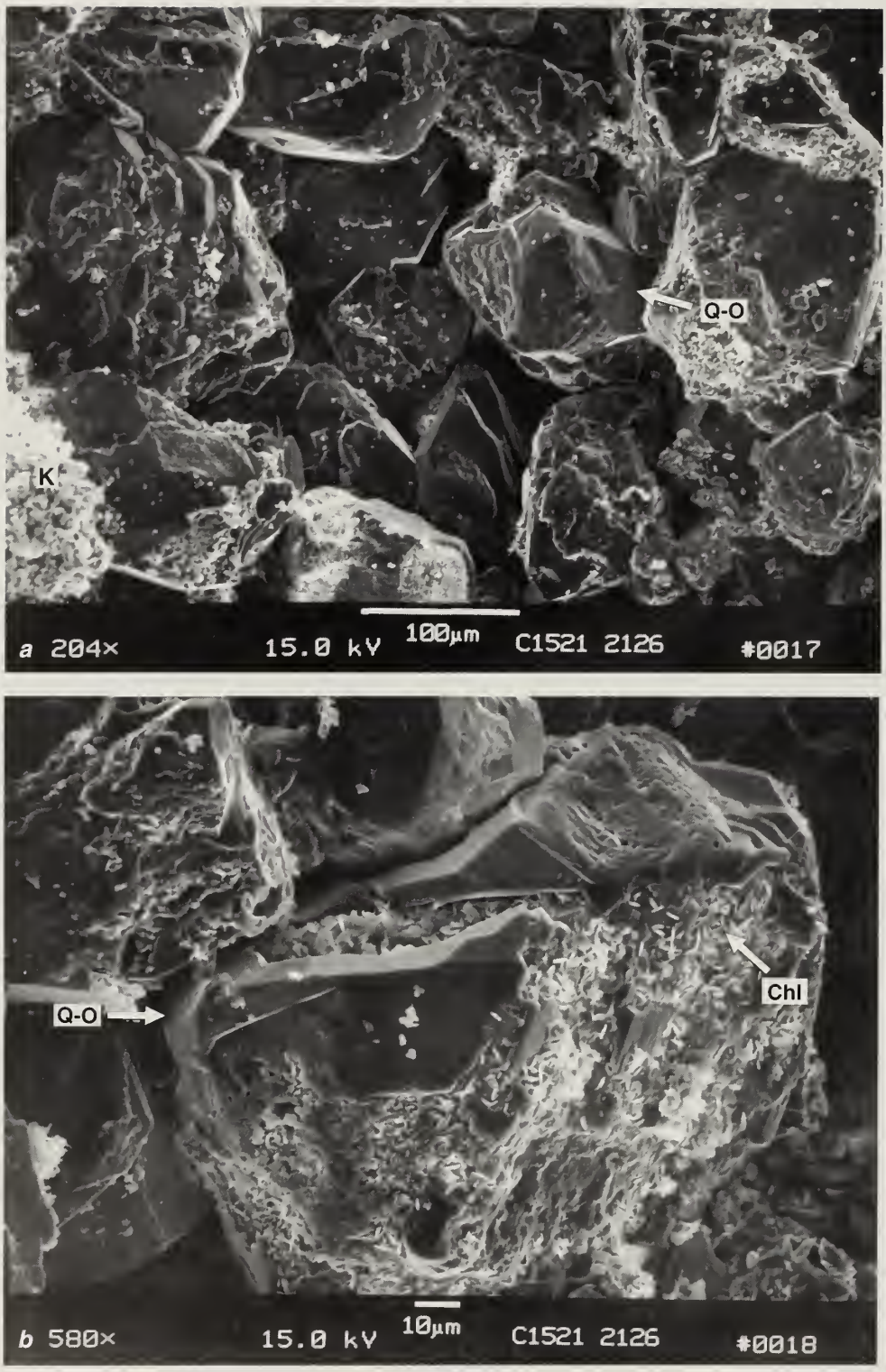

Figure 19 SEM photomicrographs of Tar Springs Sandstone. (*a*) Quartz grains with quartz overgrowths (Q-O) in a highly porous reservoir sandstone. Large pore throats are 10–30 µm in diameter. Sample is from Carter Oil, no. 3 Williams well, 2,126 feet, Sec. 2, T7S, R10E. (*b*) Quartz overgrowths (Q-O) over chlorite (Chl)-coated quartz sand grain. Small amounts of illite are associated with the iron-rich chlorite. Same sample as in 19a.

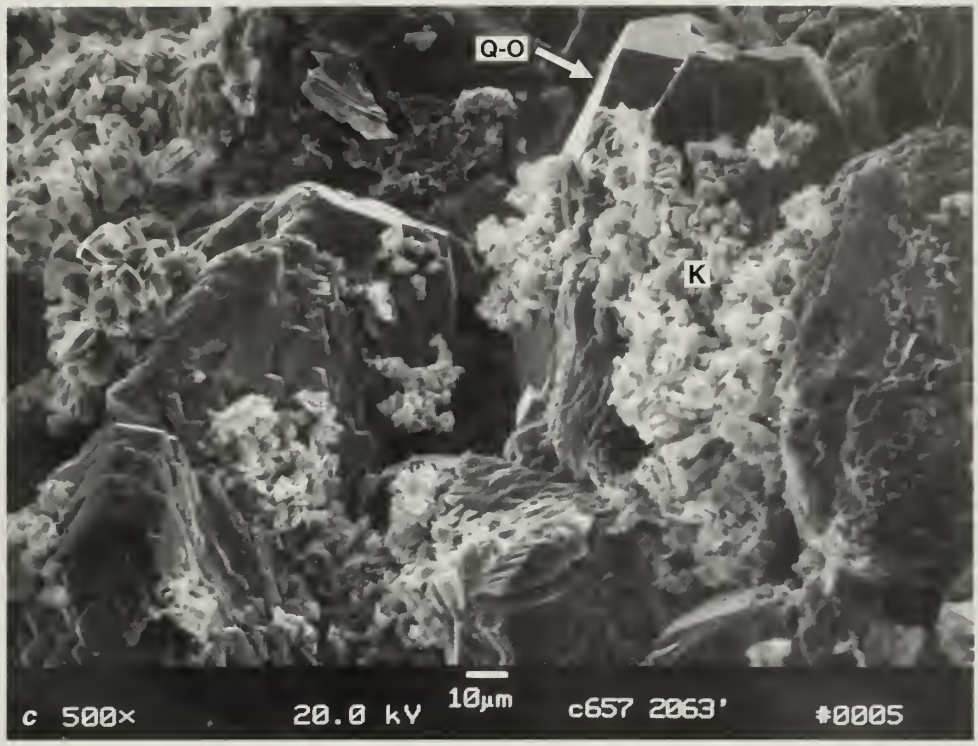

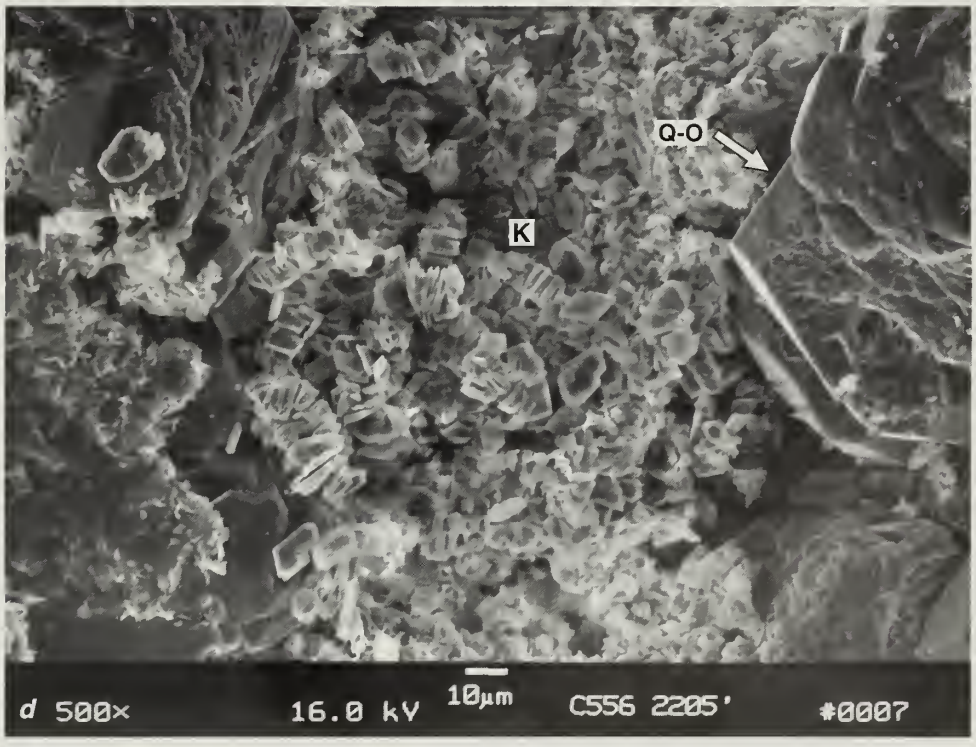

(*c*) Quartz overgrowths (Q-O) with later diagenetic kaolinite (K) and associated minor amounts of chlorite and illite clay. Pore throat in center of picture is 12 µm in diameter. Sample is from Leach and Halbert, no.1 Curry, 2,063 feet, Sec.15, T8S, R10E. (*d*) Kaolinite (K) in a pore with quartz grain overgrowths (Q-O) from a very fine-grained sandstone sample with poor porosity. Sample was primarily cemented by quartz overgrowths, but elsewhere had some calcite cement and contained abundant, partially dissolved and degraded, feldspar grains and abundant diagenetic clay minerals such as kaolinite with lesser amounts of illite. Sample is from Gulf Oil Refining Co., no. 1 J. Harlem, 2,205 feet, Sec.15, R7S, T10E.

fig. 21b). Chlorite forms rosettes (figs. 21d and 22c) that may line some pores or may be intermixed with kaolinite. SEM/EDX analysis of the chlorite showed that it is iron-rich with an Fe:Mg ratio ranging from 5:1 to 25:1. The x-ray diffraction analyses indicate the d-spacing of the 001, 002, 003 and 004 peaks for chlorite conflict with the SEM/EDX analyses and suggest that the chlorite is relatively magnesium-rich. (Moore, personal communication). No attempt was made to resolve the conflicting analyses. Mixed layered illite/smectite clays line some pores and may be intergrown with kaolinite, illite and chlorite. Fibrous illite occurs in small amounts, commonly adjacent to altered feldspar grains (fig. 21a) and intergrown or associated with other clays.

Pyrite cement that consists of 5- to 10-µm euhedral crystals or crystal aggregates occurs locally in trace amounts, commonly in siltstone to very fine-grained sandstone, and in association with detrital carbonaceous matter (figs. 23b and 24b)

Ankerite, a late stage carbonate cement ($Ca(Fe,Mg)(CO_3)_2$), is locally abundant (figs. 18b and 25). It occurs as sparry, non-baroque, pore-filling, poikilotopic clusters of clear carbonate cement that readily take a pale blue potassium ferricyanide stain, which indicates the presence of iron. Patches of this cement typically are 1 to 2 mm across and range in abundance from trace amounts to more than 10% of the rock. The ankerite cements are extinct (black) with respect to cathodo-luminescence, which indicates either that the Mn concentrations are very low or that the Fe:Mn ratio is very high (Fouke, personal communication). The SEM/EDX analysis of 29 examples of ankerite cement from four samples (see Appendix C) indicates a low amount of Mn, a highly variable Fe:Mg ratio and a Ca:Mg:Fe ratio that averages approximately 1:0.34:0.30. The SEM/EDX analysis of a broken crystal of the ankerite cement indicates that the composition of that crystal is zoned with high magnesium content on the rim and high iron content in the center (see Appendix C). The x-ray diffraction analysis indicates that the ankerite has a dolomitic rather than a calcite crystal structure and the iron content varies from 5 to 30 mole percent $FeCO_3$ (Moore, personal communication). Deer et al. (1966) note that iron continuously replaces magnesium in the dolomite crystal structure to form ankerite. When 20% or less of the magnesium positions are replaced by iron (i.e., Fe:Mg greater than or equal to 1:5), the mineral is termed "ferroan dolomite." When greater than 20% of the magnesium positions are replaced by iron, as here in all the SEM/EDX analyses of the Tar Springs (see Appendix C), the mineral is termed "ankerite." Thus, during acid clean-up or stimulation, both chlorite and the more abundant ankerite might release iron and create insoluable iron oxide gels unless appropriate iron scavengers or chelating agents are added to the stimulation fluids.

In an attempt to determine the origin of this unusual cement, the literature was reviewed and the isotopic composition was analyzed. Ankerite, particularly iron-rich ankerite such as is seen here, has been associated with lead and zinc sulfides and fluorite (Deer et al. 1966, p. 495) and thus may have formed from hydrothermal fluids. Such fluids formed the famous fluorite deposits in nearby Hardin County, just 15 miles south of Inman Field (Weller et al. 1952). Pitman et al. (1998, p.17) indicated that the ankerite cement seen in the Bethel and Cypress Sandstones in southern Illinois may have formed at the time of maximum burial about 270 million years ago during a possible hydrothermal heating event. They suggested that the Bethel and Cypress were inundated with fluids with temperatures on the order of 120°C to 140°C from deeper in the basin, which produced ankerite cement.

Carbon and oxygen isotopes of the Tar Springs ankerite cement were measured by the U.S. Geological Survey in eight samples that contained significant amounts of ankerite (see Appendix D) in an attempt to determine the source of the carbonate and the temperature of formation. The ^{13}C isotope data indicate two populations of source materials. Data from the Gulf no. 1 Harlem and Carter no. 1 Crawford wells suggest

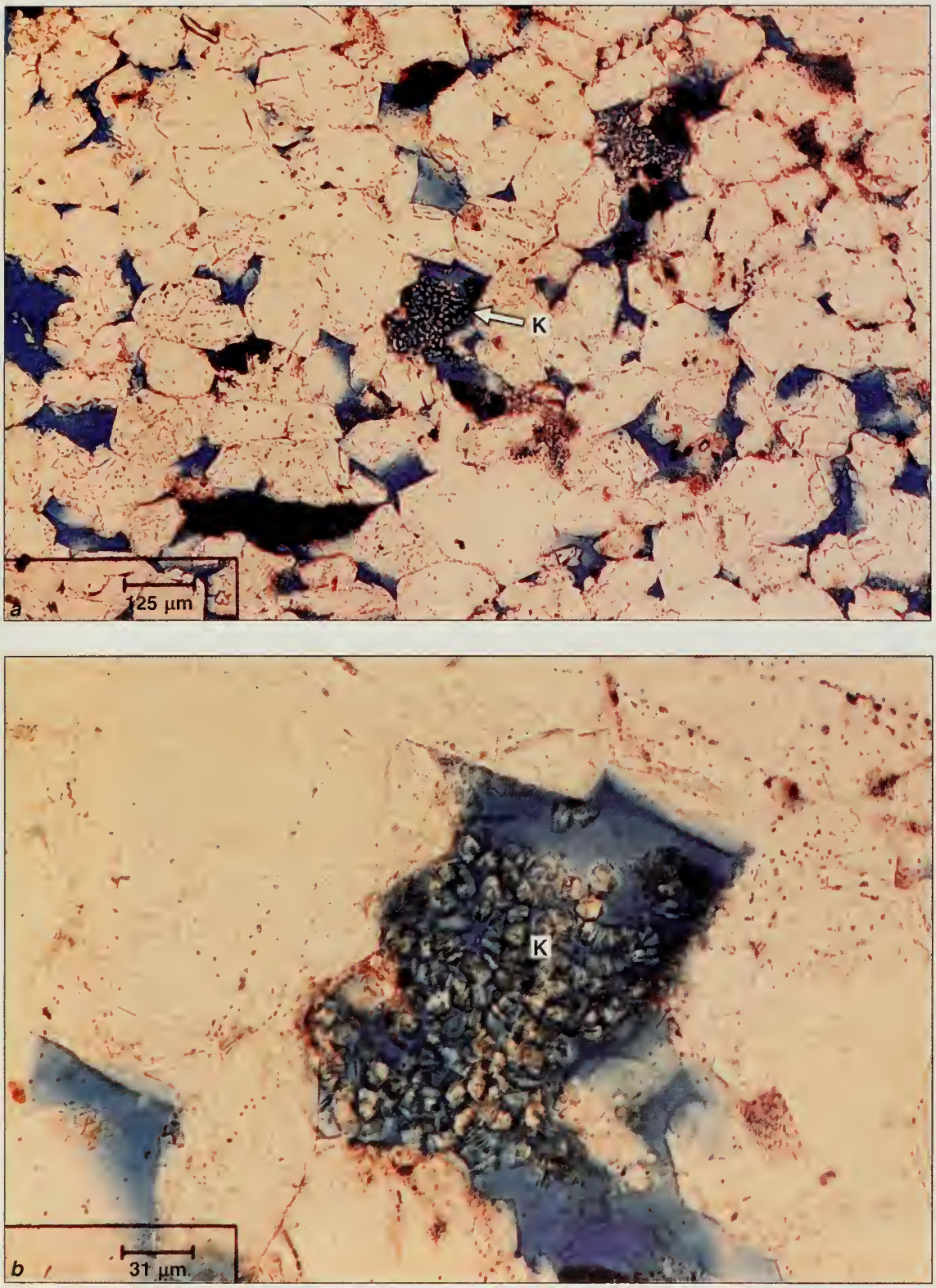

Figure 20 Thin-section photomicrographs of kaolinite formed from alteration of a feldspar grain. (*a*) Porous, quartz-cemented sandstone with grain-size clusters of kaolinite (K), which appear to have replaced a previous mineral, likely a feldspar grain, creating secondary microporosity. Sample is from Shakespeare, no. 3 Moye, 2,252.7 feet, Sec. 20, T8S, R10E, located in Inman West Consolidated Field. Bar scale = 125 μm. Plane light. (*b*) Detail of a kaolinite (K) cluster from 20a. Quartz grains are cemented by quartz overgrowth cement with euhedral faces lining the pore. The kaolinite formed later and provides largely ineffective secondary microporosity. Bar scale = 31 μm. Plane light.

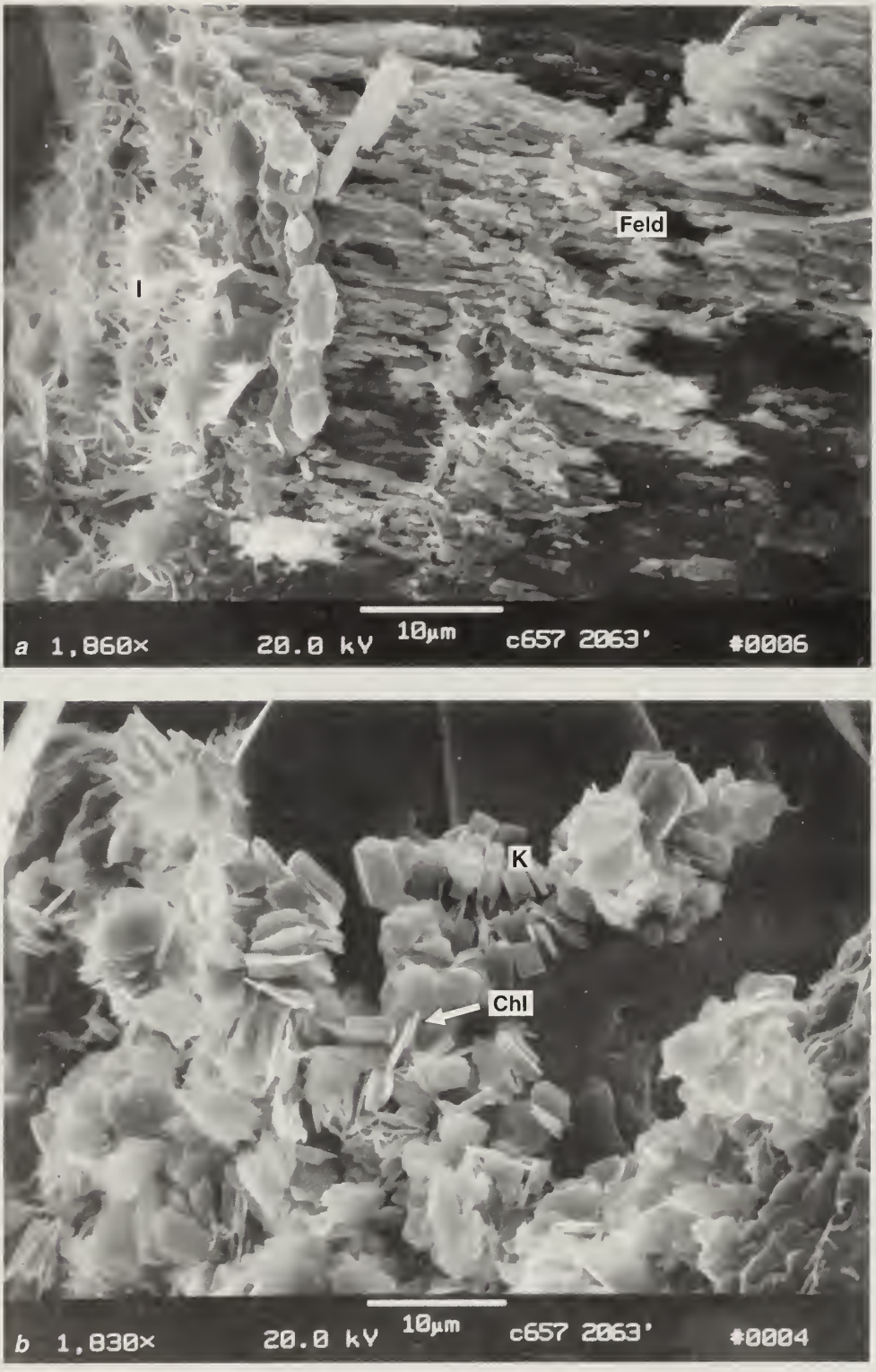

Figure 21 SEM photomicrographs of diagenetic minerals in the Tar Springs Sandstone. (*a*) Fine-grained, porous, reservoir sandstone with altered Na-feldspar (Feld) and later stage diagenetic illite (I) on left side of photo. Sample is from Leach and Halbert, no. 1 Curry, 2,063 feet, Sec. 15, T8S, R10E. (*b*) Fine-grained, porous, reservoir sandstone with diagenetic kaolinite (K) crystalized on quartz overgrowth cement. Platelets of iron-rich chlorite (Chl) are intertwined with the kaolinite crystals. Traces of later stage fibrous illite are seen on the left edge of the photo. Sample is from Halbert, no. 1 Curry, 2,063 feet, Sec.15, T8S, R10E.

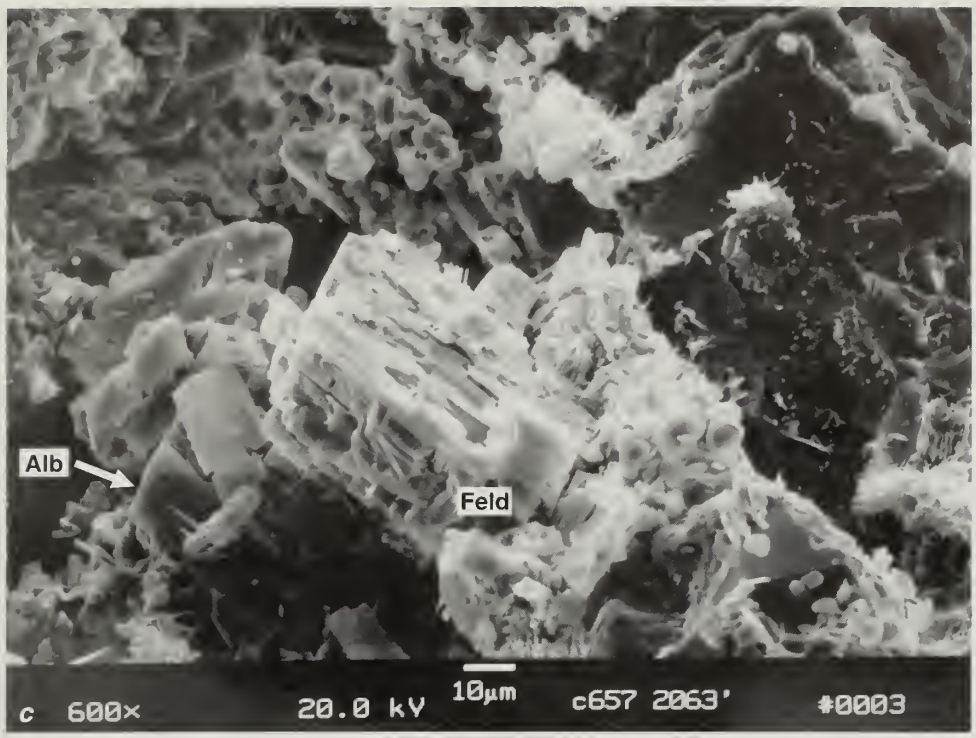

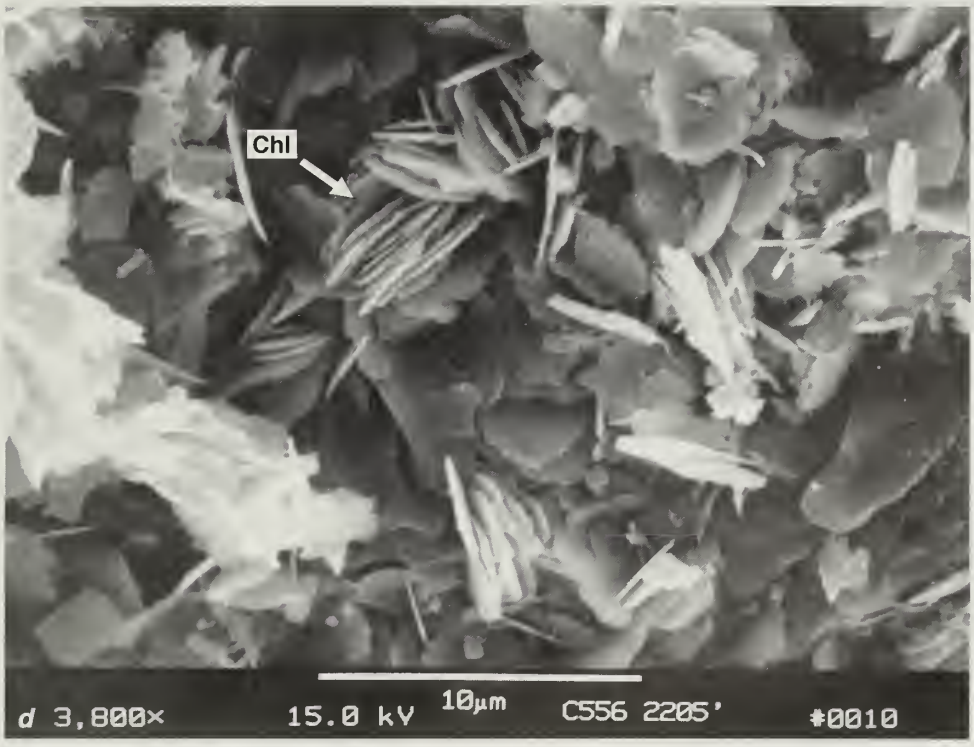

(*c*) Altered sodium-feldspar (Feld) grain in a fine-grained, porous reservoir sandstone. Kaolinite, albite (Alb) and some illite are observed lining the pores. Sample is from Halbert, no. 1 Curry, 2,063 feet, Sec.15, T8S, R10E. (*d*) Diagenetic iron-rich chlorite (Chl) rosettes with some kaolinite from a very fine-grained sandstone with low porosity. Sample is from the Gulf Refining Co., no. 1 J. Harlem, Sec.15, T7S, R10E.

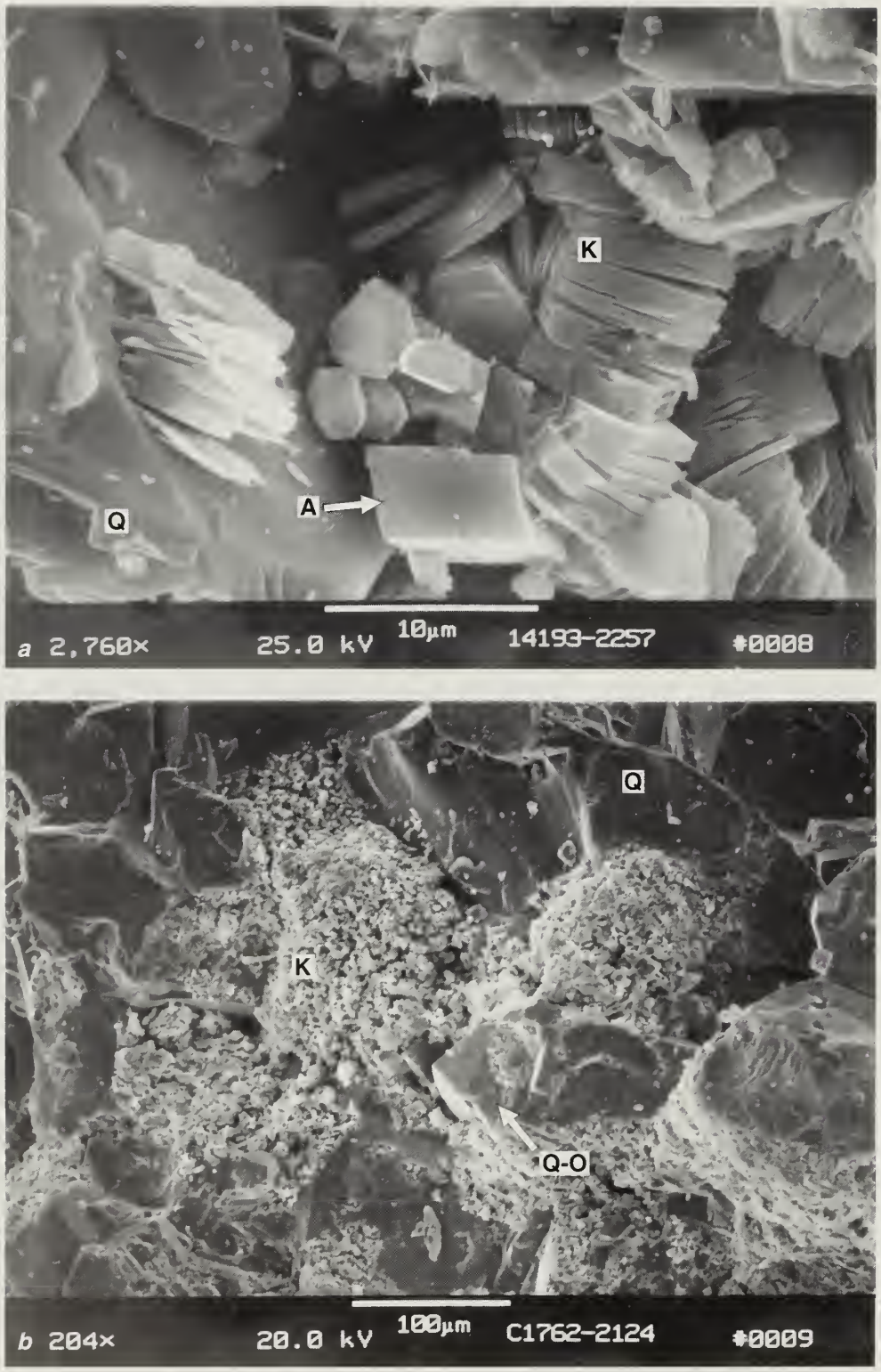

Figure 22 SEM photomicrographs of diagenetic clays in the Tar Springs Sandstone. (*a*) Diagenetic kaolinite (K) books and an ankerite (A) rhomb lying on top of a quartz overgrowth in a sandstone pore. Sample is from Shakespeare no. 3 Moye, 2,257 feet, Sec. 20, T8S, R9E located in Inman West Consolidated Field. (*b*) Clusters of diagenetic kaolinite (K) occur between quartz cemented quartz grains (Q). Kaolinite clots are the remnants of altered feldspar grains. In thin section, these grains appear cloudy and brownish as in figure 18. Euhedral minerals in the center of the photo include small albite crystals and quartz overgrowths (Q-O). Sample is from the Carter no. 1 Williams well, 2,124 feet, Sec. 27, T7S, R10E in Inman East Consolidated Field.

(*c*) Rosettes of iron-rich chlorite (Chl) growing on quartz overgrowths in a sandstone pore. Sample is from Shakespeare no. 3 Moye, 2,257 feet, Sec. 20, T8S, R9E located in Inman West Consolidated Field. (*d*) Booklets of diagenetic kaolinite (K) and round droplets of oil lie in a pore lined with quartz overgrowths (Q-O). Sample is from Shakespeare no. 3 Moye, 2,257 feet, Sec. 20, T8S, R9E located in Inman West Consolidated Field.

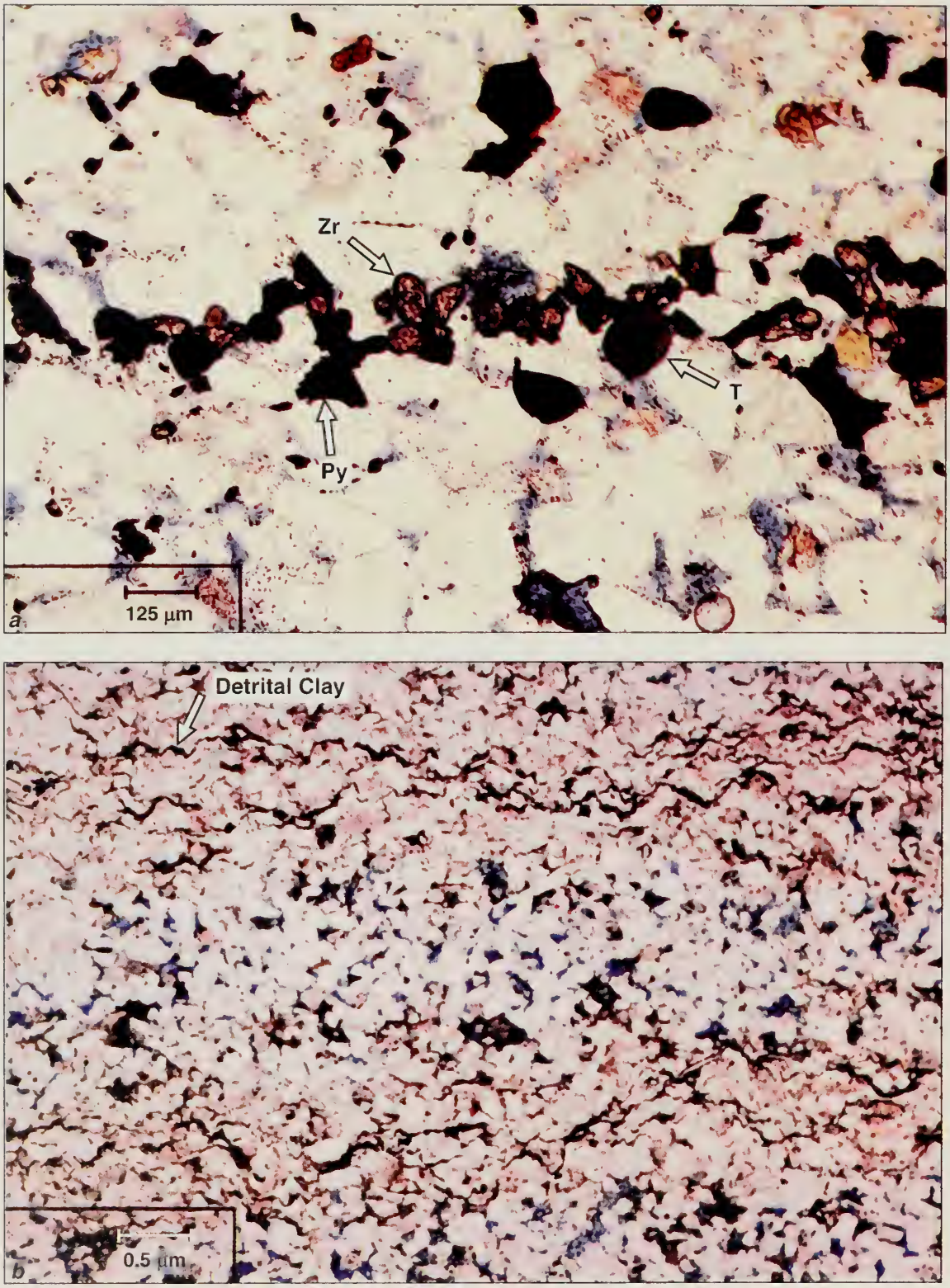

Figure 23 Thin-section photomicrographs of unusual detrital components in the Tar Springs Sandstone. (*a*) Two heavy mineral lag laminae containing sub-rounded to rounded zircon (Zr), tourmaline (T) and opaques. Note that some opaque minerals here are probably detrital magnetite and also diagenetic pyrite (Py) that formed in pore space after quartz overgrowth cement. Sample is from Sohio, TEB no. 19 well, 2,128 feet, Sec. 3, T8S, R10E, Bar scale = 125 μm. Plane light. (*b*) Very fine, low porosity sandstone laminae that contain detrital clay wisps. Sample from Shakespeare, no. 3 Moye, 2,256.9 feet, Sec. 20, T8S, R10E, located in Inman West Consolidated Field. Bar scale = 0.5 μm. Plane light.

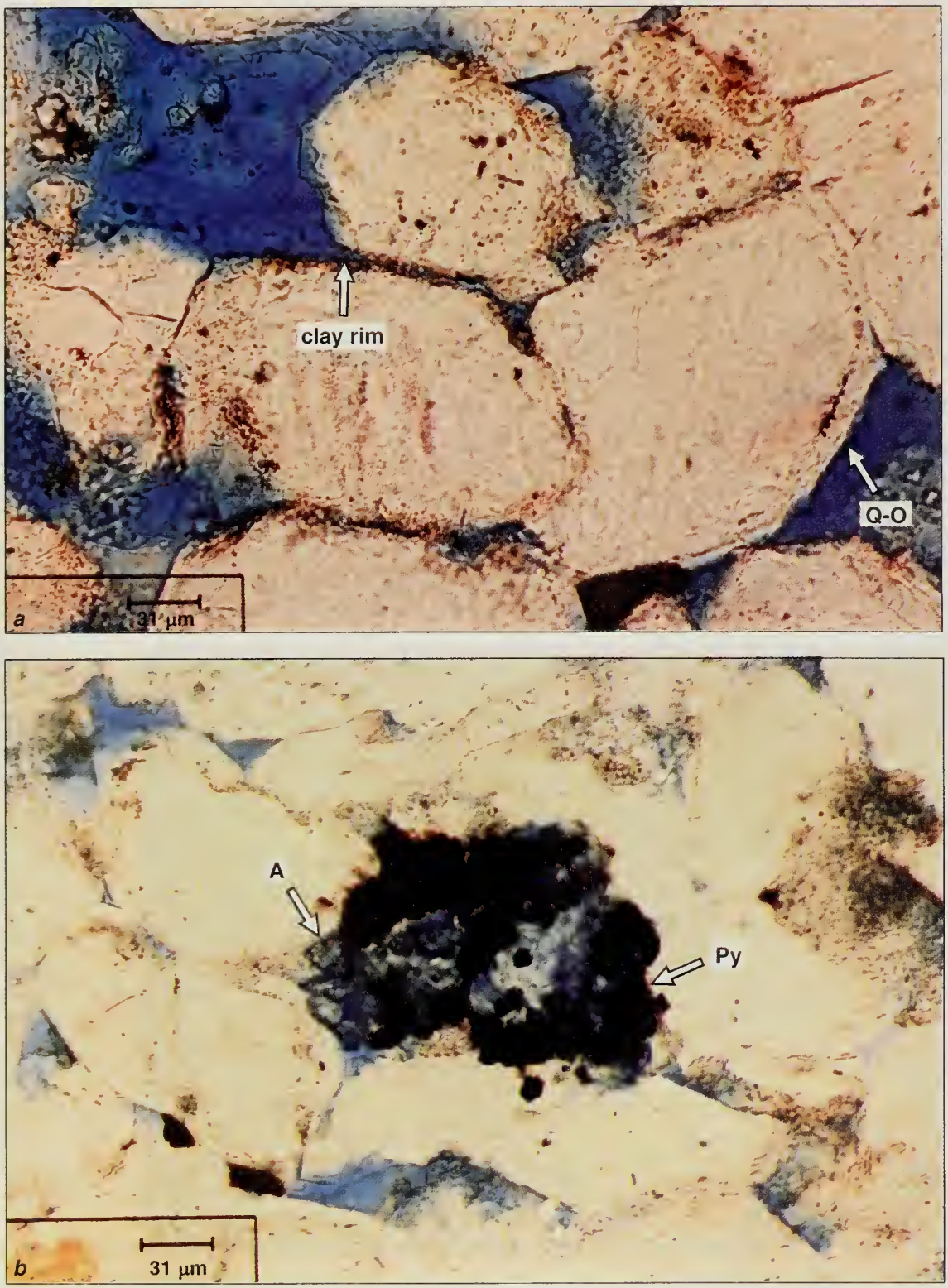

Figure 24 Thin-section photomicrographs of diagenetic features in the Tar Springs Sandstone. (*a*) Quartz overgrowths (Q-O) forming after diagenetic clay coated rims of quartz grains. Sample is from Shakespeare, no. 3 Moye, 2,252.7 feet, Sec. 20, T8S, R10E. Bar scale = 31 μm. Plane light. (*b*) Diagenetic pyrite (Py) in an ankerite (A) cement cluster. Sample is from Shakespeare, no. 3 Moye, 2,255 feet, Sec. 20, T8S, R10E, located in Inman West Consolidated Field. Bar scale = 31 μm. Plane light.

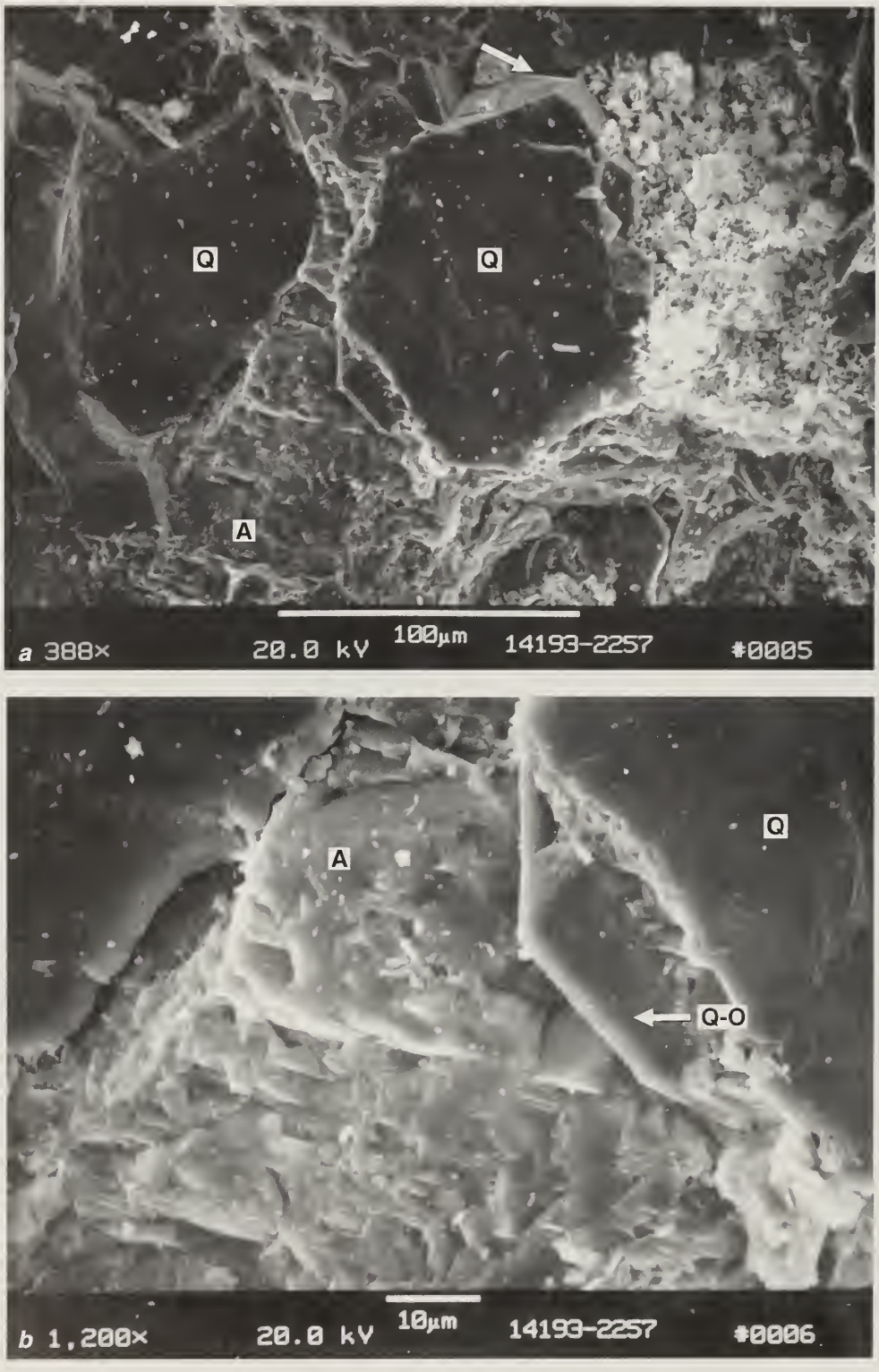

Figure 25 SEM photomicrographs of ankerite cement. (*a*) Two large quartz grains (Q) cemented by pore filling ankerite (A) cement. On the right is a kaolinite (K) cluster formed in place from the diagenetic alteration of a feldspar grain. Note the euhedral quartz overgrowths. This image is enlarged in *b*. Sample is from Shakespeare, no. 3 Moye, 2,257 feet, Sec. 20, T8S, R9E located in Inman West Consolidated Field. (*b*) Detail of figure 25a showing edges of two quartz (Q) grains and ankerite (A) cement. The quartz grain on the right is coated with diagenetic clay, followed by quartz cement, which forms the euhedral overgrowth. Finally, the ankerite cement fills the remaining volume of the pore.

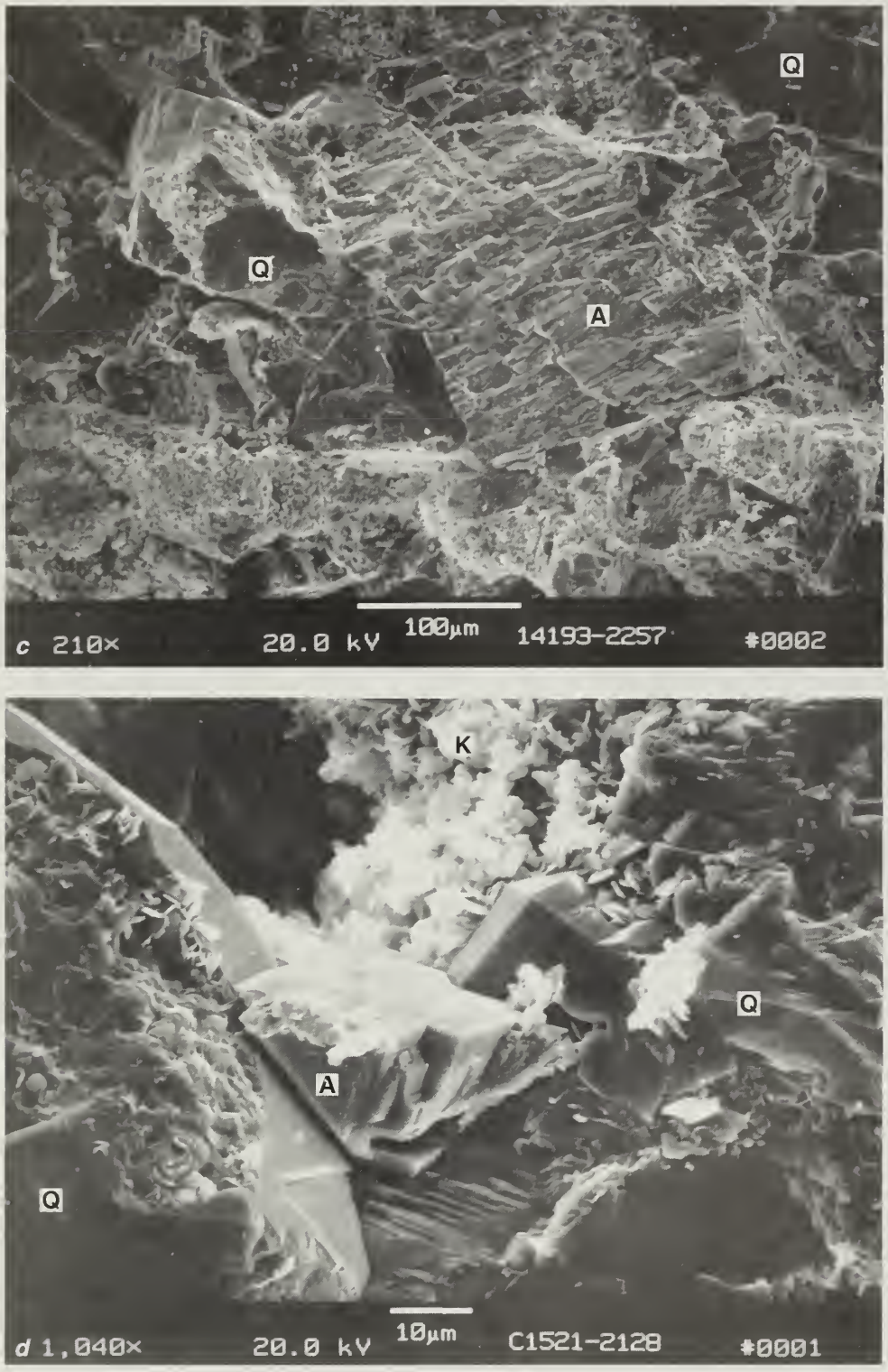

(*c*) Dense patch of ankerite (A) cement, which fills pores in Tar Springs Sandstone. Figure 22d showing kaolinite books and oil drops came from the upper left part of this photo. Sample is from Shakespeare, no. 3 Moye, 2,257 feet, Sec. 20, T8S, R9E, located in Inman West Consolidated Field. (*d*) Ankerite (A) cement formed in pore space on top of quartz overgrowths and diagenetic clays. The clays formed by feldspar alteration. EDX analysis of the ankerite indicates that it is zoned with magnesian-rich cement on the rim and is much more iron-rich in the core (see Appendix C). Sample is from the Carter, no. 3 Williams well, 2,128 feet, Sec. 27, T7S, R10E, located in Inman East Consolidated field.

that the carbonate cementation was influenced by organic matter reactions such as those involved in hydrocarbon generation. In contrast, the ^{13}C data from the Carter no. 3 Williams well samples are consistent with precipitation from a carbon source dominated by marine (inorganic) carbon (Pitman, personal communication). However, the data are not adequate to determine the temperature of formation of the ankerite (Fouke, personal communication).

Porosity Characteristics

Visible estimates of porosity in thin sections and SEM images range from very low in ankerite-cemented sandstones up to about 20% in clean sandstones (figs. 18 through 25). Core analysis data (Appendix E) indicate that typical reservoir rock contains 16% to 18% porosity. About 80% to 85% of that porosity appears in thin section and SEM images to be primary and consists of intergranular volumes that have been reduced primarily by quartz overgrowth cement and patchy ankerite cement and, to a lesser amount by, the precipitation of clay minerals and small amounts of pyrite. The primary pores have pore throats about 10 to 30 μm in diameter and long pore dimensions about the size of the sand grains. The SEM images indicate that the pores are most likely lined by quartz cement with scattered patches or clusters of diagenetic clay minerals, primarily kaolinite, along the pore walls. Kaolinite books or vermiform stacks are common (figs. 19, 20 and 22) and may fill single secondary pores where a feldspar grain has been partially or wholly dissolved (fig. 25a). Between flakes of pore-lining clay minerals, there is microporosity. Capillary forces within areas of microporosity are so strong that hydrocarbons are not likely to be moved from these locations when wells are pumped. Thus, the microporosity is considered to be ineffective in terms of reservoir production. Estimates of microporosity are, at most, a few percent of the rock volume. Secondary porosity (see below) has microporosity that is also considered ineffective.

Secondary pores constitute about 15% to 20% of the reservoir pore volume and are formed primarily by the partial or complete dissolution of feldspar grains and their alteration to clays. The feldspar grains are cloudy or may be completely replaced by clusters of clay minerals that include much microporosity. Partially altered feldspar grains are common and have a Swiss cheese or sieve-like appearance in SEM (fig. 21, a and c; fig. 22b). Diagenetic albite crystals may form on the old feldspar grains or on nearby quartz grains. Secondary pores in the altered feldspar grains are typically less than 1 μm in diameter, which is comparable with the microporosity between flakes of diagenetic clays.

Porosity and permeablity values measured on cores of the Tar Springs Sandstone from 31 wells in or near Inman East Consolidated Field are tabulated and summarized in Appendix E. In these wells the Tar Springs has an average core porosity of 17% and a geometric mean permeability of 107 md. Several of the wells have data from 40-foot long cores, which show an excellent correlation between the SP log and the measured porosity when plotted with electric log data as on figure 26. Clean SP sandstones such as those in the blocky sandstones have the greatest porosity; with values range from 17% to more than 20% in different wells. Sands with shaley SP values in the lower part of coarsening-upward SP log motifs most likely consist of layers of clean sandstone interlayered with some shale stringers and have porosities less than 17%. Other shaley SP sandstones that occur in the cap of fining-upward SP log motifs also have porosities less than 17%. The productive net pay porosity cutoff is probably near 12%. Data from siltstone or shale generally are not available as these lithologies are rarely sampled for core analysis. A few core analyses with porosities less than 8% and permeabilities less than 1 md are presumed to have come from these non-reservoir lithologies.

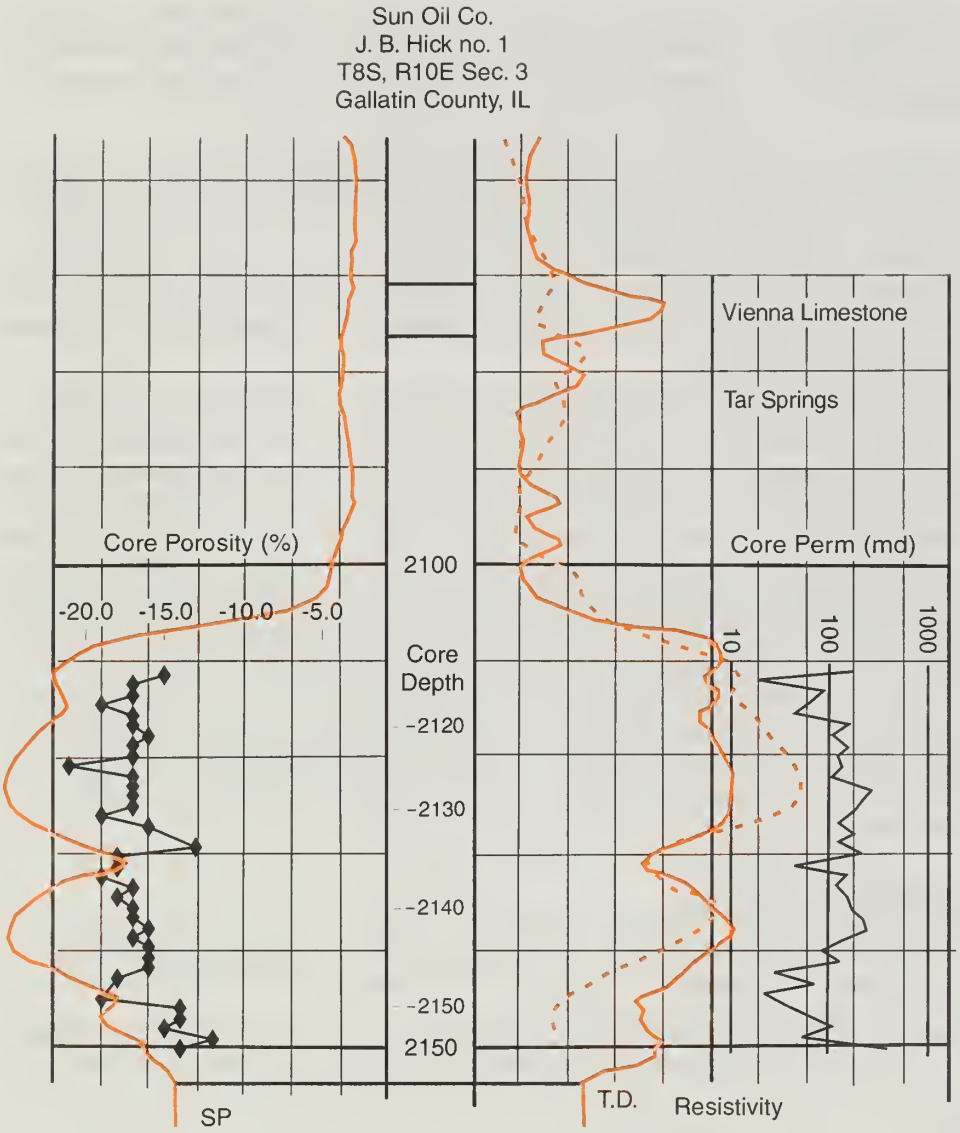

Figure 26 Core porosity and permeability plotted on SP/Resistivity log in the Inman East Consolidated Field, Sun Oil Co., J. B. Hick no. 1 well, Sec. 3, T8S, R10E. Average porosity is 17%, and permeability is 150 md in the clean sand. The Vienna Limestone is from 2,071 feet to 2,076 feet, and the Glen Dean lies below the TD of 2,154 feet.

CONCLUSIONS

The Tar Springs Sandstone is a widespread formation in the Chesterian Series (Mississippian), which was deposited in a tidally influenced, river-dominated delta on the shallow craton of Illinois, Indiana and Kentucky. This study was restricted to Illinois and concentrated on Inman East Consolidated Field in Gallatin County. The Tar Springs Sandstone consists of thick, well-sorted sands formed in delta distributary channels that this study traced across the Illinois Basin in Illinois. They are part of a generally southward-prograding delta complex. The channels in the lower part of the Tar Springs scoured downward as much as 40 feet into the underlying Glen Dean Limestone. Channel sands are stacked, accumulating in places to more than 100 feet of clean sand. Between the channels are interdistributary sandstones and mudstones deposited in bays and tidal flats as crevasse splays and channel overbank

deposits. Thus, the formation is very heterogeneous and variable in thickness. The top of the Tar Springs is commonly shaley. Thin coals or carbonaceous shales have been found in the uppermost shales. The contact with the overlying, fossiliferous, Vienna Limestone is sharp and without apparent relief.

The sandstones of the Tar Springs at Inman East Consolidated Field are composed primarily of fine to very fine-grained, well-sorted, quartzose sand, originally containing 2% to 5% feldspar grains that are now clouded and typically partially altered to clay minerals. The primary cement is quartz, which occurs as euhedral overgrowths on the quartz grains. Later cements include ankerite (an iron-rich dolomite) and a variety of clays consisting of primarily kaolinite and lesser amounts of chlorite, mixed layered illite/smectite and illite.

The hydrocarbon trap for the Tar Springs Sandstone at Inman East Consolidated Field is a combination of fault and fold closure on an uplifted horst block and up-dip stratigraphic pinchout. Inman East Consolidated Field occurs on an arching horst block formed as part of the Wabash Valley Fault System. The eastern pool or compartment of the field has up-dip closure against the Inman East Fault. The three Tar Springs compartments at Inman East Consolidated Field are all delimited by the distribution of channel sandstones and their up-dip closure against laterally equivalent and overlying shales. Porosity in the channel sandstones averages about 17%, and the geometric mean permeability is 107 md. Thinner crevasse splay sandstones, sandstones interbedded with shales, or flaser bedded sandstones have significantly less porosity and permeability. Primary pores constitute about 80% of the pore volume. The remaining secondary pores are largely from feldspar dissolution. Quartz overgrowths, with some diagenetic clay and carbonate minerals, line or fill some of the pores.

REFERENCES

Allen, G.P., D. Laurier and J. Thouvenin, 1979, Etude sedimentologique du Delta de la Mahakam: Compagnie Francaise des Petroles, Notes et Memoires 15, 156 p.

Bell, A.H., M.O. Oros, J. Van Den Berg, O. W. Sherman and R.F. Mast, 1961, Petroleum industry in Illinois, 1960: Illinois State Geological Survey, Illinois Petroleum 75, 121 p.

Butts, C., 1917, Description and correlations of the Mississippian Formations of western Kentucky *in* Mississippian Formations of western Kentucky: Kentucky Geological Survey, Series 5, v. 1, 119 p.

Butts, C., 1925, Geology and mineral resources of the Equality-Shawneetown area (parts of Gallatin and Saline Counties): Illinois State Geological Survey Bulletin 47, 76 p.

Coleman, J.M., 1976, Deltas: Processes of Deposition and Models for Exploration: Continuing Educational Publishing Co., Champaign, IL (now available from Burgess Publishing Co., Minneapolis, MN), 102 p.

Coleman, J.M., and S.M. Gagliano, 1965, Sedimentary structures—Mississippi delta plain, *in* Middleton, G.V., ed., Primary Sedimentary Structures and Their Hydrodynamic Interpretation—Symposium: Society of Economic Paleontologists and Mineralogists, Special Publication no.12, p. 133–148.

Coleman, J.M., and D.B. Prior, 1982, Deltaic environments of deposition; *in* Scholle, P.A., and D. Spearing, eds., Sandstone Depositional Environments: American Association of Petroleum Geologists, Memoir 31, p. 139–170.

Dana, P.L., and E.H. Scobey, 1941, Cross section of Chester of Illinois Basin: Bulletin of the American Association of Petroleum Geologists, v. 25, p. 871–882.

Deer, W.A., R.A. Howie and J. Zussman, 1966, An Introduction to the Rock-forming Minerals: John Wiley and Sons, New York, New York, 528 p.

Devera, J.A., 1991, Geologic map of the Glendale Quadrangle, Johnson and Pope Counties, Illinois: Illinois State Geological Survey, Geological Quadrangle Sheet IGQ-9.

Folk, S.H., and D.H. Swann, 1946, King Oil Field, Jefferson County, Illinois: Illinois State Geological Survey, Report of Investigations 119, 27 p.

Gray, H.H., 1978, Buffalo Wallow Group, Upper Chesterian (Mississippian) of Southern Indiana: Indiana Geological Survey, Occasional Paper 25, 21 p.

Grote, B., 1949, A study of the Tar Springs Sandstone in southeastern Illinois (Ph.D. dissertation): Dept. of Geology, University of Illinois, Urbana-Champaign, Illinois, 59 p.

Hatch, J.R., J.D. King and J.B. Risatti, 1991, Geochemistry of Illinois Basin oils and hydrocarbon source rocks, *in* Leighton, M. W., D. R. Kolata, D. F. Oltz and J. J. Eidel, eds., Interior Cratonic Basins: American Association of Petroleum Geologists, Memoir 51, p. 403–423.

Howard, R.H., 1987, Oil and gas pay maps of Illinois: Illinois State Geological Survey, Illinois Petroleum 84, 64 p.

Howell, J.V., 1948, Geology of Benton Field, Franklin County, Illinois: American Association of Petroleum Geologists Bulletin, v. 32, no. 5, p. 745–766.

Kvale, E.P., and A.W. Archer, 1990, Tidal deposits associated with low-sulfur coals, Brazil Fm. (Lower Pennsylvanian), Indiana: Journal of Sedimentary Petrology, v. 60, no. 4, p. 563–574.

Lamar, J.E., 1925, Geology and mineral resources of the Carbondale Quadrangle: Illinois State Geological Survey Bulletin 48, 172 p.

Lavin, H.L., 1991, The Earth through Time (4th ed.): Saunders College Publishing, Fort Worth, Texas, 649 p.

Leetaru, H.E., 1997, Sequence stratigraphy and resource assessment of the Aux Vases Sandstone in Illinois (Ph.D. dissertation): Department of Geology, University of Illinois, Urbana-Champaign, Illinois, 161 p.

Nelson, W. J., 1995, Structural features in Illinois: Illinois State Geological Survey Bulletin 100, 144 p.

Owen, D.D., 1857, General report of the geologic survey: Geological Survey of Kentucky, v. 1, p. 174 and v. 2, p. 86–87.

Petroleum Information Pipeline Production Reports, 1940 through 1997. Dwights Petroleum Information, Denver, Colorado.

Pitman, J.K., M. Henry and B. Seyler, 1998, Reservoir quality and diagenetic evolution of Upper Mississippian rocks in the Illinois Basin: Influence of a regional hydrothermal fluid-flow event during late diagenesis: U.S. Geological Survey Professional Paper 1597, 24 p.

Potter, P.E., E. Nosow, N.M. Smith, D.H. Swann and F.H. Walker, 1958, Chester cross-bedding and sandstone trends in Illinois Basin: American Association of Petroleum Geologists Bulletin, v. 42, no. 5, p. 1013–1046.

Seilacher, A., 1967, Bathymetry of trace fossils: Marine Geology, v. 5, p. 413–428.

Seilacher, A., 1978, Use of trace fossil assemblages for recognizing depositional environments, *in* Basan, P.B., ed., Trace Fossil Concepts: Society of Economic Paleontologists and Mineralogists, Short Course No. 5, p. 185–201.

Shaver, R.H., C.H. Ault, A.M. Burger, D.D. Carr, J.B. Droste, D.L. Eggert, H.H. Gray, D. Harper, N.R. Hasenmueller, W.A. Hasenmueller, A.S. Horowitz, H.C. Hutchinson, B. Keith, S.J. Keller, J. Weller, J.M.,B. Patton, D.B. Rexroad and C.E. Wier, 1986, Compendium of Paleozoic rock-unit stratigraphy in Indiana—a revision: Indiana Department of Natural Resources, Geological Survey Bulletin 59, 203 p.

Simon, J.A., and M.A., Hopkins, 1966, Sedimentary structures and morphology of Late Paleozoic sand bodies in southern Illinois: Illinois State Geologic Survey Guidebook 7, 67 p.

Smith, L.B., 1996, High-resolution sequence stratigraphy of Late Mississippian (Chesterian) mixed carbonates and siliciclastics, Illinois Basin (Ph.D. dissertation): Department of Geology, Virginia Polytechnic Institute and State University, Blacksburg, Virginia, 146 p.

Swann, D.H., 1963, Classification of Genevievian and Chesterian (Late Mississippian) rocks in Illinois: Illinois State Geologic Survey, Report of Investigations 216, 91 p.

Swann, D.H., 1964, Late Mississippian rhythmic sedimentation of the Mississippi Valley: American Association of Petroleum Geologists Bulletin, v. 79, p. 2471–2483.

Treworgy, J.D., W. J. Nelson, L.C. Furer and B.D. Keith, 1997, Subsurface sequence stratigraphy of Early Chesterian (Mississippian) mixed carbonates and siliciclastics, Illinois Basin: Eastern Section, American Association of Petroleum Geologists, Abstracts and Program, v. 14, p. 91–92.

Weller, J.M., and G.F. Ekblaw, 1940, Preliminary geologic map of parts of the Alto Pass, Jonesboro, and Thebes Quadrangles, Union, Alexander, and Jackson Counties, Illinois State Geological Survey, Report of Investigations 70, 26 p.

Weller, J.M., R.M. Grogan and F.E. Tippie, 1952, Geology of the fluorspar deposits of Illinois: Illinois State Geological Survey Bulletin 76, 147 p.

Weller, S., 1920, The Chester Series in Illinois: Journal of Geology, v. 28, p. 281–303 and 395–416.

Wescott, W.A., 1976, A model for shallow marine epeiric sea deposition: the Tar Springs Sandstone (Upper Mississippian) in southern Illinois (Master's thesis): Department of Geology, Southern Illinois University, Carbondale, Illinois, 140 p.

Wescott, W.A., 1982, Depositional setting and history of the Tar Springs Sandstone (Upper Mississippian), southern Illinois: Journal of Sedimentary Petrology, v. 52, no. 2, p. 353–366.

Willman, H.B., E. Atherton, T.C. Bushback, C. Collinson, J.C. Frye, M.E. Hopkins, J.A. Lineback and J.A. Simon, 1975, Handbook of Illinois Stratigraphy: Illinois State Geological Survey Bulletin 95, 261 p.

Workman, L. E., 1940, Sub-surface geology of Chester Series in Illinois: American Association of Petroleum Geologists Bulletin, v. 24, p. 209–224.

Worthen, A. H., 1860, Remarks on the discovery of terrestrial flora in the Mountain Limestone of Illinois (abs.): American Association for the Advancement Science Proceedings, v. 13, 312–313.

Appendix A Tar Springs Core Material in or near Inman East Consolidated Field

location	operator and farm	depth	type	ISGS core no.
White County				
15 7S 10E SE SW	J.S. Carter, Harlem no. 1	2191-2195	perm plugs	C-5736
15 7S 10E SE SE SE	Gulf, J. Harlem no. 1	2195-2205	core chips	C-556
Gallatin County				
27 7S 10E SW SW SE	Carter, Williams no. 1	2124-2130	core chips	C-1762
27 7S 10E NE SW SE	Carter, Williams no. 3	2115-2134	core chips	C-1521
30 7S 10E NE NE SW	Wausau Petrol., Mobly no. 1	2180-2185	perm plugs	C-5487
20 8S 9E NW NW NE	Shakespeare, no. 3 Moye	2246-2258	core	C-14193
3 8S 10E NW CNW	Sohio, Teb no. 19	2117-2142	core plugs	C-5263
11 8S 10E NE SE NW	Carter, Crawford no. 1	2084-2091	core chips	C-644
15 8S 10E SW SW NW	R. Halbert, Curry no. 1	2057-2074	core chips	C-657

Appendix B Inman East Consolidated Field—Visual Petrographic Estimates of Mineral Content and Porosity Types (volume percent)

short API	well name/IP	location	ISGS core no.	depth	facies[1]	grain size[2]	bedding[3]	quartz	clay and altered feldspar[4]	other[5]	carbonate	porosity primary	porosity secondary
554	Carter Oil no. 3 Williams	27 7S 10E	C-521	2,115	top FU	vf-f Ss	pl	80	8	1 to 2	tr	5	5?
	IP = 181 BOD			2,116	top blky	vf-f Ss	pl	70	7 to 10	tr	tr to 1	14	6
				2,117	top blky	vf-f Ss	pl	74	12	1	tr to 1	10	2
				2,118	top blky	vf-f Ss	pl	80	7 to 8	tr	tr to 1	7	2
				2,119	top blky	vf-f Ss	pl	76	11	6	1	8	2
				2,121	blky	vf-f Ss	pl	80	2+	5	2	8	2
				2,125	blky	vf-f Ss	pl	68	1 to 2	1 to 2	10	17	3
				2,126	blky	vf-f Ss	pl	60	4 to 6	2	15 to 20	13	2
				2,127	blky	vf-f Ss		69	5 to 9	2	12 to 15	10	2
				2,128	SP break	vf-f Ss	pl	75	3 to 5?	2 to 3	15 to 20	5	1
				2,129	top blky	vf-f Ss	pl	70 to 76	2 to 4	1 to 2	12 to 15	7	3
				2,130	blky	vf-f Ss	pl	71	4 to 6	1 to 2	5 to 8	10	3
				2,131	blky	vf-f Ss	pl	75	6 to 9	2 to 3	2 to 5	5	2
				2,132	blky	vf-f Ss	pl	70	4 to 8	2 to 5	5 to 8	13	3
				2,133	base blky	vf-f Ss	pl	75	5 to 8	2 to 3	8 to 10	4	1
222	Leach no. 1 Curray	15 8S 10E	C-657	2,057	blky	f Ss	rpl	78	8	2	2	8	2
	IP = 240 BOD			2,060	blky	f Ss		70	10	2	3	10	5
5736	Carter no. 1A Crawford	11 8S 10E	C-644	2,085	blky	f Ss	pl					16	4
	IP = 9 BOD			2,086	blky	mf Ss	rpl	75 to 77	2 to 3	1	2 to 3	17	3
				2,087	blky	mf Ss	rpl	75 to 80	1 to 2	1 to 2	1	14	3
				2,088	blky	f Ss	rpl	75 to 80	2 to 5	1	1 to 2	17	3
				2,089	blky	mf Ss	xbed	75 to 80	2 to 5	1	2 to 4	17	3
				2,091	blky	m Ss	lam	75 to 80	4 to 5		tr	11	2
2072	Sohio no. 19 TEB	3 8S 10E	C-5263	2,117	top blky	vf-f Ss		74	3 to 6	3 to 5	1 to 2	13	2
	IP = 0 BOD			2,121	top blky	f Ss	pl	78	2 to 4	2 to 3	1 to 2	15	3
				2,125	blky	vf-f Ss	pl	73	3 to 5?	1 to 2	1	16	2
				2,128	blky	vf-f Ss	pl	75	3 to 5?	3 to 4	1	16	2
				2,131	blky	vf-f Ss	pl	80	2 to 5	1 to 2	1	14	2
				2,133	blky	f Ss	pl	75	2 to 3	1 to 2	2 to 3	14	3
				2,136	blky	f Ss	pl	70 to 75	5 to 9	1 to 2	1 to 2	10	4
				2,138	blky	f Ss	hom-pl	70 to 75	5 to 8		1 to 2	13	3
				2,142	blky	vf-f Ss	hom-pl	70 to 75	4 to 6		1?	14	3
2800	Shaw no. 1 Mobly	30 7S 10E	C-5487	2,181	blky	f Ss	hom				2 to 4	10	3
	IP = 6 BOD			2,182	blky	f Ss	xbed	73 to 79	4 to 7	1	2 to 4	11	3
				2,183	blky	f Ss	hom	76	5 to 7	2	1	14	3
				2,184	blky	mf Ss	hom	70 to 75	2 to 3	1 to 2	2 to 3	13	5
				2,185	blky	mf Ss	hom	70 to 75	5 to 7	2 to 3	1	13	5
				2,186	blky	mf Ss	hom	70 to 75	4 to 6	tr	1	12	3

433	Gulf no. 1 Harlem	15 7S 10E	C-556	2,195	no log	v-f Ss	pl	75 to 80	4 to 6	1 to 2	2 to 3	9	4
IP = 0 BOD				2,197	no log	vf-f Ss	rpl	75 to 80	4 to 6	1.5	2 to 3	10	4
				2,198	no log	vf-f Ss	rpl	75 to 80	2 to 4	1	1	15	2
				2,199	no log	vf-f Ss	pl	75 to 80	2 to 4	1	tr	13	2
				2,200	no log	f Ss	pl	75 to 80	2 to 3	?	2 to 5	11	2
				2,201	no log	vf-f Ss	pl	75 to 80	2 to 3	?	4 to 6	10	3
				2,202	no log	vf-f Ss	hom	75 to 80	3 to 4		6 to 8	9	2
				2,203	no log	vf-f Ss	rpl	75 to 80	2 to 4	1	2 to 5	10	3
				2,204	no log	f Ss	rpl	75 to 80	2 to 3	1	2 to 5	10	3
				2,205	no log	vf-f Ss	rpl	70 to 75	4 to 5		5 to 8	10	3
352	Carter Oil no. 1 Williams	27 7S 10E	C-1762	2,124	top FU	f Ss	pl-rpl	80 to 85	3 to 5	4 to 6	6 to 8	2	?
IP = 0 BOD				2,125A	silty	silt	pl	62	5 to 7	24	5	2	?
				2,125B	silty	f Ss	pl	80	3 to 4	5	8 to 10	3	?
				2,126	flaser	vf-f Ss	pl	75	11 to 18	5 to 8	tr	1	?
				2,127B4	flaser	vf-f Ss	rpl	80	7 to 10	5 to 8	2	3	?
				2,127A11	flaser	f Ss	rpl	74	5 to 7	5 to 7	7 to 11	5 to 8	?
				2,128B5	flaser	vf-f Ss	rpl	82	5 to 7	8 to 10	tr	1 to 2	?
				2,128A5	flaser	vf Ss	rpl	80	9 to 12	6	tr	1	?
				2,128C5	flaser	f Ss	rpl	81	3 to 5	5	3 to 4	4 to 6	?
7338	Carter no. 1 Harlem	15 7S 10E	C-5736	2,091.5	blky	f Ss	hom	70 to 75	3 to 5	1	1	16	3
IP = 0 BOD				2,093.5	blky	vf Ss	pl	70 to 80	3 to 4		1	12	3
				2,094.5	blky	vf Ss	hom	70 to 75	4 to 6		1	16	3
				2,095.5	base blky	vf Ss	lam	70 to 80	5 to 8		1	11	3

[1] Facies: FU, fining-upward; blky, blocky; SP, spontaneous potential.
[2] Grain size: m, medium; mf, medium fine; f, fine; vf, very fine; Ss, sandstone.
[3] Bedding: pl, planar laminated; rpl, rippled; xbed, cross-bedded; lam, laminated; hom, homogeneous.
[4] Clay and altered feldspar, diagenic clay, altered feldspar.
[5] Other: lithic clasts, pyrite, heavy minerals and detrital silt and clay; tr, trace amount.

Appendix C SEM-EDX Analyses of Ankerite, Calcite, and Chlorite

ankerite cements core ID	depth	$Ca(Fe,Mg,Mn)(CO_3)_2$ atom percents[1]				atomic ratios					
(see Appendix A)		Ca	Fe	Mg	Mn	Ca/Ca	Fe/Ca	Mg/Ca	Mn/Ca	Fe/Mg	remarks
C-1762	2,124	25.89	7.84	11.05	1.08	1	0.30	0.43	0.04	0.71	
C-1762	2,124	17.84	5.21	13.07	0.63	1	0.29	0.73	0.04	0.40	
C-1762	2,124	18.19	5.84	13.65	0.76	1	0.32	0.75	0.04	0.43	
C-14193	2,257.6	19.78	8.47	11.79	0.68	1	0.43	0.60	0.03	0.72	
C-14193	2,257.6	24.86	8.84	4.7	0.9	1	0.36	0.19	0.04	1.88	
C-14193	2,257.6	24.69	8.88	5.6	0.61	1	0.36	0.23	0.02	1.59	
C-14193	2,257.6	21.15	6.18	21.08	0.85	1	0.29	1.00	0.04	0.29	
C-14193	2,257.6	23.84	8.21	15.74	0.79	1	0.34	0.66	0.03	0.52	
C-556	2,205	25.66	6.11	15.19	0.53	1	0.24	0.59	0.02	0.40	
C-556	2,205	25.81	13.3	6.11	n/d[2]	1	0.52	0.24		2.18	
C-556	2,205	29.2	8.27	7.67	n/d	1	0.28	0.26		1.08	
C-556	2,205	24.74	12.38	8.88	n/d	1	0.50	0.36		1.39	
C-556	2,205	36.67	7.95	3.09	n/d	1	0.22	0.08		2.57	
C-556	2,205	29.2	8.27	7.67	n/d	1	0.28	0.26		1.08	
C-556	2,205	25.81	13.3	6.61	n/d	1	0.52	0.26	2.01		
C-1521	2,128	25.84	8.07	11.76	0.61	1	0.31	0.46	0.02	0.69	
C-1521	2,128	26.77	8.35	11.67	1.08	1	0.31	0.44	0.04	0.72	
C-1521	2,128	24.88	8.11	11.44	0.56	1	0.33	0.46	0.02	0.71	
C-1521	2,128	15.53	4.81	9.73	n/d	1	0.31	0.63		0.49	outer surface-top
C-1521	2,128	16.44	4.63	11.14	n/d	1	0.28	0.68		0.42	outer layer-side
C-1521	2,128	16.45	4.64	11.13	n/d	1	0.28	0.68		0.42	adj check-outer layer-side
C-1521	2,128	21.19	6.77	5.03	n/d	1	0.32	0.24		1.35	2nd layer
C-1521	2,128	20.43	6	5.36	n/d	1	0.29	0.26		1.12	adj. 2nd layer
C-1521	2,128	21.15	8.71	1.58	n/d	1	0.41	0.07		5.51	3rd layer
C-1521	2,128	19.92	8.27	4.31	n/d	1	0.42	0.22		1.92	adj. 3rd layer
C-1521	2,128	22.71	8.88	1.09	n/d	1	0.39	0.05		8.15	4th layer
C-1521	2,128	20.05	8.22	2.15	n/d	1	0.41	0.11		3.82	adj 4th layer
C-1521	2,126	28.49	13.95	4.95	n/d	1	0.49	0.17		2.82	
C-1521	2,126	27.77	10.5	8.98	n/d	1	0.38	0.32		1.17	
					average	1	0.30	0.34		0.88	

Appendix C SEM-EDX Analyses *continued*

calcite cements core ID (see Appendix A)	depth	$(Ca,Fe,Mg)CO_3$ atomic percents Ca	Fe	Mg	Mn	atomic ratios Ca/Ca	Fe/Ca	Mg/Ca	Mn	Fe/Mg
C-556	2,205	46.38	0.96	1.33	0.33	1	0.02	0.03	0.01	0.72

chlorite cements core ID (see Appendix A)	depth	$(Mg,Al,Fe)_{12}\{(Si,Al)_8O_{20}\}(OH)_{16}$ atomic percents Mg	Al	Fe	Ca	Si	K	atomic ratios Fe/Mg
C-14193	2,257.6	7.79	n/c[3]	16.59	0.47	16.76	n/d	2.13
C-1521	2,128	3.79	13.67	5.88	0.57	15.12	n/d	1.55
C-556	2,205	0.58	6.86	14.68	0.37	17.19	n/d	25.31
C-1521	2,126	0.92	8.79	4.91	n/d	n/c	0.78	5.34

[1] from Deer et al., 1966.
[2] n/d, not detected.
[3] n/c, not counted.

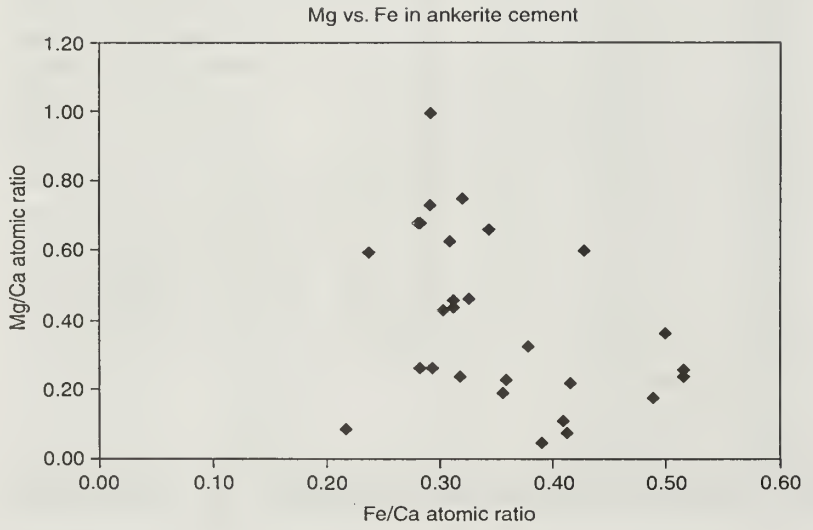

Appendix D Carbon and Oxygen Isotope Analyses[1] of Carbonate Cements

sample well	location	depth	calcite[2]		dolomite		ISGS	
			$\delta^{18}O$	$\delta^{13}C$	$\delta^{18}O$	$\delta^{13}C$	core no.	est. ankerite %
Gulf no.1 Harlem	15 7S 10E	2,205	-8.18	-7.22	-6.35	-2.69	C-556	5 to 8%
Gulf no.1 Harlem	15 7S 10E	2,202	-7.1	-6.12	-6.39	-2.8	C-556	4 to 6%
Gulf no.1 Harlem	15 7S 10E	2,202	-7.19	-6.35			C-556	4 to 6%
Carter Oil no. 1A Crawford	11 8S 10E	2,086	-5.43	-6.62	-4.54	-3.53	C-644	2 to 3%
Carter Oil no. 1A Crawford	11 8S 10E	2,086	-5.24	-6.61	-4.69	-2.34	C-644	2 to 3%
Carter no. 3 Williams	27 7S 10E	2,125	-7.02	-2.02	-6.75	-1.9	C-1521	~10%
Carter no. 3 Williams	27 7S 10E	2,126	-6.62	-1.97	-6.6	-1.95	C-1521	15 to 20%
Carter no. 3 Williams	27 7S 10E	2,126	-6.66	-2			C-1521	15 to 20%
Carter no. 3 Williams	27 7S 10E	2,127	-6.29	-2.43	-6.08	-2.17	C-1521	12 to 15%
Carter no. 3 Williams	27 7S 10E	2,128	-6.15	-2.36	-5.97	-2.17	C-1521	15 to 20%
Carter no. 3 Williams	27 7S 10E	2,128		-6.13	-2.13		C-1521	15 to 20%
Carter no. 3 Williams	27 7S 10E	2,129	-6.27	-2.42	-6.08	-2.21	C-1521	12 to 15%
Carter no. 3 Williams	27 7S 10E	2,129			-6.39	-2.18	C-1521	12 to 15%

[1] Analyses were performed by U.S. Geological Survey.

[2] Carbon and oxgen isotope ratios were obtained by a timed-dissolution procedure based on the different reaction rates for the different minerals. The CO_2 evolved during the first hour after reaction with phosphoric acid is attributed to calcite, and gas recovered after several hours of reaction is attributed to dolomite.

Appendix E Inman East Consolidated Field Core Analysis Data

API number	well name	no.	location	depth	porosity percent	air permeability horiz	air permeability vert	oil sat	water sat	avg por	geom mean perm	median horiz. perm
120590055400	Williams	3	27 7S 10E	2,115.5	13.6	6.5	2.8			15	22	20
120590055400	Williams	3	27 7S 10E	2,116.5	13.0	3.5	1.1					
120590055400	Williams	3	27 7S 10E	2,117.5	12.1	5.1	2.8					
120590055400	Williams	3	27 7S 10E	2,118.5	12.1	51	2.7					
120590055400	Williams	3	27 7S 10E	2,119.5	17.9	18	10					
120590055400	Williams	3	27 7S 10E	2,120.5	14.7	20	7.4					
120590055400	Williams	3	27 7S 10E	2,121.5	19.4	250	55					
120590055400	Williams	3	27 7S 10E	2,125.5	19.8	201	81					
120590055400	Williams	3	27 7S 10E	2,126.5	14.6	60	37					
120590055400	Williams	3	27 7S 10E	2,127.5	12.6	35	40					
120590055400	Williams	3	27 7S 10E	2,128.5	12.1	6.1	4.4					
120590055400	Williams	3	27 7S 10E	2,129.5	14.3	15	6.1					
120590055400	Williams	3	27 7S 10E	2,130.5	16.0	31	12					
120590055400	Williams	3	27 7S 10E	2,131.5	14.1	6.9	31					
120590055400	Williams	3	27 7S 10E	2,132.5	14.4	24	28					
120590055400	Williams	3	27 7S 10E	2,133.5	14.3	20	13					
120590057600	J.H. Tedford	1	33 7S 10E	2,121.5	17.1	35		19.9	30.4	18	39	37
120590057600	J.H. Tedford	1	33 7S 10E	2,122.5	16.8	80		25	28			
120590057600	J.H. Tedford	1	33 7S 10E	2,123.5	18.6	62	38	19.9	31.8			
120590057600	J.H. Tedford	1	33 7S 10E	2,124.5	19.0	37		26.9	33.4			
120590057600	J.H. Tedford	1	33 7S 10E	2,125.5	18.7	14		23.6	34.8			
120590057700	Tedford	2	33 7S 10E	2,245.3	16.7	43		21	40.7	17	39	35
120590057700	Tedford	2	33 7S 10E	2,246	17.2	35		18.6	36.6			
120590057700	Tedford	2	33 7S 10E	2,246.8	14.6	25		17.8	49.3			
120590058100	Busiek	C-5	34 7S 10E	2,119.5	16.9	16		17.7	34.3	16	83	99
120590058100	Busiek	C-5	34 7S 10E	2,120.5	16.2	67		20.2	21.6			
120590058100	Busiek	C-5	34 7S 10E	2,121.5	14.3	99		22.4	22.4			
120590058100	Busiek	C-5	34 7S 10E	2,122.5	19.7	121		21.3	21.8			
120590058100	Busiek	C-5	34 7S 10E	2,124.5	15.2	145		22.4	31.6			
120590058100	Busiek	C-5	34 7S 10E	2,125.5	16.9	156		20.1	28.4			
120590058100	Busiek	C-5	34 7S 10E	2,126.5	17.5	71		19.4	33.2			
120590058100	Busiek	C-5	34 7S 10E	2,127.5	16.1	112		21.2	36			
120590058100	Busiek	C-5	34 7S 10E	2,128.5	18.3	59		19.1	40.4			
120590058100	Busiek	C-5	34 7S 10E	2,129.5	17.3	39		20.2	35.9			
120590058100	Busiek	C-5	34 7S 10E	2,131.5	15.3	65		18.3	38			
120590058100	Busiek	C-5	34 7S 10E	2,132.5	15.4	45		17.5	46.1			
120590058100	Busiek	C-5	34 7S 10E	2,133.5	16.2	155		21.8	30.4			

Continued

Appendix E *Continued* Inman East Consolidated Field Core Analysis Data

API number	well name	no.	location	depth	porosity percent	air permeability horiz	air permeability vert	oil sat	water sat	avg por	geom mean perm	median horiz perm
120590058100	Busiek	C-5	34 7S 10E	2,134.5	15.6	51		19.9	25.7			
120590058100	Busiek	C-5	34 7S 10E	2,135.5	15.9	129		20.8	31.5			
120590058100	Busiek	C-5	34 7S 10E	2,136.5	13.2	157		16.7	33.4			
120590058100	Busiek	C-5	34 7S 10E	2,137.5	16.3	154		20.2	31.9			
120590058200	Busiek	C-4	34 7S 10E	2,122.5	17.6	56		19.2	44.8	18	94	98
120590058200	Busiek	C-4	34 7S 10E	2,123.5	18.6	98		22.6	43.5			
120590058200	Busiek	C-4	34 7S 10E	2,124.5	16.7	69		20.4	33			
120590058200	Busiek	C-4	34 7S 10E	2,125.5	19.5	118		22.6	38.5			
120590058200	Busiek	C-4	34 7S 10E	2,126.5	15.3	86		28.9	34.6			
120590058200	Busiek	C-4	34 7S 10E	2,118.5	17.6	56		19.2	44.8			
120590058200	Busiek	C-4	34 7S 10E	2,119.5	18.6	98		22.6	43.5			
120590058200	Busiek	C-4	34 7S 10E	2,120.5	16.7	69		20.4	33			
120590058200	Busiek	C-4	34 7S 10E	2,121.5	19.5	118		22.6	38.5			
120590058200	Busiek	C-4	34 7S 10E	2,122.5	15.3	86		20.9	34.6			
120590058200	Busiek	C-4	34 7S 10E	2,124	18.3	80		18.6	46.5			
120590058200	Busiek	C-4	34 7S 10E	2,125	19.9	118		18.1	42.7			
120590058200	Busiek	C-4	34 7S 10E	2,126	20.3	102		15.8	48.3			
120590058200	Busiek	C-4	34 7S 10E	2,127.5	20.4	157		19.7	50.6			
120590058200	Busiek	C-4	34 7S 10E	2,128.5	17.1	123		19.3	48.5			
120590058200	Busiek	C-4	34 7S 10E	2,129.5	18.9	43		16.9	47			
120590058200	Busiek	C-4	34 7S 10E	2,130.5	19.0	95		14.7	34.2			
120590058200	Busiek	C-4	34 7S 10E	2,132	17.2	195		15.1	34.9			
120590058200	Busiek	C-4	34 7S 10E	2,133	18.2	182		9.8	32.4			
120590058200	Busiek	C-4	34 7S 10E	2,134	18.2	178		15.4	39			
120590058200	Busiek	C-4	34 7S 10E	2,135	20.1	165		15.9	39.7			
120590058200	Busiek	C-4	34 7S 10E	2,136.5	18.3	109		0	58.7			
120590058200	Busiek	C-4	34 7S 10E	2,137.5	18.0	33		0	61.2			
120590058200	Busiek	C-4	347S 10E	2,138.5	19.0	54		13.7	34.2			
120590058300	Busiek	C-2	34 7S 10E	2,122.5	16.8	110		22	36.9	16	118	114
120590058300	Busiek	C-2	34 7S 10E	2,123.5	18.5	118		20	40.5			
120590058300	Busiek	C-2	34 7S 10E	2,124.5	19.1	227		20.4	38.2			
120590058300	Busiek	C-2	34 7S 10E	2,125.5	13.8	48		7.3	49.3			
120590058300	Busiek	C-2	34 7S 10E	2,126.5	14.6	75		12.3	46.8			
120590058300	Busiek	C-2	34 7S 10E	2,129.5	16.3	146		18.2	45.4			
120590058300	Busiek	C-2	34 7S 10E	2,130.5	15.4	225		22.1	31.2			
120590058300	Busiek	C-2	34 7S 10E	2,131.5	15.2	108		21.7	32.2			
120590058500	Busiek	11-B	34 7S 10E	2,124.5	13.5	11		20	25	17	52	71
120590058500	Busiek	11-B	34 7S 10E	2,125.5	14.4	15		20.8	21.5			

120590058500	Busiek	11-B	34 7S 10E	2,126.5	17.0	27	18.2	33				
120590058500	Busiek	11-B	34 7S 10E	2,127.5	17.1	23	0	76				
120590058500	Busiek	11-B	34 7S 10E	2,128.5	11.2	28	23.2	22.3				
120590058500	Busiek	11-B	34 7S 10E	2,129.5	16.7	102	18	25				
120590058500	Busiek	11-B	34 7S 10E	2,130.5	17.3	53	17.4	34.1				
120590058500	Busiek	11-B	34 7S 10E	2,131.5	18.3	43	18.1	26.2				
120590058500	Busiek	11-B	34 7S 10E	2,132.5	19.2	84	15.1	31.2				
120590058500	Busiek	11-B	34 7S 10E	2,133.5	18.2	96	15.9	33.5				
120590058500	Busiek	11-B	34 7S 10E	2,134.5	19.2	89	19.3	31.2				
120590058500	Busiek	11-B	34 7S 10E	2,135.5	18.7	25	16.6	34.8				
120590058500	Busiek	11-B	34 7S 10E	2,136.5	16.5	103	18.8	30.9				
120590058500	Busiek	11-B	34 7S 10E	2,137.5	17.8	144	16.3	31.5				
120590058500	Busiek	11-B	34 7S 10E	2,138.5	17.7	71	16.4	29.4				
120590058500	Busiek	11-B	34 7S 10E	2,139.5	17.8	71	14.6	37.1				
120590058500	Busiek	11-B	34 7S 10E	2,140.5	15.2	165	11.8	15.2				
120590058900	Busiek	B-2	34 7S 10E	2,128.5	15.6	111	25.6	27	18	129	112	
120590058900	Busiek	B-2	34 7S 10E	2,129.5	17.9	106	24	26.8				
120590058900	Busiek	B-2	34 7S 10E	2,130.5	18.4	71	22.8	31.4				
120590058900	Busiek	B-2	34 7S 10E	2,131.5	19.8	253	24.8	29.3				
120590058900	Busiek	B-2	34 7S 10E	2,132.5	16.3	166	25.8	25.8				
120590059000	Busick	1B	34 7S 10E	2,122.5	14.3	4.4	8.4	37.8	18	20	23	
120590059000	Busick	1B	34 7S 10E	2,123.5	14.9	3.5	18.1	31				
120590059000	Busick	1B	34 7S 10E	2,124.5	16.1	5	14.3	49.6				
120590059000	Busick	1B	34 7S 10E	2,125.5	19.4	3	8.2	59.5				
120590059000	Busick	1B	34 7S 10E	2,126.5	18.5	38	19.6	39.2				
120590059000	Busick	1B	34 7S 10E	2,127.5	20.3	156	22.2	29.6				
120590059000	Busick	1B	34 7S 10E	2,128.5	16.9	180	27.2	23.1				
120590059000	Busick	1B	34 7S 10E	2,129.5	18.8	92	22.9	25.6				
120590059000	Busick	1B	34 7S 10E	2,130.5	18.5	74	29.7	21.1				
120590059000	Busick	1B	34 7S 10E	2,131.5	18.9	7.4	20.6	25.6				
120590060600	Stoffieth	4	34 7S 10E	2,122.5	17.0	17	15.9	39.4	18	92	100	
120590060600	Stoffieth	4	34 7S 10E	2,123.5	14.6	21	11.6	42.5				
120590060600	Stoffieth	4	34 7S 10E	2,124.5	18.1	28	19.3	35.9				
120590060600	Stoffieth	4	34 7S 10E	2,125.5	17.7	44	18.1	32.8				
120590060600	Stoffieth	4	34 7S 10E	2,126.5	18.4	109	20.6	34.8				
120590060600	Stoffieth	4	34 7S 10E	2,127.5	19.6	98	19.9	40.3				
120590060600	Stoffieth	4	34 7S 10E	2,128.5	19.5	106	20	39				
120590060600	Stoffieth	4	34 7S 10E	2,129.5	19.5	83	21	39				
120590060600	Stoffieth	4	34 7S 10E	2,130.5	16.8	81	15.5	32.8				
120590060600	Stoffieth	4	34 7S 10E	2,131.5	17.9	8.6	12.3	45.3				
120590060600	Stoffieth	4	34 7S 10E	2,132.5	18.6	62	19.4	33.4				
120590060600	Stoffieth	4	34 7S 10E	2,133.2	22.0	82	16.4	40.8				
120590060600	Stoffieth	4	34 7S 10E	2,140.5	18.5	512	17.6	62.2				

Continued

Appendix E *Continued* Inman East Consolidated Field Core Analysis Data

API number	well name	no.	location	depth	porosity percent	air permeability horiz	air permeability vert	oil sat	water sat	avg por	geom mean perm	median horiz perm
120590060600	Stoffieth	4	34 7S 10E	2,141.5	19.1	220		21	33			
120590060600	Stoffieth	4	34 7S 10E	2,142.5	17.8	298		18	35.4			
120590060600	Stoffieth	4	34 7S 10E	2,143.5	18.0	403		20.6	25.6			
120590060600	Stoffieth	4	34 7S 10E	2,144.5	19.6	381		21.4	24			
120590060600	Stoffieth	4	34 7S 10E	2,145.5	18.0	83		18.9	33.9			
120590060600	Stoffieth	4	34 7S 10E	2,146.5	17.3	68		17.9	37.6			
120590060600	Stoffieth	4	34 7S 10E	2,147.5	20.2	105		18.3	32.2			
120590060600	Stoffieth	4	34 7S 10E	2,148.5	19.5	149		13.3	37.4			
120590060600	Stoffieth	4	34 7S 10E	2,149.5	17.4	102		10.9	37.4			
120590060600	Stoffieth	4	34 7S 10E	2,150.5	17.1	115		19.9	36.8			
120590060600	Stoffieth	4	34 7S 10E	2,151.3	20.1	162		16.4	37.8			
120590081600	Big Barn	25	3 8S 10E	2,121	17.0	141.0		28	28	17	151	140
120590081600	Big Barn	25	3 8S 10E	2,122	17.0	97.0		25	29			
120590081600	Big Barn	25	3 8S 10E	2,123	18.0	149.0		27	25			
120590081600	Big Barn	25	3 8S 10E	2,124	16.0	84.0		29	22			
120590081600	Big Barn	25	3 8S 10E	2,125	19.0	603.0		21	25			
120590081600	Big Barn	25	3 8S 10E	2,126	16.0	262.0		19	27			
120590081600	Big Barn	25	3 8S 10E	2,127	16.0	155.0		24	21			
120590081600	Big Barn	25	3 8S 10E	2,128	15.0	219.0		28	21			
120590081600	Big Barn	25	3 8S 10E	2,129	16.0	270.0		24	21			
120590081600	Big Barn	25	3 8S 10E	2,130	16.0	243.0		23	23			
120590081600	Big Barn	25	3 8S 10E	2,131	17.0	123.0		21	24			
120590081600	Big Barn	25	3 8S 10E	2,132	17.0	113.0		27	19			
120590081600	Big Barn	25	3 8S 10E	2,133	15.0	59.0		23	27			
120590081600	Big Barn	25	3 8S 10E	2,134	16.0	117.0		26	22			
120590081600	Big Barn	25	3 8S 10E	2,135	18.0	120.0		25	26			
120590081600	Big Barn	25	3 8S 10E	2,136	18.0	108.0		21	27			
120590081600	Big Barn	25	3 8S 10E	2,137	20.0	140.0		19	27			
120590082000	Hick	1	3 8S 10E	2,117	15.0	180.0		21	26	17	108	128
120590082000	Hick	1	3 8S 10E	2,118	17.0	18.0		17	38			
120590082000	Hick	1	3 8S 10E	2,119	17.0	91.0		18	38			
120590082000	Hick	1	3 8S 10E	2,120	19.0	65.0		18	31			
120590082000	Hick	1	3 8S 10E	2,121	17.0	45.0		21	27			
120590082000	Hick	1	3 8S 10E	2,122	17.0	152.0		22	27			
120590082000	Hick	1	3 8S 10E	2,123	16.0	107.0		21	28			
120590082000	Hick	1	3 8S 10E	2,124	17.0	154.0		24	28			
120590082000	Hick	1	3 8S 10E	2,125	17.0	123.0		25	23			
120590082000	Hick	1	3 8S 10E	2,126	21.0	134.0		17	30			
120590082000	Hick	1	3 8S 10E	2,127	17.0	106.0		20	34			

120590082000	Hick	1	3 8S 10E	2,128	17.0	276.0		20	31			
120590082000	Hick	1	3 8S 10E	2,129	17.0	226.0		24	37			
120590082000	Hick	1	3 8S 10E	2,130	17.0	186.0		20	34			
120590082000	Hick	1	3 8S 10E	2,131	19.0	129.0		19	33			
120590082000	Hick	1	3 8S 10E	2,132	16.0	176.0		25	27			
120590082000	Hick	1	3 8S 10E	2,134	13.0	127.0		24	24			
120590082000	Hick	1	3 8S 10E	2,135	18.0	216.0		26	28			
120590082000	Hick	1	3 8S 10E	2,136	18.0	46.0	28	22	28			
120590082000	Hick	1	3 8S 10E	2,137	19.0	154.0	103	16	31			
120590082000	Hick	1	3 8S 10E	2,138	17.0	121.0	120	15	37			
120590082000	Hick	1	3 8S 10E	2,139	18.0	159.0	188	15	33			
120590082000	Hick	1	3 8S 10E	2,140	17.0	171.0	84	16	26			
120590082000	Hick	1	3 8S 10E	2,141	17.0	229.0	218	16	29			
120590082000	Hick	1	3 8S 10E	2,142	16.0	242.0	220	22	29			
120590082000	Hick	1	3 8S 10E	2,143	17.0	135.0	86	20	29			
120590082000	Hick	1	3 8S 10E	2,144	16.0	88.0	56	17	34			
120590082000	Hick	1	3 8S 10E	2,145	16.0	134.0	177	17	32			
120590082000	Hick	1	3 8S 10E	2,146	16.0	28.0	34	19	27			
120590082000	Hick	1	3 8S 10E	2,145	16.0	134.0	177	17	32			
120590082000	Hick	1	3 8S 10E	2,146	16.0	28.0	34	19	27			
120590082000	Hick	1	3 8S 10E	2,147	18.0	73.0	24	17	33			
120590082000	Hick	1	3 8S 10E	2,149	19.0	23.0	15	14	40			
120590082000	Hick	1	3 8S 10E	2,150	14.0	38.0	25	6	42			
120590082000	Hick	1	3 8S 10E	2,151	14.0	67.0	60	21	29			
120590082000	Hick	1	3 8S 10E	2,152	15.0	112.0	124	15	31			
120590082000	Hick	1	3 8S 10E	2,153	12.0	56.0	40	25	16			
120590082000	Hick	1	3 8S 10E	2,154	14.0	422.0		0	79			
120590082100	Hick	2	3 8S 10E	2,102	17.0	115.0		18	28	18	96	121
120590082100	Hick	2	3 8S 10E	2,103	16.0	58.0		20	28			
120590082100	Hick	2	3 8S 10E	2,104	17.0	143.0		21	29			
120590082100	Hick	2	3 8S 10E	2,105	19.0	94.0		18	30			
120590082100	Hick	2	3 8S 10E	2,106	20.0	136.0		20	31			
120590082100	Hick	2	3 8S 10E	2,107	18.0	98.0		14	33			
120590082100	Hick	2	3 8S 10E	2,108	18.0	24.0		16	28			
120590082100	Hick	2	3 8S 10E	2,109	17.0	73.0		16	45			
120590082100	Hick	2	3 8S 10E	2,110	18.0	98.0		16	26			
120590082100	Hick	2	3 8S 10E	2,111	18.0	153.0		14	34			
120590082100	Hick	2	3 8S 10E	2,112	20.0	169.0		20	31			
120590082100	Hick	2	3 8S 10E	2,113	19.0	126.0		23	28			
120590082100	Hick	2	3 8S 10E	2,114	18.0	76.0		18	30			
120590082100	Hick	2	3 8S 10E	2,115	18.0	206.0		25	24			
120590082100	Hick	2	3 8S 10E	2,116	18.0	66.0		23	30			
120590082100	Hick	2	3 8S 10E	2,117	15.0	79.0		19	23			
120590082100	Hick	2	3 8S 10E	2,118	17.0	67.0		20	31			

Continued

Appendix E *Continued* Inman East Consolidated Field Core Analysis Data

API number	well name	no.	location	depth	porosity percent	air permeability horiz	air permeability vert	oil sat	water sat	avg por	geom mean perm	median horiz perm
120590082100	Hick	2	3 8S 10E	2,119	17.0	81.0		20	35			
120590082100	Hick	2	3 8S 10E	2,120	19.0	180.0		20	30			
120590082100	Hick	2	3 8E 10E	2,121	17.0	144.0		21	26			
120590082100	Hick	2	3 8S 10E	2,122	17.0	245.0		20	36			
120590082100	Hick	2	3 8S 10E	2,123	18.0	274.0		14	25			
120590082100	Hick	2	3 8S 10E	2,124	18.0	198.0		16	25			
120590082100	Hick	2	3 8S 10E	2,125	16.0	0.1		0	76			
120590082100	Hick	2	3 8S 10E	2,126	17.0	170.0		18	28			
120590082100	Hick	2	3 8S 10E	2,127	18.0	170.0		18	31			
120590082100	Hick	2	3 8S 10E	2,128	16.0	193.0		16	26			
120590082100	Hick	2	3 8S 10E	2,129	19.0	195.0		17	28			
120590082100	Hick	2	3 8S 10E	2,132	19.0	198.0		15	30			
120590082100	Hick	2	3 8S 10E	2,133	18.0	74.0		12	32			
120590082100	Hick	2	3 8S 10E	2,134	18.0	161.0		20	27			
120590082100	Hick	2	3 8S 10E	2,135	19.0	88.0		17	31			
120590082100	Hick	2	3 8S 10E	2,136	19.0	91.0		18	39			
120590082100	Hick	2	3 8S 10E	2,137	21.0	36.0		18	32			
120590082100	Hick	2	3 8S 10E	2,138	18.0	115.0		18	32			
120590082100	Hick	2	3 8S 10E	2,139	17.0	247.0		17	29			
120590082300	Hick	4	3 8S 10E	2,128	17.0	128.0		22	24	17	94	117
120590082300	Hick	4	3 8S 10E	2,129	17.0	250.0		23	32			
120590082300	Hick	4	3 8S 10E	2,130	17.0	50.0		20	32			
120590082300	Hick	4	3 8S 10E	2,131	17.0	128.0		26	29			
120590082300	Hick	4	3 8S 10E	2,132	17.0	114.0		21	33			
120590082300	Hick	4	3 8S 10E	2,133	17.0	38.0		17	40			
120590082300	Hick	4	3 8S 10E	2,134	16.0	150.0		21	31			
120590082300	Hick	4	3 8S 10E	2,135	19.0	120.0		27	29			
120590082300	Hick	4	3 8S 10E	2,136	22.0	69.0		17	32			
120590082300	Hick	4	3 8S 10E	2,137	18.0	123.0		22	32			
120590082300	Hick	4	3 8S 10E	2,138	17.0	31.0		20	37			
120590082300	Hick	4	3 8S 10E	2,139	14.0	109.0		23	38			
120590082400	Jessie Hick	5	3 8S 10E	2,116	19.0	54.0		21	40	19	130	136
120590082400	Jessie Hick	5	3 8S 10E	2,117	19.0	160.0		20	33			
120590082400	Jessie Hick	5	3 8S 10E	2,118	19.0	144.0		20	35			
120590082400	Jessie Hick	5	3 8S 10E	2,119	17.0	104.0		24	30			
120590082400	Jessie Hick	5	3 8S 10E	2,120	17.0	128.0		19	30			
120590082400	Jessie Hick	5	3 8S 10E	2,121	19.0	75.0		20	33			
120590082400	Jessie Hick	5	3 8S 10E	2,122	17.0	173.0		21	29			

120590082400	Jessie Hick	5	3 8S 10E	2,123	19.0	197.0	21	28				
120590082400	Jessie Hick	5	3 8S 10E	2,124	19.0	60.0	23	32				
120590082400	Jessie Hick	5	3 8S 10E	2,125	17.0	98.0	22	35				
120590082400	Jessie Hick	5	3 8S 10E	2,126	18.0	121.0	24	29				
120590082400	Jessie Hick	5	3 8S 10E	2,127	18.0	230.0	19	28				
120590082400	Jessie Hick	5	3 8S 10E	2,128	18.0	110.0	20	32				
120590082400	Jessie Hick	5	3 8S 10E	2,129	19.0	107.0	23	30				
120590082400	Jessie Hick	5	3 8S 10E	2,130	19.0	251.0	24	40				
120590082400	Jessie Hick	5	3 8S 10E	2,131	20.0	210.0	21	36				
120590082400	Jessie Hick	5	3 8S 10E	2,132	18.0	21.0	22	37				
120590082400	Jessie Hick	5	3 8S 10E	2,133	19.0	153.0	21	38				
120590082400	Jessie Hick	5	3 8S 10E	2,134	20.0	377.0	22	32				
120590082400	Jessie Hick	5	3 8S 10E	2,135	20.0	92.0	22	37				
120590082400	Jessie Hick	5	3 8S 10E	2,136	20.0	257.0	19	34				
120590082400	Jessie Hick	5	3 8S 10E	2,137	18.0	252.0	21	36				
120590084100	TEB	1	3 8S 10E	2,136	15.0	201.0			14	102		138
120590084100	TEB	1	3 8S 10E	2,137	14.0	16.0						
120590084100	TEB	1	3 8S 10E	2,138	14.0	45.0						
120590084100	TEB	1	3 8S 10E	2,139	15.0	70.0						
120590084100	TEB	1	3 8S 10E	2,140	14.0	65.0						
120590084100	TEB	1	3 8S 10E	2,141	15.0	247.0						
120590084100	TEB	1	3 8S 10E	2,142	15.0	181.0						
120590084100	TEB	1	3 8S 10E	2,144	14.0	42.0						
120590084100	TEB	1	3 8S 10E	2,145	15.0	52.0	19	28				
120590084100	TEB	1	3 8S 10E	2,146	15.0	236.0	23	30				
120590084100	TEB	1	3 8S 10E	2,147	15.0	245.0	20	30				
120590084100	TEB	1	3 8S 10E	2,148	14.0	155.0	23	44				
120590084100	TEB	1	3 8S 10E	2,149	12.0	192.0	27	22				
120590084100	TEB	1	3 8S 10E	2,150	14.0	121.0	22	20				
120590084200	TEB	2	3 8S 10E	2,132	21.0	90.0	19	36	19	136		142
120590084200	TEB	2	3 8S 10E	2,133	21.0	131.0	19	30				
120590084200	TEB	2	3 8S 10E	2,134	20.0	185.0	21	28				
120590084200	TEB	2	3 8S 10E	2,135	19.0	158.0	23	23				
120590084200	TEB	2	3 8S 10E	2,136	18.0	152.0	23	17				
120590084200	TEB	2	3 8S 10E	2,138	20.0	172.0	19	25				
120590084200	TEB	2	3 8S 10E	2,139	18.0	132.0	19	32				
120590084200	TEB	2	3 8S 10E	2,140	16.0	117.0	23	23				
120590084200	TEB	2	3 8S 10E	2,142	15.0	273.0	19	23				
120590084200	TEB	2	3 8S 10E	2,143	18.0	59.0	16	27				
120590084300	TEB	3	3 8S 10E	2,123	18.0	76.0	20	43	18	94		110
120590084300	TEB	3	3 8S 10E	2,124	19.0	93.0	19	41				
120590084300	TEB	3	3 8S 10E	2,125	18.0	160.0	20	36				
120590084300	TEB	3	3 8S 10E	2,126	18.0	61.0	16	43				
120590084300	TEB	3	3 8S 10E	2,127	19.0	70.0	17	40				

Continued

Appendix E *Continued* Inman East Consolidated Field Core Analysis Data

API number	well name	no.	location	depth	porosity percent	air permeability horiz	air permeability vert	oil Sat	water Sat	avg por	geom mean perm	median horiz perm
120590084300	TEB	3	3 8S 10E	2,128	18.0	24.0		19	42			
120590084300	TEB	3	3 8S 10E	2,129	17.0	110.0		19	42			
120590084300	TEB	3	3 8S 10E	2,130	19.0	127.0		24	35			
120590084300	TEB	3	3 8S 10E	2,131	19.0	43.0		23	41			
120590084300	TEB	3	3 8S 10E	2,132	18.0	145.0		20	42			
120590084300	TEB	3	3 8S 10E	2,133	19.0	333.0		17	38			
120590084300	TEB	3	3 8S 10E	2,134	21.0	15.0		17	47			
120590084300	TEB	3	3 8S 10E	2,135	16.0	233.0		22	48			
120590084300	TEB	3	3 8S 10E	2,136	16.0	181.0		23	32			
120590084300	TEB	3	3 8S 10E	2,137	20.0	186.0		17	39			
120590084400	TEB	4	3 8S 10E	2,121	18.0	120.0		24	28	19	115	116
120590084400	TEB	4	3 8S 10E	2,122	18.0	134.0		21	27			
120590084400	TEB	4	3 8S 10E	2,123	19.0	54.0		20	29			
120590084400	TEB	4	3 8S 10E	2,124	17.0	116.0		23	28			
120590084400	TEB	4	3 8S 10E	2,125	17.0	48.0		19	26			
120590084400	TEB	4	3 8S 10E	2,126	17.0	80.0		17	30			
120590084400	TEB	4	3 8S 10E	2,127	18.0	88.0		16	25			
120590084400	TEB	4	3 8S 10E	2,131	19.0	78.0						
120590084400	TEB	4	3 8S 10E	2,132	21.0	74.0						
120590084400	TEB	4	3 8S 10E	2,133	20.0	110.0						
120590084400	TEB	4	3 8S 10E	2,134	19.0	140.0						
120590084400	TEB	4	3 8S 10E	3,135	21.0	230.0						
120590084400	TEB	4	3 8S 10E	2,136	20.0	270.0						
120590084400	TEB	4	3 8S 10E	2,137	20.0	215.0						
120590084400	TEB	4	3 8S 10E	2,138	20.0	184.0						
120590084400	TEB	4	3 8S 10E	2,139	20.0	355.0						
120590084400	TEB	4	3 8S 10E	2,140	20.0	40.0						
120590084500	TEB	5	3 8S 10E	2,124	18.0	21.0		20	36	18	58	122
120590084500	TEB	5	3 8S 10E	2,125	17.0	16.0		20	37			
120590084500	TEB	5	3 8S 10E	2,126	14.0	5.0		20	45			
120590084500	TEB	5	3 8S 10E	2,127	15.0	0.1			42			
120590084500	TEB	5	3 8S 10E	2,128	20.0	86.0		19	32			
120590084500	TEB	5	3 8S 10E	2,129	17.0	126.0		22	29			
120590084500	TEB	5	3 8S 10E	2,130	17.0	117.0		18	30			
120590084500	TEB	5	3 8S 10E	2,131	21.0	177.0		20	36			
120590084500	TEB	5	3 8S 10E	2,132	19.0	129.0		22	32			
120590084500	TEB	5	3 8S 10E	2,133	21.0	73.0		18	32			
120590084500	TEB	5	3 8S 10E	2,134	16.0	89.0		21	34			

120590084500	TEB	5	3 8S 10E	2,135	19.0	141.0	17	30				
120590084500	TEB	5	3 8S 10E	2,136	18.0	278.0	20	33				
120590084500	TEB	5	3 8S 10E	2,137	19.0	198.0	23	31				
120590084500	TEB	5	3 8S 10E	2,138	19.0	248.0	15	40				
120590084500	TEB	5	3 8S 10E	2,139	20.0	256.0	17	40				
120590084800	TEB	8	3 8S 10E	2,119	18.0	32.0	25	34	17	101	117	
120590084800	TEB	8	3 8S 10E	2,120	16.0	99.0	28	31				
120590084800	TEB	8	3 8S 10E	2,121	19.0	130.0	19	28				
120590084800	TEB	8	3 8S 10E	2,122	18.0	183.0	21	31				
120590084800	TEB	8	3 8S 10E	2,123	17.0	59.0	21	32				
120590084800	TEB	8	3 8S 10E	2,124	17.0	40.0	22	35				
120590084800	TEB	8	3 8S 10E	2,125	18.0	42.0	20	42				
120590084800	TEB	8	3 8S 10E	2,126	17.0	48.0	22	32				
120590084800	TEB	8	3 8S 10E	2,127	18.0	107.0	24	29				
120590084800	TEB	8	3 8S 10E	2,128	20.0	162.0	22	26				
120590084800	TEB	8	3 8S 10E	2,129	18.0	100.0	24	3				
120590084800	TEB	8	3 8S 10E	2,130	18.0	200.0	22	31				
120590084800	TEB	8	3 8S 10E	2,131	15.0	126.0	26	38				
120590084800	TEB	8	3 8S 10E	2,132	16.0	220.0	25	24				
120590084800	TEB	8	3 8S 10E	2,133	16.0	234.0	17	42				
120590084800	TEB	8	3 8S 10E	2,134	16.0	144.0	21	40				
120590085500	Busiek	D-1	4 8S 10E	2,126	18.0	79.0	25	29	18	77	87	
120590085500	Busiek	D-1	4 8S 10E	2,127	16.0	94.0	27	24				
120590085500	Busiek	D-1	4 8S 10E	2,128	17.0	107.0	25	35				
120590085500	Busiek	D-1	4 8S 10E	2,129	18.0	48.0	21	27				
120590085500	Busiek	D-1	4 8S 10E	2,130	19.0	57.0	21	30				
120590085500	Busiek	D-1	4 8S 10E	2,131	19.0	99.0	28	27				
120590092400	Murphy	6	10 8S 10E	2,106	20.0	277.0	24	37	19	78	99	
120590092400	Murphy	6	10 8S 10E	2,107	18.0	137.0	23	32				
120590092400	Murphy	6	10 8S 10E	2,108	17.0	210.0	24	30				
120590092400	Murphy	6	10 8S 10E	2,109	18.0	242.0	22	25				
120590092400	Murphy	6	10 8S 10E	2,110	18.0	184.0	23	26				
120590092400	Murphy	6	10 8S 10E	2,111	18.0	307.0	27	27				
120590092400	Murphy	6	10 8S 10E	2,112	20.0	223.0	25	26				
120590092400	Murphy	6	10 8S 10E	2,113	21.0	100.0	25	28				
120590092400	Murphy	6	10 8S 10E	2,114	20.0	54.0	20	31				
120590092400	Murphy	6	10 8S 10E	2,115	22.0	45.0	23	29				
120590092400	Murphy	6	10 8S 10E	2,116	20.0	31.0	22	26				
120590092400	Murphy	6	10 8S 10E	2,117	18.0	42.0	23	21				
120590092400	Murphy	6	10 8S 10E	2,118	21.0	95.0	23	24				
120590092400	Murphy	6	10 8S 10E	2,119	18.0	14.0	26	26				
120590092400	Murphy	6	10 8S 10E	2,120	20.0	16.0	25	22				
120590092400	Murphy	6	10 8S 10E	2,121	18.0	99.0	22	27				
120590092400	Murphy	6	10 8S 10E	2,123	19.0	498.0	26	26				

Continued

Appendix E *Continued* Inman East Consolidated Field Core Analysis Data

API number	well name	no.	location	depth	porosity percent	air permeability horiz	air permeability vert	oil Sat	water Sat	avg por	geom mean perm	median horiz perm
120590092400	Murphy	6	10 8S 10E	2,124	20.0	118.0		27	24			
120590092400	Murphy	6	10 8S 10E	2,125	20.0	67.0		26	18			
120590092400	Murphy	6	10 8S 10E	2,126	20.0	400.0		26	19			
120590092400	Murphy	6	10 8S 10E	2,127	22.0	43.0		17	39			
120590092400	Murphy	6	10 8S 10E	2,128	18.0	2.0		20	37			
120590092400	Murphy	6	10 8S 10E	2,129	19.0	14.0		15	40			
120590019400	Busick	1	11 8S 10E	2,040	19.0	10.0		13	44	17	58	55
120590019400	Busick	1	11 8S 10E	2,041	19.0	9.0		13	45			
120590019400	Busick	1	11 8S 10E	2,042	19.0	15.0		15	43			
120590019400	Busick	1	11 8S 10E	2,043	15.0	6.0		18	34			
120590019400	Busick	1	11 8S 10E	2,044	11.0	160.0		19	28			
120590019400	Busick	1	11 8S 10E	2,045	14.0	55.0		22	34			
120590019400	Busick	1	11 8S 10E	2,046	14.0	270.0		24	32			
120590019400	Busick	1	11 8S 10E	2,047	18.0	254.0		20	28			
120590019400	Busick	1	11 8S 10E	2,048	20.0	161.0		20	31			
120590019400	Busick	1	11 8S 10E	2,049	20.0	138.0		16	26			
120590019400	Busick	1	11 8S 10E	2,050	19.0	247.0		19	32			
120590019400	Busick	1	11 8S 10E	2,051	19.0	189.0		16	28			
120590019400	Busick	1	11 8S 10E	2,052	18.0	34.0		171	47			
120590019400	Busick	1	11 8S 10E	2,053	19.0	41.0		15	32			
120590019400	Busick	1	11 8S 10E	2,054	16.0	40.0		17	37			
120590020500	Kerwin	2	11 8S 10E	2,053	15.0	96.0		21	34	15	218	394
120590020500	Kerwin	2	11 8S 10E	2,054	15.0	15.0		18	34			
120590020500	Kerwin	2	11 8S 10E	2,055	14.0	394.0		19	23			
120590020500	Kerwin	2	11 8S 10E	2,056	14.0	318.0		21	26			
120590020500	Kerwin	2	11 8S 10E	2,057	14.0	549.0		21	33			
120590020500	Kerwin	2	11 8S 10E	2,059	16.0	411.0		14	26			
120590020500	Kerwin	2	11 8S 10E	2,061	16.0	583.0		21	33			
120590021900	Curry	1	15 8S 10E	2,092	10.0	21.0		10	41	10	5	7
120590021900	Curry	1	15 8S 10E	2,093	8.0	7.0		5	51			
120590021900	Curry	1	15 8S 10E	2,094	12.0	7.0		10	36			
120590021900	Curry	1	15 8S 10E	2,094	13.0	18.0		7	40			
120590021900	Curry	1	15 8S 10E	2,095	7.0	0.1		0	66			
120590025800	Egyptian Tie & Timber Co.	1	16 8S 10E	2,071	19.0	740.0		29		18	417	363
120590025800	Egyptian Tie & Timber Co.	1	16 8S 10E	2,073	18.0	365.0		26				
120590025800	Egyptian Tie & Timber Co.	1	16 8S 10E	2,075	16.0	310.0		33				

120590025800	Egyptian Tie & Timber Co.	1	16 8S 10E	2,079	17.0	360.0	31				
120590026800	Leach	1	16 8S 10E	2,072	12.0	66.0	22	31	15	79	52
120590026800	Leach	1	16 8S 10E	2,073	16.0	335.0	29	9			
120590026800	Leach	1	16 8S 10E	2,074	17.0	860.0	28	5			
120590026800	Leach	1	16 8S 10E	2,075	17.0	510.0	30	10			
120590026800	Leach	1	16 8S 10E	2,076	11.0	24.0	21	12			
120590026800	Leach	1	16 8S 10E	2,077	16.0	38.0	12	52			
120590026800	Leach	1	16 8S 10E	2,078	14.0	15.0	0	46			
120590026800	Leach	1	16 8S 10E	2,079	14.0	12.0	14	29			
120590026900	Leach	2	16 8S 10E	2,085	18.0	170.0	25		18	187	172
120590026900	Leach	2	16 8S 10E	2,086	18.0	222.0	21				
120590026900	Leach	2	16 8S 10E	2,084	17.8	172.0					
120590031900	Egyptian Tie & Timber Co.	1	16 8S 10E	2,096	14.0	26.0	8		16	159	120
120590031900	Egyptian Tie & Timber Co.	1	16 8S 10E	2,097	10.0	190.0	21				
120590031900	Egyptian Tie & Timber Co.	1	16 8S 10E	2,099	13.0	157.0	22				
120590031900	Egyptian Tie & Timber Co.	1	16 8S 10E	2,100	17.0	69.0	16				
120590031900	Egyptian Tie & Timber Co.	1	16 8S 10E	2,101	16.0	151.0	13				
120590031900	Egyptian Tie & Timber Co.	1	16 8S 10E	2,102	16.0	152.0	7				
120590031900	Egyptian Tie & Timber Co.	1	16 8S 10E	2,103	15.0	88.0					
120590031900	Egyptian Tie & Timber Co.	1	16 8S 10E	2,105	23.0	74.0					
120590097900	Egyptian	14	16 8S 10E	2,214	17.6	25.0			19	22	30
120590097900	Egyptian	14	16 8S 10E	2,215	19.5	11.0					
120590097900	Egyptian	14	16 8S 10E	2,216	20.1	42.0					
120590097900	Egyptian	14	16 8S 10E	2,217	18.8	39.0					
120590097900	Egyptian	14	16 8S 10E	2,218	20.5	40.0					
120590097900	Egyptian	14	16 8S 10E	2,219	20.9	44.0					
120590097900	Egyptian	14	16 8S 10E	2,220	20.8	50.0					
120590097900	Egyptian	14	16 8S 10E	2,221	20.4	40.0					
120590097900	Egyptian	14	16 8S 10E	2,222	17.3	8.0					
120590097900	Egyptian	14	16 8S 10E	2,223	18.6	3.8					
120590097900	Egyptian	14	16 8S 10E	2,224	19.9	26.0					
120590097900	Egyptian	14	16 8S 10E	2,225	19.1	16.0					
120590097900	Egyptian	14	16 8S 10E	2,226	18.5	75.0					
120590097900	Egyptian	14	16 8S 10E	2,227	13.8	30.0					
120590097900	Egyptian	14	16 8S 10E	2,228	14.6	4.1					
Inman Field Averages									17	102	112